Dear Dr. Karlsson,

We would like to thank you for your attention to our manuscript and the three reviewers for their comments. We are pleased that all three reviewers liked the manuscript and consider it to be publishable in 'The Cryosphere'. We appreciate both their interest in our study, and their constructive comments, and we have paid great attention to the feedbacks provided in revising our manuscript.

We have provided a response to each reviewer, including details of any edits to the manuscript. Minor text edits are detailed in these responses and the more substantive revisions consist of:

1) We have clarified our methodology and the conclusions we draw from our results.

2) We provide a Supplementary Information file which contains additional tables and figures, as requested by the reviewers, to help in the interpretation of the results.

Note that all the material included in the Appendix of the original version of the manuscript has also been moved in this Supplementary Information file.

Please do not hesitate to get in touch should any further modifications be required, or any clarification on our response to reviewers.

Best regards,
Vincent Verjans, on behalf of authors

Referee 1

We thank this reviewer for their compliments and feedback. Our response to these comments is below, the referees original text is given in red throughout and our response is in black.

A) General comments

Although it is clear they are aware of the extreme variability of firn density in the percolation zone, they do not comment on the difficulty of up-scaling from a single point measurement to the model scale. It would be very useful to have a discussion, early on in the paper, about what features of the observed data a good model, fed by their input data, could be expected to reproduce. Perhaps the overall densification rate? Perhaps the amount of refrozen meltwater in the profile? Certainly not the position and size of ice layers as this is notoriously variable.

We recognize that one would not expect a firn model to reproduce with great precision the number of ice layers observed and their exact location, especially given the spatial variability of firn structure, the 5.5 km resolution of the Regional Climate Model used as forcing and the use of a constant surface density. However, we think that the assessment of the ability of a firn model to produce *representative* ice layers and a density profile varying in depth is valuable for some applications, especially for the meltwater routing.

In the manuscript, we try to highlight the ability of the models tested to match observed values of FAC and 10 m temperature. These variables give, in our opinion, a good perspective on how well a particular model reproduces the bulk conditions of the upper firn column.

As you suggested, we added a paragraph at the beginning of Sect. 4 in order to clarify the way in which we compare model results to observations to the reader.
Section 4: *Results of simulations and observations are inter-compared based on the firn air content (FAC; the depth integrated porosity in a firn column) over the top 15 m of firn and the temperature at 10m depth. Comparing the modelled FAC and 10 m depth temperature values with observed data depicts the ability of the tested models to reproduce the bulk condition of the upper firn column. We also qualitatively assess the degree to which the models to form a 'realistic' ice layer distribution and depth-density profile. One would not expect simulated values of either to match observations precisely given the high spatial variability of firn structure (Marchenko et al., 2017), but it is indicative of the models' performance in reproducing heterogeneity in firn density.*

Given this preliminary discussion the authors would be able to concentrate on the differences in model outputs, which are interesting and illuminating, and could avoid putting too much weight on the comparison with observed data. Small changes would probably be enough; for example, if Figures 4, 5, 8 and 10 had a very pale grey indication of the observed data in the background, the model outputs would be easier to compare with each other and the reader would be led away from the idea that the model output "should" reproduce the point observations in detail.

In our paper we do not aim to single out a specific water flow scheme or model configuration as "best" in comparison with observations. We focus on giving the reader an extensive overview of the behaviour and differences in outputs of the three schemes tested. We hope that the modifications made in response to your comment above, amongst others, addresses this comment.

We additionally changed Figures 4, 5, 8 and 10 as you suggested by giving a pale grey colour to the observed depth-density profile.

The descriptions of what each model is doing are very good and show great insight into how these quite complex models work. However, the mass of material in the Results section is rather overwhelming and the authors might consider whether all of it is needed. It may be that all the results are indeed required, in order to justify the points made in the Discussion section. In that case, maybe the answer would be to move some material into a Supplementary Material section.
We agree with you that the manuscript is long. We have considered to move parts of the Results section to the Supplementary Material. However, we think that the clarity and coherence of the study would be affected by any such move and we took the decision to keep the entirety of the Results section in the main manuscript.

The statement (p.8 l.26) that water cannot fill the entire pore space because otherwise there would not be enough space for the liquid to freeze is a bit confusing. Is it equivalent to saying that as water in a saturated layer freezes, the part that won't fit is expelled into another layer? What about the possibility that a saturated layer expands on freezing?

Our approach in this study has been to implement the SNOWPACK liquid water schemes with the greatest fidelity possible. The deviations we make from the original schemes are only related to the age and depth scales that differ by orders of magnitude between seasonal snow and firn. Because the SNOWPACK scheme uses the correction for the saturation that you refer to, we have decided to implement the same. Please note that this correction (that, at saturation, water does not fill the entire porosity of the firn) is in good agreement with the laboratory findings of Yamaguchi et al. (2010).

We add a statement to this effect in the revised manuscript in Sect. 3.2:
It is reasonable to use this correction factor since Yamaguchi et al. (2010) found that trapped air still occupies 10 % of the porosity in saturated snow.

It would be worthwhile looking at each use of “therefore” to ensure that the authors really do mean a strong causal connection; the alternative might be to use the weaker ‘so” or even “and”.

In the revised manuscript we looked again at our uses of “therefore” and removed or replaced several ones.

B) Specific comments

For all the specific editorial comments, we agreed with the reviewer and made modifications as suggested.

Concerning the comment:

p.6 l.26 “the depth from which firn density does not reach”? Not clear what is meant here

We replaced the statement by “the depth below which all layers have density higher than the pore close-off value (830 kg m^{-3})”, as suggested by another referee.

Referee 2

We thank this reviewer for his compliments and feedback. Our response to his comments is below, the referees original text is given in red throughout and our response is in black.

General comments

The authors selected from the SUMup dataset few density profiles for validation, but left aside other profiles contained in that same dataset. Some of these missing measurements can be deemed redundant, but other firn observations, such as the PARCA cores, are important to understand the performance of the model through time.

We greatly value the existence of the SUMup and PARCA datasets because they enable an extensive evaluation of firn densification modelling against observations in general. These are thus very valuable for any firn modelling study at the ice-sheet wide scale.

Since we, to our knowledge, are the first study to perform firn densification simulations using these more physically complex liquid water flow schemes, we preferred to focus our analysis on the performance of the different schemes at four sites chosen on the basis that they represented a range of climatological and glaciological settings. Including more sites would have necessitated a reduction in the detail of our analysis which would have had a detrimental effect on its thoroughness. Reviewer 1 in fact complimented the study in this respect.

We agree that the performance of the model through time is important, but given the current length of the manuscript we feel that an assessment of this is beyond the scope of this study. We will certainly consider this in future work however and have added a comment in the Conclusion of the revised manuscript to this effect.

Another flaw of the manuscript is the lack of context regarding the modelling approaches used here as well as the absence of comparison of the results with previous similar work. It is important to know if the results presented here were already known or expected or if they constitute a novelty of this study.

We thank the reviewer for bringing these papers to our attention. In this revised version, we took care to refer more to both existing modelling studies and observational studies as you advised. For example, we added references to Langen et al. (2017) and Steger et al. (2017b), in which model experiments were performed at KAN-U with different firn models/liquid water schemes/climatic forcing. We discuss the differences with our results in section 5. We also included references to Marchenko et al. (2017) who highlighted the large spatial variability of firn structure and to Miller et al. (2018) who measured discharge rates in firn aquifers. We performed further simulations with runoff rates in aquifers calibrated in accordance with the observations of Miller et al. (2018) and discuss these briefly. We think these additions improve the quality of the manuscript.

References to Marchenko et al. (2017)
Section 4: *We also qualitatively assess the degree to which the models to form a 'realistic' ice layer distribution and depth-density profile. One would not expect simulated values of either to match observations precisely given the high spatial variability of firn structure (Marchenko et al., 2017), but it is indicative of the models' performance in reproducing heterogeneity in firn density.*

Section 5: *On the other hand, comparisons between modelled and observed density profiles are strongly affected by the choice and accuracy of the densification formulation, the variability of surface density, several other factors influencing model outputs mentioned above and possible uncertainties in field measurements. Such uncertainties are related to the strong spatial variability of firn structure (Marchenko et al., 2017), which can be observed by comparing density profiles of cores drilled at nearby locations.*

Reference to Miller et al. (2018)
Section 3.4.2: *Miller et al. (2018) found discharge rates within the firn aquifer to be 4.3 x 10^{-6} m s^{-1} by borehole dilution tests in the field. We tested this approach in our model by applying this value as a constant discharge rate for aquifers formed in our simulations. We found however that, using this approach, an aquifer was not sustained; suggesting that such discharge rates must be dependent on the total amount of water within the aquifer and are likely temporally variable.*

Reference to Langen et al. (2017) and Steger et al. (2017b)
Section 5: *We compare the results reached at KAN-U with previous firn modelling studies at this site. Langen et al. (2017) also used the CROCUS densification scheme and a water flow scheme conceptually comparable to R1M but with a simplified solving process of the RE. Their results show a density profile entirely at ice density from 4 m depth and an overestimation of the temperature at 10 m depth (+3 to +5 K). In our study, the R1M results show lower deep densities and a 10 m temperature underestimation. These discrepancies can be attributed to differences in 1) model implementation, 2) climatic forcing and 3) details of the water flow scheme. Model resolution is likely of importance here: Langen et al. (2017) used a coarser vertical resolution, disfavouring the formation of thin impermeable layers, allowing liquid water to flow more readily to greater depths and refreeze, thus causing greater density and higher temperature values. Steger et al. (2017b) used the SNOWPACK densification model (recall: we use different densification physics to SNOWPACK in this study) with a bucket scheme, similar to BK, and the same climatic forcing as in this study. Their model output shows a firn column fully compacted to ice at KAN-U. They attribute this to the overestimation of densification rates by the densification model used and also argued that some other effects*

could be at play such as the surface density applied. The 10 m temperature is underestimated in their result, likely due to the absence of percolation of water through ice and thus no latent heat release at depth.

Some of the reasons that could explain the model performance, such as potential biases in the forcing data or the effect of the impermeability threshold on the calculated FAC, are not even mentioned. These sources of bias should be quantified and discussed.

Concerning the RCM forcing data, we briefly mention that any bias in the climatic forcing would affect model results in Sect. 5.

We do not discuss this issue of RCM validation and uncertainty in-depth in the manuscript because we consider that the main goal of this study is to investigate the impact of different liquid water schemes on model performance. At the present state, we consider the biases arising from the liquid water scheme and the densification model as much greater than the uncertainty arising from the RCM. We think that discussing the validity of the climate model is beyond the scope of this study and such discussions are extensively covered in the existing literature.

We added additional references to Noël et al. (2018) and Ligtenberg et al. (2018) in Sect. 2.2 of the revised version of the manuscript. These papers evaluate RACMO2.3p2 and assess the effects of recent developments of the RCM on firn models respectively. Please note that the biases reported in Noël et al. (2018) are further reduced in our study because we use the RCM at a 5.5 km resolution. In Noël et al. (2018), there are detailed comparison between modelled and observed values of snowfall (see Fig. 11) and the estimated uncertainty integrated over the GrIS and specific catchments is 10 %. Also, it is shown (Figs 5 and 10b) that melt rates are well reproduced along the K-transect and at a South-East Greenland site, which are areas corresponding to the four sites of model experiments in our study. In Noël et al. (2018), radiative fluxes, which are the primary drivers of melt rates, are also demonstrated to be in good agreement with measurements from the PROMICE weather stations (Fig. 4) and their validation is further detailed in the supplementary material.
Section 2.2: *We refer to Noël et al. (2018) for a detailed discussion about the performance of RACMO2.3p2 on GrIS and related uncertainties. Additionally, Ligtenberg et al. (2018) have demonstrated the impact of recent developments in RACMO2.3p2 on firn modelling, mostly yielding improvements in modelled densification.*

Considering the impact of the impermeability threshold on the FAC, this is one of the main point of investigation of this study. At every site, we vary the impermeability threshold of each of the flow scheme and quantify the change in FAC due to these variations. The relative changes of FAC between simulations are given in the text and the absolute values as well as their discrepancy with the observed FAC are provided in the Tables. We also try to provide explanations of why an increase/decrease of the impermeability threshold can cause a modification of the modelled FAC.
We recognize that the discussion about the DPM results at KAN-U in Sect. 5 was speculative, in part because the prescribed impermeability threshold was limiting the amount of refreezing allowed in individual layers. Therefore, we have decided to remove this specific part of the text (p.22 l.23-30 in the original manuscript).

Specific comments

p.1 l.13 The abstract could benefit from being more quantitative and more specific.
We added quantifications of the increase in melt over the GrIS and an order of magnitude of the changes in modelled firn densities due to the use of different flow schemes. We specified the main uncertainties affecting the performance of the water flow schemes implemented. We also specified the processes that firn models should better represent for reaching improved results.

p.1 l.17 I believe the appropriate word is just "bucket approach". "tipping" gives the idea that the bucket/layer is emptied into the next bucket/layer. The water rather fills the layer's capacity and the excess water overflows into the next layer.
We agree with this and have replaced “tipping bucket approach” by “bucket approach” in the entire text.

p.1 l.21 Quantify
We proceeded to the suggested modifications: we quantify the trend of increase in surface melt and the upper limit of inter-model differences of porosity that we reach in our simulations.

p.1 l.26 Please list the main ones.
We proceeded to the suggested modification: we give as examples the snow grain structure and the presence of ice layers.

p.1 l.28 Name them.
We proceeded to the suggested modification by naming the microstructural effects, the wet snow metamorphism and the temperature sensitivity.

p.2 l.10 Please clarify this sentence and give reference.
We could not find any reference to this sentence and so have removed it from the revised manuscript.

p.2 l.29 Maybe "through the pores" ?

We proceeded to the change suggested.

p.3 l.5 Maybe implemented or combined with?
We proceeded to the change suggested.

p.4 l.1 It would be useful to know how the HL and KM densification schemes are forced. Are the accumulation and temperature considered constant?

HL and KM are forced with exactly the same three hourly climatic forcing as CROCUS. In the KM model, the firn temperature is used instead of the annual mean temperature for the diffusion process, as proposed in Steger et al. (2017). For the grain growth process, we use the 10 m depth temperature instead of the annual mean because the release of latent heat is not captured by the latter value. For the HL model, we use the firn temperature instead of the annual mean as in Lundin et al. (2017). This allows for seasonal variability in densification rates and accounts for latent heat release. For both the HL and KM, we use the mean accumulation rate over the lifetime of any firn layer instead of the mean annual accumulation rate (see Stevens 2018) because this approximates the overburden stress better.

These information are added in Sect. 4.1 in the revised manuscript.

p.5 l.6 Please give these values.
We added the specification of the surface density values in Sect. 2.4.

p.6 l.11 More density profiles are available at NASA-SE and DYE-2 from the PARCA campaign. Considering that they are freely accessible in the SUMup dataset, they should be included in the comparison. More measurements are available at KAN_U in 2015, 16, 17. Considering that these surveys are close in time, it might be deemed unnecessary to add them to the comparison. But they should be mentioned and leaving available data out should be justified. I believe there is also a density profile from the firn aquifer location from 2016.

We addressed the issue of simulating firn density at more locations and proceeding to comparisons with more observations in the response to your general comments. Please note that we took care to justify our approach at the end of Sect. 2.4.

p.6 l.13 I am missing a description of the temperature measurement that is being used in the validation. Here would be the appropriate place to describe them.

We added details of the temperature measurement used at KAN-U in Sect. 2.4 of the revised manuscript. At all the other sites, the temperature measurement comes with the source cited for the density data. We specify this also in Sect. 2.4 of the revised manuscript.

p.6 l.26 Maybe: ... is the depth below which all layers have density higher than the pore close off density.
We proceeded to the change suggested.

p.7 l.16 Please refer to section 2.4.2 where lateral runoff is detailed.
The BK model does not use the same runoff routine as the R1M and DPM. In the BK, all the water percolating until an impermeable ice layer is treated as immediate lateral runoff. We modified the manuscript in Sect. 3.1 in order to clarify this point.

p.8 Eq.(11) theta and its unit are actually not defined clearly in a sentence.
θ and its units are defined in p.4 Eq.(3). We added a sentence in the manuscript to refer the reader back to this equation for the definition of θ.

p.8 l.13 maybe "tuning" coefficients?
We proceeded to the modification suggested.

p.9 l.4 This value of irreducible water content was used in https://doi.org/10.5194/tc-6-743-2012 and https://doi.org/10.3389/feart.2017.00003 where it was described as:
"The irreducible water content is set to a relatively low value of 2% of the pore volume to mimic processes that allow an effective vertical water transport to lower layers, such as piping"

Here you use that same value for a model that solves these processes explicitly and therefore a low irreducible water content is questionable. Why not using the Coleou and Lesaffre formulation?

Throughout the entire implementation of R1M and DPM, we have taken care to remain as close as possible to the original SNOWPACK implementation. In the SNOWPACK implementation, the value of 0.02 is used for θ_r instead of the Coléou and Lesaffre formulation.

We would like to point out the difference between the water holding capacity θ_h of the BK and the residual water content θ_r of the R1m and DPM. θ_h is meant to simulate retention of water by capillary tension against gravity. The capillary tension is however explicitly modelled when applying the Richards Equation. The residual water content refers to the saturation at which the mobile water loses its continuity in the porous medium, and water flow becomes impossible (see for example Szymkiewicz (2009)). Thus, the water holding capacity should represent the effects of both this residual water saturation and of the capillary forces exerted when firn effective saturation is greater than zero (that is, when the volumetric water content is greater than the residual water content).

p.9 l.7 Is the following related to the sentence above: "... but in case of refreezing, can approach zero and must be adjusted accordingly"? If yes, then the word "another" is misleading. If not then please develop the refreezing issue as the provided information is insufficient to understand why an adjustment is necessary.

We agree with your comment and have modified this paragraph accordingly. We hope that it now provides better clarity.

p.9 l.9 In theory, water content below irreducible water content should not suffer gravity as capillary forces dominate. It is also unclear why changing from 0.75 to 0.9 addresses this issue. Please clarify.

We agree that in theory, the value of θ should be allowed to equal and to remain at a fixed θ_r value. However, the numerical requirement of keeping Se strictly greater than zero leads the model to adjust θ_r when θ approaches θ_r and minimal flow rates thus persist.

We clarify this point in Sect. 3.2 of the revised manuscript.

Note that gravity-driven flow occurs in the model as a function of the hydraulic conductivity, which depends on the effective saturation. Since the effective saturation must remain above zero, very low flow rates persist in layers close to θ_r. In other words, because Se cannot be set to zero, extremely low rates of water flow are modelled, and over long periods of time (weeks or months) this leads any layer to fall below the threshold we use to consider the firn column dry. The use of 0.9 instead of 0.75 leads to higher values of θ_r when θ approaches zero. In turn, this causes the effective saturation value to be lower. Lower effective saturation values lead to lower hydraulic conductivity and thus decreased flow rates.

p.9 l.23 Please point at section 2.4.2 for runoff calculation.
We proceeded to the modification suggested.

p.11 l.15 Please compare this number to field observations:
Schneebeli, M.: Development and stability of preferential flow paths in a layered snowpack, in: Biogeochemistry of Seasonally Snow-Covered Catchments (Proceedings of a Boulder Symposium July 1995), edited by: Tonnessen, K., Williams, M., and Tranter, M., 89–95, AHS Publ. no. 228, 1995.

Marsh, P. and Woo, M.-K.: Meltwater movement in natural heterogeneous snow covers, Water Resour. Res., 21, 1710–1716, doi:10.1029/WR021i011p01710, 1985.

Williams et al. Visualizing meltwater flow through snow at the centimetre-to-metre scale using a snow guillotine *Hydrol. Process.* **24**, 2098–2110 (2010)

The parameter Θ is the threshold saturation value in the preferential flow domain at which point water is assumed to flow back to the matrix flow domain. This is purely used as a tuning coefficient to reach the best agreement possible between modelled and observed ice layer formation and runoff rates by Wever et al. (2016) and Θ is difficult to compare to any observation.

The parameter N should not be confused with the parameter F. The latter represent the proportion of the snowpack where preferential flow can occur. As explained at the beginning of Sect. 3.3, we do not follow the regression relation derived in Wever et al. (2016) for this parameter but we take a constant value of 0.2 in line with observations of Marsh and Woo (1984) and Williams et al. (2010). The parameter N represents the number of active flowpaths for preferential flow. As an example in a 1 m^{-2} section of a snowpack and using F = 0.2, a single flowpath of area 0.2 m^{-2} would correspond to N = 1 whereas 10 flowpaths of area 0.02 m^{-2} would correspond to N = 10. Wever et al. (2016) briefly discuss the difficulty to constrain the N parameter with observations: it is possible to detect the number of flowpaths that formed in a dye tracing experiment but it is much more difficult to evaluate how many flowpaths were active simultaneously. As a consequence, similarly to what has been done for Θ, they proceeded to the calibration of N by minimizing the mismatch between the final output of the model and their observations of runoff and ice layer formation in alpine snow.

p.11 l.24 Point at the section where the time step of the water scheme is introduced.
We proceeded to the modification suggested.

p.11 l.25 Unclear whether this sentence applies to both R1M and DPM or just to DPM.
We modified the manuscript to clarify this point.

p.12 l.3 Please discuss the chosen runoff rates and aquifer dynamics compared to
Miller, O., Solomon, D. K., Miège, C., Koenig, L., Forster, R., Schmerr, N., Montgomery, L. (2018). Direct evidence of meltwater flow within a firn aquifer in southeast Greenland. Geophysical Research Letters, 45, 207–215. https://doi.org/10.1002/2017GL075707

We thank you for pointing us to this interesting and complementary observational study. We performed additional simulations by applying the runoff rates measured in that study in the simulated aquifers and discuss these new outputs and their implications at the end of Sect. 3.4.2.

p.12 l.4 Not in BK?
In this study, BK assumes instantaneous runoff when percolating water reaches an impermeable layer. Only the water held due to the water holding capacity can remain in firn layers. We clarified this point in Sect. 3.1 of the revised manuscript.

p.12 l.5 Isn't it allowed anywhere the water flow is impeded?
We have modified Sect. 3.4.2 to provide greater clarity.

p.12 l.10 The phrasing here and the structure of the section is rather confusing. It presents first the ponding on at the bottom of the column, then the lateral runoff that applies everywhere in the column, and finally reintroduce the ponding and show that the runoff rates do not allow the build up of aquifer. An alternative would be to present the runoff rates that apply on any ponding water in the column, then show that it does not allow the build up of aquifer, and finally present the aquifer-specific handling of ponding water as an exception.
As mentioned in the previous answer, we have modified Sect. 3.4.2 to provide greater clarity. We think that this concern is now addressed.

p.13 l.8 A major omission in this manuscript is the comparison of the forcing data to other estimations of accumulation, meltwater production and surface temperature at these sites. In all the following sections, overestimated FAC could be due to overestimated snowfall or underestimated meltwater input. Subsurface temperature bias could also be due to biased forcing skin temperature. One obvious pitfall would be to tune firn models so that they can reproduce observations using inaccurate forcing from a RCM. Please discuss this issue and refer to the appropriate literature to validate the forcing used here.

We address your concerns concerning the RCM forcing in the general comments. Again, we agree with you that the climatic forcing brings in a potential bias. But we consider the investigation of this bias as beyond the scope of this study and we assume that the biases related to the liquid water scheme and the firn densification model are greater in amplitude.

p.14 l.7 Here an in the following, a "reasonable" match between modeled and simulated density is often presented after an over- or underestimation of FAC. The two quantity being linked, they should reflect the same conclusions.

We modified the manuscript to ensure that any comparison between different profiles is quantified. In this particular case, the differences in FAC of each of the flow schemes with respect to the observed value are given in the previous lines. A close agreement in FAC values reflect a good agreement with the mean density. Additionally, we refer the reader to the figures of density profiles (Fig. 4a in this case) when we discuss the agreement with the observed density in more details.

p.14 l.31 relative to the original BK run or relative to observations? Check throughout the manuscript that for each of these relative change, the baseline is clearly specified.

We clarified that this is with respect to BK wh02 ip810 on this line. We also made sure that the comparative basis is clear throughout the paper, especially in Sect. 4.3 and 4.4.

p.15 l.33 How does the impermeability criteria relate to the layer thickness? A thick layer can refreeze large amounts of water without being categorized impermeable while minor refreezing in small layers immediately cause saturation and subsequent runoff.

The layer thickness is dependent on the model resolution used. In this study, we attach great importance to using a very fine vertical resolution in order to minimize approximations when solving the Richards Equation and also approximations such as the one you are highlighting. The layers' thickness is determined by the accumulation at every 3h time step modelled by the RCM and we apply merging only for layers less than 0.02 m thick.

It is true that thinner layers require less absolute refreezing to have their density raised to the impermeability threshold. Note however that this is partly counteracted by the lower cold content of a thin layer than a thick layer for a given temperature. Thus, thinner layer also have a lower refreezing capacity.

p.16 l.5 give depth range
We proceeded to the modification suggested.

p.16 l.21 It seems that the grain size parametrization has a great impact on the result although there is no observation of firn grain size or clear constrains on the grain growth modules in firn models. This could be highlighted more. The abstract, for example, could be more specific than "numerous uncertainties surrounding firn micro- and macro-structure...".

We modified the abstract to explicitly mention the importance of grain-size on the water flow scheme. We also modified the Discussion section to highlight the spread in results that can be due to the grain-size formulation. We agree that it is important to emphasize this because grain metamorphism in firn is poorly constrained by observations and thus subject to important uncertainties.

p.16 l.26 This sentence is unnecessary. The following presentation is sufficient for a result section. In the discussion part however, this spread of outcome for different compaction schemes can be brought up again and an appropriate reference where the schemes are being compared can be given.
We removed this sentence as suggested. We highlight further the need for intercomparison experiments in the Discussion section, such as the one of Lundin et al. (2017).

p.16 l.29 Give bias in the text.
We proceeded to the modification suggested.

p.16 l.31 At this site, valuable observations were made by http://dx.doi.org/10.1038/nclimate2899 http://dx.doi.org/10.5194/tc-9-2163-2015 and doi: 10.1017/aog.2016.2 The output of a firn model forced by HIRHAM RCM is presented here: https://doi.org/10.3389/feart.2016.00110 and another model forced by RACMO is presented here: https://doi.org/10.3389/feart.2017.00003 and https://doi.org/10.5194/tc-11-2507-2017. Please compare forcing and model results.

We address the issue of climatic forcing and further use of observations in our answers to your general comments. Please note that we use here the drilled KAN-U core provided by one of your suggested references (Machguth et al., 2016).
Thank you for highlighting the absence of comparison with previous modelling studies. We now compare the results of this study to the ones of the references you mention (Langen et al., 2017; Steger et al., 2017b) in the Discussion section.

p.16 l.33 Why stopping in 2013?

Drilled cores at KAN-U show that the site turned to bare ice after 2013, thus with almost no remaining firn layer. This study focuses on the simulation of water flow in firn and bare ice conditions are irrelevant for this because of the absence of downward percolation. Therefore, we stop the simulation in 2013.

p.16 l.33 Does that mean that this is ablation area?

The RCM simulated climate indeed indicates that the KAN-U site is turning into ablation area over the recent years. This is further confirmed by drilled cores (see previous answer).

p.17 l.16 Mention the role of runoff in this case.

We proceeded to the modification suggested.

p.18 l.5 It could also increase the structural strength of the firn.

It is true that higher densities cause stronger firn and thus decreased densification rates. However, when the impermeability threshold is increased from 810 to 830 kg m^{-3}, the increased strength of the simulated ice layers does not lead to a FAC decrease. Indeed, all other things being equal, a layer at 810 kg m^{-3} in an ip810 simulation will further densify faster than a layer at 830 kg m^{-3} in an ip830 simulation. But this faster densification only occurs because the density is lower (and thus the strength decreased) and the result is that the FAC contribution of that particular layer will always remain higher in the ip810 simulation. On the contrary, the higher load exerted by the denser layer of the ip830 simulation on the firn below will cause faster densification and thus decreased FAC in the ip830 simulation.

p.19 l.18 Please give the observed value.

The observed value is already given in p.19 l.15. If you think it is necessary to repeat this value, we would proceed to this adjustment.

p.21 l.11 Meaning bare ice during the summer or ablation area.

This means bare ice in summer indeed. However, it is not necessarily ablation area because the internal accumulation component of the Surface Mass Balance must be accounted for. In this particular case, it is important because a lot of meltwater refreezes locally in the firn column (see Table 5) and this keeps total accumulation above ablation.

p.21 l.15 Why is runoff combined with refreezing here? A more interesting comparison would be solid input + refreezing (mass gain) compared to runoff (mass loss). This would be another formulation of the surface mass balance.

Here we only use this additional statement to provide an explanation to the reader of why the sinks of liquid water (refreezing and runoff) exceed the sources of liquid water (surface melt and rain), which violates mass conservation if one looks only at a single year. We do not combine runoff and refreezing for assessing any other variable and we agree with your statement of Surface Mass Balance quantification. However, we think that the manuscript is already long and so we do not provide this detailed quantification of annual Surface Mass Balance.

p.21 l.15 Maybe split this sentence.
We proceeded to the modification suggested.

p.21 l.19 The difference between R1M and DPM as well as the sensitivity of DPM to its internal parameters was discussed in Wever et al. 2016. Please compare your results to their work on alpine snowpack. Do you see the same patterns? Did they see for example the sensitivity of DPM to the grain size formulation?

In their study, Wever et al. (2016) also showed the greater ability of DPM to produce ice layers than R1M. We added this valuable comparison in the Discussion section. However, Wever et al. (2016) only tested the sensitivity of their model to their tuning parameters Θ and N, that we keep constant in this study (see Sect. 3.3 and Sect. 4). They did not try different grain-size formulations and it is thus impossible to know if they have noticed an important sensitivity of the flow schemes to grain-size, as we do in this study.

p.21 l.20 Here "greater retention" seem to contradict with favored lateral runoff. Please clarify.

Indeed the term “greater retention” is confusing and inappropriate. We replaced it by “slower downward percolation”.

p.21 l.25 I believe "biases" cannot be hot or cold. Please rephrase.

We proceeded to a rephrasing as demanded.

p.21 l.28 This is quite surprising when the BK wh02 was made to mimic piping processes and R1M is supposed to ignore it. Please discuss.

We modified Sect. 5 in the manuscript to discuss more the agreement between R1M and BK and what this implies for situations in which BK is tuned to mimic preferential flow.

p.22 l.23 Due to the impermeability threshold, the ice density in the model is very low (max. 830 kg/m3 vs. ~900kg/m3 at KAN_U and vs. 917kg/m3 in the FAC calculation). This skews completely the comparison of FAC. Here DPM gives the same FAC as the firn cores in spite of simulating completely saturated firn below 2.5 m.

We agree with your comment and so have removed this section from the revised version of the manuscript.

p.23 l.13 Can your experiment tell anything about what should be developed/improved in the DPM ?

We think indeed that our study provides some insights of which aspects of DPM should be improved. We modified the manuscript to highlight these more clearly by summarizing the three main shortfalls of DPM. Note that these modifications are made further in the Discussion section:
We highlight (1) that too much water is transported through preferential flow or at exaggerated depths as demonstrated by the consistent overestimation of 10 m temperature, (2) the need to consider lateral flow as the tendency to underestimate FAC shows and (3) the large sensitivity of the ice layer formation process to grain size, which should be overcome or should be addressed by further observational studies of grain metamorphism in firn.

p.23 l.14 I do not understand why the presented biases may be related to a sensitivity of the model to temperature. Could you specify?

We argue that the densification models are not well suited for conditions where the refreezing of meltwater causes latent heat release and thus higher firn temperatures. We think that these high temperatures cause overestimated densification rates as has been pointed out in previous studies (e.g. Steger et al., 2017a). We modified the manuscript to clarify this point.

p.23 l.29 Maybe "water flow" ?
We proceeded to the modification suggested.

p.24 l.21 Be more specific here, there has been work in Greenland and elsewhere about the spatial heterogeneity in firn (and in FAC). One source could be doi: 10.1017/jog.2016.118

We modified the manuscript to emphasize that observational constrains of firn structure are affected by strong spatial variability and we cite the reference you suggested.

p.25 l.23 Rephrase. It deteriorates the performance of the model or "explains the mismatch". But the validation (the act of validating) in itself is always possible.

The validation is affected by the fact that the liquid water scheme is far from being the only component of the firn model to influence depth-density profiles. Thus there are many sources of uncertainty at play and the problem of compensating errors can arise. Continuous measurements of liquid water content would provide a more direct way to validate liquid water schemes, but such measurements are not available. We modified the manuscript to clarify this point.

p.25 l.25 Be specific. You have identified some crucial but unconstrained parameters such as grain size. Or are you referring to processes not yet explored? The second half of this sentence is also very redundant with the firt part.

We modified the manuscript to identify more clearly the poorly constrained complexities affecting the flow scheme. We split the sentence in two separate sentences. The second part of the statement is meant to identify the processes not immediately related to the flow scheme that must be better represented to reach more accurate modelled firn densities in the percolation area. We hope that the rephrasing helps clarify all of this.

p.26 l.6 Please give websites for PROMICE and DOI for SUMup.

We proceeded to the modifications requested.

p.27 l.12 1 m w.eq. I guess?

The variable is the volumetric water content. Thus it is the ratio between the amount of water (in m w.e.) in a layer and the thickness of the layer (regardless of the density of the layer).

p.27 l.17 It seems that this minimum liquid water for refreezing is supposed to solve the same issue (necessary residual water in all layers) as eq. 19. How do these two steps work together?

Indeed, this 0.01 % value and the adjustment of θ_r have the same numerical purpose: the effective saturation of any layer cannot reach zero. However, they influence different processes: θ_r influences flow rates and the 0.01 % value influences refreezing rates. The restriction on refreezing rates comes into play only once θ falls below 10^{-4} (0.01 %), whereas the adjustment of θ_r is required as soon as θ approaches 0.02. Please note that the amounts of refreezing that are omitted due to this 0.01 % value would be a negligible fraction of the total refreezing in any of our simulation but is only required for numerical purposes.

p.27 l.18 Is time step meant here? Or step in the iterative solving of water movement?

Yes, time step is meant here. At any point in the solving of the RE, a layer cannot be completely dry. The artificial initialisation of all layers at θ_{dry} is executed only at the beginning of the flow routine and not at every iterative step. Therefore, the complete refreezing can only be applied at the end of the flow routine and not at the end of every iterative step. The latter case would lead to layers being dry when the next iterative step starts.

p.27 l.20 Here the convergence criteria is also used as a liquid water threshold for dry conditions. Maybe you could give different names to these variables even though they have the same value.

We replaced the use of ε_θ by its numerical value 10^{-5} as suggested (it is used only once, so we preferred not to define a new variable name).

Referee 3

We thank this reviewer for their compliments and feedback. Our response to these comments is below, the referees original text is given in red throughout and our response is in black.

General comments

1) Measured temperature was used for the validation of models. Simulated runoff was also discussed. However, figures for these results were not shown. Lack of figures sometimes makes difficult to understand in detail. In TC, authors can use a supplement file to show figures relatively less important. Therefore, figures of them should be added using a supplement to support the discussion in the main text (see minor comment P13 L22-28, P14 L14-15).

We thank you for this constructive suggestion. We have added in a Supplementary Information file the figures of the evolution of annual runoff and annual refreezing, showed with the annual fluxes of meltwater as a basis of comparison. This can indeed help the reader to have a better overview of the evolution of these variables in time. We also added figures of the evolution of the modelled temperature profiles. This is especially valuable for highlighting how the use of different flow schemes affect the thermal properties of the modelled firn layer. As an example, it is easy for the reader to see how DPM tends to bring too much heat at great depths using figures S5 and S6. Please note that we did not add figures showing the differences between modelled temperature profiles and measured temperature profiles in time. Firstly, the evolution of the temperature in depth has not been measured systematically at all the sites tested. Also, our point of view, supported by Referee 1 and Referee 2, is that we should not expect a model configuration to reproduce precisely a point measurement for the following reasons: (i) the climatic forcing comes from a Regional Climate Model of 5.5 km horizontal resolution, (ii) firn properties show large spatial variability. We added more clarification about argument (ii) in the introduction of Sect. 4 and in Sect. 5 in the revised version of the manuscript. We use a comparison with the 10 m depth firn temperature because we think that this gives a good evaluation of the ability of the different models to reproduce the bulk thermal properties of the firn layer. However, we think that showing a detailed difference of the modelled and measured temperature in depth and in time may mislead the reader to think that the model is expected to reproduce observed values with great precision despite (i), (ii) and the many sources of additional uncertainty that we highlight in the manuscript.
Section 4: *Comparing the modelled FAC and 10 m depth temperature values with observed data depicts the ability of the tested models to reproduce the bulk condition of the upper firn column. We also qualitatively assess the degree to which the models to form a 'realistic' ice layer distribution and depth-density profile. One would not expect simulated values of either to match observations precisely given the high spatial variability of firn structure (Marchenko et al., 2017), but it is indicative of the models' performance in reproducing heterogeneity in firn density.*
Section 5: *On the other hand, comparisons between modelled and observed density profiles are strongly affected by the choice and accuracy of the densification formulation, the variability of surface density, several other factors influencing model outputs mentioned above and possible uncertainties in field measurements. Such uncertainties are related to the strong spatial variability of firn structure (Marchenko et al., 2017), which can be observed by comparing density profiles of cores drilled at nearby locations.*

2) The simulation in this paper was performed for four fields. Tables were provided for results in each field showing total or averaged simulated values. I would like to suggest that the author provide a table which shows the comprehensive result to see the difference between fields about simulation results (see minor comment in P19L5 and P22L26). This is not prerequisite for acceptance, but it will help to understand the overall result.

We have also added in the Supplementary Information file a table that summarizes the difference between measured and modelled values of each flow scheme at every site for the FAC15 and the 10 m temperature. We did not put the table in the main text of the manuscript because most of the values are already given in the Tables 2, 3, 4 and 5. We hope that this fulfils your request of a comprehensive table.

3) Although the main target of this study was the validation of liquid water infiltration model, density and temperature data were used instead of liquid water content for validation. It leads to the limitation of the validation itself. Discussion about the limitation because of this is also necessary.
The limitations of the validation process for firn percolation schemes is one of the challenges that our study highlights. Examples of such limitations are the unavailability of liquid water flow measurements in firn and the competing effects of other processes on the density profile (compaction, surface density, etc.). We modified the conclusion section in the revised manuscript in order to ensure this was adequately addressed:
There is no large scale detailed observation available of liquid water content and percolation pattern during melting events in firn. This renders the validation of a particular flow scheme difficult and validation relies on temperature and density profiles. However, there are a number of effects that influence firn density and temperature, all potentially contributing to mismatch between modelled and observed values.

4) This simulation study can provide several suggestions for a laboratory experiment and field observation required to improve the model. Although limitations are written in conclusion, detailed discussion about limitation and suggestion of new experiment and observation (e.g. liquid water infiltration experiment into firn or observation of liquid water.) will be informative for future research.

Our study tries to outline the limitations of current liquid water flow scheme when applied within firn models. We have additionally modified the revised version of the manuscript in order to provide a detailed summary of the shortcomings of DPM in the Discussion section. We hope that our findings could help laboratory and field researchers to design experiments that would address the numerous uncertainties highlighted throughout the article. We leave it up to these specialists to identify the experiments that would best address these limitations as this is beyond our area of expertise.
Section 5: *We highlight (1) that too much water is transported through preferential flow or at exaggerated depths as demonstrated by the consistent overestimation of 10 m temperature, (2) the need to consider lateral flow as the tendency to underestimate FAC shows and (3) the large sensitivity of the ice layer formation process to grain size, which should be overcome or should be addressed by further observational studies of grain metamorphism in firn.*

Specific comments

P8 L26-27 In this sentence and Eq. (17), the saturated water content was estimated as i/w (0.917?) of pore space. It seems to be used for convenience in calculation. Yamaguchi et al. (2010) obtained the saturated water content was about 90% of pore space in their gravity drainage column experiment. Although they are coincidence, this paper had better be referred to show that the assumption in Eq. (17) is consistent.

Our approach in this study has been to implement the DPM flow scheme following the SNOWPACK dual permeability water scheme with the greatest fidelity possible. Because the SNOWPACK scheme uses that correction for the saturation, we have decided to implement the same. Indeed, this correction for saturated water content is in good agreement with the findings of Yamaguchi et al. (2010). We mention this in the revised form of the manuscript as you suggested and we also refer to the laboratory study of Yamaguchi et al. (2010).

P13 L22-28 Figures for simulated runoff had better to be shown in a supplement.

As we explained in the answer to your major comment 1), these figures have been added to a Supplementary Information file.

P14 L14-15 Comparison between observation and simulation of temperature also needs a figure in a supplement.

This point has also been addressed in the answer to your major comment 1).

P17 L18-30 In terms of average value, DPM had a good agreement. However, the simulated result of DPM was a constant value for vertical and maximum density was underestimated. In my opinion, the depiction "good agreement" feels not suitable (depiction "average density is reasonable" may be OK). The state of this result had better be that present liquid water infiltration scheme has limitation and requires future improvement.

We proceeded to the suggested modification.

P19L5 Here, densification model had a larger effect than water infiltration model. Is this trend only this place or common for all four places? Comprehensive table comparing between fields about this will help to check this question. (This is suggested in major comments.)

We have also added in the Supplementary Information a table that summarizes the difference between measured and modelled values of each densification scheme at every site for the FAC15 and the 10 m temperature. By comparing the values of both tables that have been added in the Supplementary Information, the reader can have a good overview of the respective effect of the choice of the water schemes and of the choice of the densification model.

Please note also that we address the great variability at all sites due to the densification scheme used in the Discussion and Conclusion sections. To emphasize this more, we added in the Discussion section a mention to the need for more firn models intercomparison experiments.

P20 L27 L31 Fig8f? Recheck the figure number
This was a typo in the first version of the paper. Thank you for pointing this out.

P22 L7-9 Is it mean that the simulation using BK and R1M were performed by CROCUS whereas DPM was performed by SNOWPACK? If so, the difference in results receives the effect of the difference of numerical snowpack model. Did authors check the difference of them performing a simulation with the same water infiltration scheme? SNOWPACK has Bucket and RE scheme comparable with BK and R1M, respectively.

This is not the case. All water schemes were always used with the same densification model (CROCUS for the sites DYE-2, NASA-SE and KAN-U, HL for the FA13 site as explained in the text). This was indeed to avoid differences in results to arise from the use of different firn densification models. The DPM water scheme implemented in the firn model is a reproduction of the dual permeability water scheme that was implemented in SNOWPACK by Wever et al. (2016). What we explain in this paragraph is that a simulation performed by the full SNOWPACK model would be different from our simulations because SNOWPACK has different physics for densification and grain growth for example (which have not been implemented in the firn model). We modified the revised version of the manuscript in order to clarify this.

P22 L26 This results seems that the DPM is not suitable for this place (actually, improvement is necessary for preferential flow scheme). As discussed in P17 L4-8, BK and R1M reproduce surface ponding and refreeze. If a suitable model is different depending on the field, the most suitable scheme had better be shown for each field. Comprehensive table suggested in a major comment is useful to show a comparison between fields.

This results suggests indeed that the current form of DPM is not suitable for the conditions at KAN-U. We attached great importance throughout the entire study to show the performances of each of the flow schemes (BK, R1M, DPM) at the four different sites and not to systematically pick the water scheme that gave results in closest agreement with observations. This is because the aim of this study is to give a first overview of the performance of physically based water schemes of snow models (R1M and DPM) when applied in firn models and to compare these with the common bucket scheme (BK). We do not argue about whether a particular model is better than the other and we try to provide some ways of improvements for further development of water flow schemes in firn models. By highlighting the deficiencies of DPM, we also hope to orientate future modelling efforts. We hope that the tables added in the Supplementary Information satisfy your requests of comprehensive tables. Please, note also that this specific part of the Discussion section has been removed from the revised version of the manuscript. In accordance with the point of view of other referees, we deemed it too speculative.

Development of physically based liquid water schemes for Greenland firn-densification models

Vincent Verjans[1], Amber Leeson[2], C. Max Stevens[3], Michael MacFerrin[4], Brice Noël[5] and Michiel R. van den Broeke[5]

[1] Lancaster Environment Centre, Lancaster University, Lancaster, LA1 4YW, UK.
[2] Lancaster Environment Centre / Data Science Institute, Lancaster University, Lancaster, LA1 4YW, UK
[3] Department of Earth and Space Sciences, University of Washington, Seattle, WA, USA
[4] Cooperative Institute for Research in Environmental Sciences, University of Colorado, Boulder, CO USA
[5] Institute for Marine and Atmospheric research Utrecht, Utrecht University, Utrecht, the Netherlands

Correspondence to: Vincent Verjans (v.verjans@lancaster.ac.uk)

Abstract.

As surface melt is increasing (+11.4 Gt yr^{-2}) on the Greenland ice sheet (GrIS), quantifying the retention capacity of the firn layer is critical to link meltwater production to meltwater runoff. Firn-densification models have so far relied on empirical approaches to account for the percolation-refreezing process, and more physically based representations of liquid water flow might ~~therefore~~ bring improvements to model performance. Here we implement three types of water percolation schemes into the Community Firn Model: the ~~tipping~~ bucket approach, the Richards Equation in a single-domain and the Richards Equation in a dual-domain, which accounts for partitioning between matrix and fast preferential flow. We investigate their impact on firn densification at four locations on the GrIS and compare model results with observations. We find that for all of the flow schemes, significant discrepancies remain with respect to observed firn density, particularly the density variability in depth, and that inter-model differences are large (porosity of the upper 15 m firn varies by up to 47 %).~~.~~ The simple bucket scheme is as efficient in replicating observed density profiles as the single-domain Richards Equation and the~~. The~~ most physically detailed dual-domain scheme does not necessarily reach best agreement with observed data. However, we find that the implementation of preferential flow does allow for more frequent ice layer formation and for deeper percolation. We also find that the firn model is more sensitive to the choice of densification scheme than to the choice of water percolation scheme. The disagreements with observations and the spread in model results demonstrate that progress towards an accurate description of water flow in firn is necessary. The numerous uncertainties about~~surrounding~~ firn ~~micro- and macro-~~structure (e.g. grain size and shape, presence of ice layers) and about~~,~~ its hydraulic properties, as well as~~and~~ the one dimensionality of firn models render the implementation of physically based percolation schemes difficult. Additionally, the performance~~An improved understanding~~ of ~~the parameters affecting evolution of polar~~ firn models is still affected by~~, of~~ the various effects affecting ~~of the climatic forcing on~~ the densification process such as microstructural effects, wet snow metamorphism and temperature sensitivity when meltwater is present. ~~more accurate treatment of liquid water would benefit further developments.~~

1 Introduction

Estimating the properties of the firn layer – and how it evolves under a warming climate – is a critical step in measuring the ice sheets' contribution to sea level rise, yet it remains one of the key sources of uncertainty in present assessments (McMillan et al., 2016). Accurate estimates of firn thickness and density are required for the conversion of space-borne measurements of volume change into mass change (e.g. McMillan et al., 2016; Shepherd et al., 2018). Also, assessments of the Greenland and Antarctic ice sheets' contribution to sea level require information on firn density and spatial distribution in order to calculate meltwater retention potential and the capacity of firn to buffer the flow of meltwater to the ocean (Harper et al., 2012; Machguth et al., 2016; van den Broeke et al., 2016). Surface melting has become more widespread and intense on the Greenland Ice Sheet (GrIS), with annual total melt rates rising by 11.4 Gt yr^{-2} between 1991 and 2015 (van Angelen et al., 2014; van den Broeke et al., 2016). ~~Most of this increase in melting has occurred in the percolation zone, where a firn layer is present year-round.~~ This melt water percolates into the firn layer, where it can refreeze, run off, or remain liquid in temperate firn. Refreezing of liquid water in firn, known as internal accumulation, has an impact both on ice-sheet mass balance and on heat fluxes from the surface to the ice sheet (van Pelt et al., 2012). As such, understanding physical processes in firn, including in particular the transport of liquid water, is becoming increasingly important in order to accurately constrain and predict the mass balance of the GrIS (van den Broeke et al., 2016).

Densification of dry firn is typically modelled as a function of near-surface air temperature and accumulation (Herron and Langway, 1980; Arthern et al., 2010; Li and Zwally, 2011; Simonsen et al., 2013; Morris and Wingham, 2014; Kuipers Munneke et al., 2015a,b). If applied to wet firn, these models are often modified to include a simplified representation of liquid water percolation, the bucket~~'tipping bucket'~~ scheme, which assumes flow and refreezing through the firn column occur in a single time step (Simonsen et al., 2013; Kuipers Munneke et al., 2015b; Steger et al., 2017a). Observations have shown that, in reality~~(Simonsen et al., 2013; Kuipers Munneke et al., 2015b; Steger et al., 2017). Observations have shown that, in actuality~~, liquid water transport in firn is characterised by flow patterns that are heterogeneous in space and time (Pfeffer and Humphrey, 1996; Humphrey et al., 2012). Incorporation of liquid water schemes representing such flow patterns would enable~~-~~ models to better represent the transport of mass and heat through the firn; these schemes might also improve modelled densification in wet firn conditions (Kuipers Munneke et al., 2014; van As et al., 2016; Meyer and Hewitt, 2017).~~(Kuipers Munneke et al., 2014; van As et al., 2016).~~ Liquid water flow however, is a complex function of several properties and processes that are difficult to constrain by observations and, as a corollary, are difficult to represent in these models (e.g. presence of impermeable ice layers, snow hydraulic properties, grain-size, lateral runoff). The infiltration of water through firn can be partitioned between the progressive advance of a uniform wetting front through the pores~~porosity~~, called matrix flow, and fast, localised, preferential flow (Waldner et al., 2004; Katsushima et al., 2013). This dual-nature of water flow has been reported in observations of the firn layer of the GrIS, where preferential flow pathways come in the form of discrete vertical conduits and are crucial to effectively transport surface meltwater in deep subfreezing firn (Pfeffer and Humphrey, 1996; Parry et al., 2007;

Humphrey et al., 2012; Cox et al., 2015). The detection of Perennial Firn Aquifers (PFA), in which large amounts (140 Gt) of liquid water is stored year round in deep firn, further emphasises the importance of firn hydrology on the GrIS mass balance (Forster et al., 2014; Koenig et al., 2014).~~(Forster et al., 2014; Koenig et al., 2014).~~ Snow modellers~~models~~ have developed liquid water schemes based on the Richards Equation (RE) to simulate matrix flow (Hirashima et al., 2010; Wever et al., 2014; D'Amboise et al., 2017). The RE is a continuity equation describing water flow in unsaturated porous media and is widely used in hydrological models. Recently, a preferential flow scheme has been included in the SNOWPACK model to account for heterogeneous percolation (Wever et al., 2016). Until now however, such developments have not been implemented in~~translated into~~ firn-densification models.

In this study, we describe and compare liquid water schemes of different levels of physical complexity from snow models, and we apply these in combination with firn-densification models in order to evaluate the impact of the treatment of liquid water flow on modelled firn densification and temperature. We use the Community Firn Model (CFM) as the modelling framework for our study; the CFM is able to simulate numerous physical processes in firn and includes a large choice of governing formulations for densification. We use the common~~ tipping~~ bucket approach and also develop schemes for liquid water flow in firn following physically based advances in snow models (Wever et al., 2014, 2016; D'Amboise et al., 2017).
We simulate liquid water flow and firn densification starting from 1980 at four sites on the GrIS: DYE-2, NASA-SE, KAN-U and a PFA site (Fig. 1). These sites were chosen because they are collocated with recently drilled firn cores which allow a direct comparison of model results with observations. By comparing simulated firn densification to observations at these sites, we investigate the sensitivity of the system to the choice of liquid water flow scheme and the sensitivity of the flow schemes to various parameterisations of firn structural properties. Finally, we perform simulations with a range of firn-densification formulae and assess the relative importance of the choice of liquid water flow scheme to the choice of the underlying densification equation.

2 Firn Model and Data

In this study we use and further develop the CFM, an open-source firn-densification modelling framework. We refer the reader to Stevens (2018) for details and briefly summarise the main characteristics here. The CFM is one-dimensional and works in a Lagrangian framework; it is forced at its upper boundary by observed or modelled values for accumulation, surface temperature, surface density, rain, and snow melt. The CFM includes many of the commonly used dry firn-densification schemes (e.g. Herron and Langway, 1980; Helsen et al., 2008; Arthern et al., 2010; Li and Zwally, 2011; Morris and Wingham, 2014; Kuipers Munneke et al., 2015b). We refer the reader to the original publications for details on the different densification schemes and briefly outline the expressions used in our simulations in this section.

2.1 Dry firn-densification model

As a base case, we use the firn-densification~~-~~ formulation implemented in the snow model CROCUS (Vionnet et al., 2012), Eq. (1). It has previously been used in model studies of firn densification on the GrIS and also on polar ice caps (Gascon et al., 2014; Langen et al., 2017). This model is formulated so that densification is based on the overburden stress:

$$\frac{d\rho}{dt} = \rho\,\frac{\sigma}{\eta} \qquad (1)$$

where ρ is the density of the firn (kg m^{-3}), σ is the stress due to weight of the upper layers (kg m^{-1} s^{-2}) and η is the snow viscosity (kg m^{-1} s^{-1}) following the parameterisation:

$$\eta = f_1 f_2 \eta_0 \frac{\rho}{c_\eta} \exp\left[a_\eta (T_0 - T) + b_\eta \rho\right] \cancel{\left[a_\eta (273.15 - T) + b_\eta \rho\right]} \qquad (2)$$

where η_0 = 7.62237 kg s^{-1} m^{-1}, a_η = 0.1 K^{-1}, b_η= 0.023 m^3 kg^{-1}~~, and~~ T is the firn temperature (K) and T_0 = 273.15 K.~~).~~ The parameter c_η is set to 358 kg m^{-3} as suggested by van Kampenhout et al. (2017) when using Eq. (1) for polar firn. There are two additional correction factors, f_1 and f_2 , depending on firn microstructural properties. The factor f_1 accounts for the presence of liquid water:

$$f_1 = \frac{1}{1+60\,\theta} \qquad (3)$$

where θ is the volumetric water content (m^3 m^{-3}). In this study, we neglect the change in snow viscosity for grain-sizes smaller than 0.3 mm by keeping the constant value f_2 = 4 (after Langen et al., 2017; van Kampenhout et al., 2017).

Several firn-densification equations have been derived and calibrated for the GrIS specifically. We favoured the use of Eq. (1) as our base case because (i) most of these calibrated schemes were developed for dry firn densification whereas the CROCUS formulation accounts for the presence of liquid water explicitly, (ii) applying a percolation scheme in a stress-based densification model rather than in an accumulation-rate-based model ensures that the redistribution of mass associated with percolation will affect the densification appropriately and (iii) the CROCUS densification scheme is currently used by the regional climate model MAR and by the Earth System Model CESM to quantify firn densification on the GrIS (Fettweis et al., 2017; van Kampenhout et al., 2017)~~(Fettweis et al., 2017; van Kampenhout et al., 2017)~~.

2.2 Climatic forcing

To force the model at its upper boundary we use three-hourly skin temperature, melt, snowfall, rain and sublimation fields simulated by the latest version of the RACMO2 regional climate model (RACMO2.3p2, Noël et al., 2018). This model has a 5.5 km horizontal resolution grid and has been explicitly adapted for use over the polar ice sheets. We refer to Noël et al. (2018) for a detailed discussion about the performance of RACMO2.3p2 on GrIS and related uncertainties. Additionally, Ligtenberg et al. (2018) have demonstrated the impact of recent developments in RACMO2.3p2 on firn modelling, mostly yielding improvements in modelled densification.

If the solid input rate (snowfall – sublimation) is negative over a time step, the CFM treats it as~~by~~ a corresponding mass loss in~~for~~ the surface layer;~~, and~~ liquid water is evaporated before solid mass gets sublimated. The temperature of a newly accumulated snow layer is defined as the skin temperature at that time step. Deep temperatures in the model are thus mostly determined by the mean surface temperature applied during the spin-up process (Sect. 2.5) together with latent heat release through refreezing. We use a Neumann boundary condition for the temperature at the bottom of the domain and use a 250 m deep column to account for the large thermal mass of the ice sheet during the transient run.

In addition to latent heat release due to refreezing, the CFM accounts for heat conduction through the different layers to determine the temperature profile. In accordance with previous firn modelling studies (Kuipers Munneke et al., 2015a; Steger et al., 2017a), we make the firn conductivity, k_s, ~~(Kuipers Munneke et al., 2015a; Steger et al., 2017), we make the firn conductivity,~~ $\cancel{k_s,}$ a function of density following Anderson (1976):

$$k_s = 0.021 + 2.5\left(\frac{\rho}{1000}\right)^2 \quad (4)$$

Another boundary condition is the density of every fresh snow layer deposited at the surface. To reduce the sources of possible uncertainties, we simply use a constant and site-specific surface density according to the surface value of the drilled firn cores instead of a parameterised formulation (see Sect. 2.4).~~.~~

2.3 Grain-size

The temporal evolution of grain-size in firn is poorly understood and observational constraints are scarce. However, the grain-size is a key variable for the RE, and the flow schemes used in this study thus require an initial grain-size and a grain-growth rate. For the former, we use the empirical formulation of Linow et al. (2012) derived from observations of snow samples from Antarctica and Greenland:

$$r_0 = \left(b_0 + b_1(T_{av} - T_0) + b_2\cancel{(T_{av} - 273.15) + b_2}\,\dot{b}\,\frac{\rho_i}{\rho_w}\right) \quad (5)$$

where~~Where~~ ρ_i is the ice density (917 kg m^{-3}), ρ_w that of liquid water (1000 kg m^{-3}), $\dot{b}$ is the mean annual accumulation rate (m w.e. yr^{-1}), T_{av} the mean annual surface temperature (K) and b_0, b_1 and b_2 are calibration parameters taking the values 0.781 m, 0.0085 m K^{-1} and -0.279 yr (m w.e.)$^{-1}$ respectively.

For grain growth rate, the relationship proposed by Katsushima et al. (2009) is applied:

$$\frac{dr}{dt} = \frac{1}{8\,r^2\,10^9}\,min\left[\frac{2}{\pi}\left(1.28\ 10^{-8} + 4.22\ 10^{-10}\left(\theta_{weight,\%}\right)^3\right), 6.9410^{-8}\right] \quad (6)$$

where r is the grain radius (m) and $\theta_{weight,\%}$ is the mass liquid water content expressed in percent and is thus related to θ (see Eq. (3)):

$$\theta_{weight,\%} = 100\,\frac{\theta\,\rho_w(\rho_i - \rho)}{\rho_i\,\rho} \quad (7)$$

Equation (6) combines a wet snow metamorphism formula and a higher limit of growth rate of ice particles, both derived from laboratory measurements.

To study the sensitivity of the model to the grain-size implementation, we also use an alternative option based on the approach for West-Antarctic firn of Arthern et al. (2010);~~:~~ the grain radius in newly deposited layers (r_0) has the constant value of 0.1 mm and the grain growth rate is formulated as:

$$\frac{dr}{dt} = \frac{1}{2\,r}\, k_g \exp\left(\frac{-E_g}{RT}\right) \cancel{exp\left(\frac{-E_g}{R\,T}\right)} \qquad (8)$$

where E_g is the activation energy for grain growth (42.4 kJ mol^{-1}), R is the gas constant (8.314 J mol^{-1} K^{-1}) and ~~-~~k_g a parameter that takes the value 1.3 10^{-7} m^2 s^{-1}. Note that Eq. (8) does not take the impact of liquid water presence on firn metamorphism into account.

2.4 Study sites

We perform ~~model~~ simulations at four study sites in~~of~~ the percolation zone of the GrIS: NASA-SE, DYE-2, KAN-U and FA13 (perennial Firn Aquifer) (Fig. 1). The sites have different climatic conditions (Figs. 1 and 2) and well-documented firn cores are available here, which we use in order to assess the performance of the different flow schemes. NASA-SE (66.48ºN, 42.50ºW, 2372 m a.s.l.) is located in the upper part of the percolation zone with a mean annual temperature of -20°C and relatively low melt rates (50 mm yr^{-1}). DYE-2 (66.48ºN, 46.28ºW, 2126 m a.s.l.) is a slightly warmer site (T_{av} = -18°C), and melt is about three times greater than at NASA-SE (150 mm yr^{-1}). KAN-U (67.00ºN, 47.03ºW, 1838 m a.s.l.) is near the equilibrium line altitude and has warmer temperatures (T_{av} = -8°C) and significant melting (280 mm yr^{-1}). FA13 (66.18ºN, 39.04ºW, 1563 m a.s.l., T_{av} = -13°C) is a location known to contain~~where~~ a firn aquifer ~~has been recently discovered~~ (Foster et al., 2014). The persistence of deep saturated layers year round is due to the coupling of high melt rates (587 mm w.e. yr^{-1}) with high accumulation rates (1002 mm w.e. yr^{-1}) (Kuipers Munneke et al., 2014). We perform transient firn-model simulations for each site until the date that a core was drilled. The cores at NASA-SE and DYE-2 were drilled in spring of the years 2016 and 2017 respectively, as part of the FirnCover project. The cores at KAN-U (Machguth et al., 2016) and at FA13 (Koenig et al., 2014) were drilled in spring 2013. The firn temperature measurements were given in the sources mentioned for the density data, except at KAN-U for which it comes from the PROMICE dataset. The fixed surface densities for DYE-2, NASA-SE, KAN-U and FA13 are 325, 240, 325 and 365 kg m^{-3} respectively and were taken in accordance with the surface density of the drilled cores.

2.5 Spin-up and domain definition

In order to simulate the evolution of the firn layer in time, we start the transient simulation from an initial state in equilibrium with a reference climate. In accordance with previous GrIS firn studies (Kuipers Munneke et al., 2015b; Steger et al., 2017a), we take the 1960-1979 climate as reference climate because it predates the onset of the general warming of Greenland and the subsequent increase in surface melt.~~(Kuipers Munneke et al., 2015b; Steger et al., 2017), we take the 1960-1979 climate as reference climate because it predates the onset of the general warming of Greenland and the subsequent increase in surface melt.~~ We iterate over the reference climate until 70 m w.e. of snow has been accumulated, which ensures the entire firn column is refreshed. The number of iterations over the reference climate is thus site-specific. This spin-up process starts from an analytical solution for the density profile (Herron and Langway, 1980) with temperatures corrected to account for latent heat release by refreezing (Reeh, 2008). During the spin-up process we use the simple~~ percolation~~ bucket approach, and the more advanced flow schemes, detailed in the next section, are turned on only at the end of the spin-up for the transient simulation. This is because using the advanced schemes over long periods is computationally expensive. The domain on which the flow calculations are applied is a subset of the entire CFM domain; this sub-domain is defined each time the flow routine is called in the transient run. The bottom of the sub-domain is defined as the depth below~~from~~ which all layers have~~firn~~ density higher than~~does not reach values below~~ the pore close-off value (830 kg m^{-3}), because infiltration of liquid water becomes negligible at this point. The thickness of the layers deposited in every three hourly time step determines the vertical resolution, and we apply a merging process only to individual layers less than 2 cm thick (see Supplementary Material S1.8~~Appendix A8~~).

3 Liquid water schemes

The water flow schemes are added to the dry-densification model detailed in Sect. 2.1 and are thus also effectively one-dimensional, representing no lateral exchange of heat and mass although lateral runoff is used as a mass sink. In this section, we present the three different flow schemes that we implement in the CFM: (1) the Bucket method (BK), (2) a single-domain Richards Equation scheme (R1M) and (3) a dual-permeability Richards Equation scheme (DPM). Because of its robustness and ease of implementation, BK is the current 'state-of-the-art' in firn-densification models that are interactively coupled to regional climate models. R1M is used in several stand-alone snow models to describe water flow (Hirashima et al., 2010; Wever et al., 2014; D'Amboise et al., 2017), and DPM is entirely based on the scheme implemented in the snow model SNOWPACK (Wever et al., 2016), where dual-permeability means that separate domains for matrix flow and preferential flow coexist with liquid water exchanged between these domains.

3.1 Bucket model

The bucket~~'tipping bucket'~~ percolation scheme is commonly used to account for the vertical transport of meltwater in firn models, though the precise form of its implementation is variable. Each layer in the model can refreeze meltwater according to its 'cold content', i.e. the energy required to raise the temperature of the layer to the melting point. Starting from the surface, the meltwater may percolate through successive layers, thus allowing for refreezing at depth. Meltwater is progressively depleted due to refreezing and retention according to each layers' water-holding capacity, which is the part of the water that is stored in some of the available pore space and not subject to vertical transfer. The water-holding capacity acts as an approximation of the effect of capillary forces on water retention. Percolation proceeds until all the meltwater is stored (refrozen or retained) or until it reaches a layer with a density exceeding the impermeability threshold (780-830 kg m^{-3}), at which point all the water in excess is instantly treated as lateral runoff~~ is assumed~~. The BK thus requires two parameters: the water-holding capacity and the impermeability threshold. We test two possibilities for the former and three for the latter. The water-holding capacity can be prescribed by the calculations of Coléou and Lesaffre (1998) for the mass proportion of water in a firn layer, W_w:

$$W_w = 0.057\ \frac{\rho_i - \rho}{\rho} \tag{9}$$

This mass proportion is then converted to the water-holding capacity, θ_h:

$$\theta_h = \frac{W_w}{(1-W_w)}\ \frac{\rho\,\rho_i}{\rho_w(\rho_i - \rho)} \tag{10}$$

Using constant values of the water-holding capacity is also common practice (Reijmer et al., 2012; Steger et al., 2017a).~~(Reijmer et al., 2012; Steger et al., 2017).~~ Our base case scenario uses a fixed θ_h at 0.02, or 2% of the pore space available for liquid water retention. This low value assumes effective downward percolation and is meant to account for vertical preferential flow (Reijmer et al., 2012). For that reason, we consider this as a good basis for comparison with the DPM that explicitly accounts for such ~~vertical preferential~~ flow.

We test three values for the impermeability threshold; these were selected in accordance with Gregory et al. (2014), who tested firn permeability of Antarctic samples in a lab and reported that impermeability can occur over density values ranging from 780 kg m^{-3} to 840 kg m^{-3}. We thus take our three test values to be 780 kg m^{-3}, 810 kg m^{-3} and 830 kg m^{-3}, respectively the lower bound and middle of this range and a commonly-used value of pore close-off density.

3.2 Richards Equation

Vertical movement of water in a variably saturated porous medium can be described by the one-dimensional version of the RE:

$$\frac{\partial\theta}{\partial t} - \frac{\partial}{\partial z}\left[K(\theta)\left(\frac{\partial h}{\partial z} + 1\right)\right] = 0 \tag{11}$$

where K is the hydraulic conductivity (m s^{-1}), h is the pressure head (m),~~) and~~ z is the vertical coordinate (m, taken positive downwards) and θ is as defined in Eq. (3). The +1 term accounts for the effect of gravity. The RE is an equation expressing the mass conservation law and Darcy's law and it includes the 'suction head', i.e. the suction force exerted at the surface of individual grains.

A water-retention curve describes the relationship between θ and h required by Eq. (11). We use the van Genuchten (1980)~~We use the van Genuchten (1980)~~ model which is typically applied in studies of liquid water flow through snow (Jordan, 1995; Hirashima et al., 2014; Wever et al., 2014; D'Amboise et al., 2017):

$$\theta = \theta_r + (\theta_{sat} - \theta_r)\frac{(1+(\alpha|h|^n)^{-m}}{Sc} \tag{12}$$

where θ_r is the residual water content (m^3 m^{-3}), θ_{sat} is the volumetric liquid water content at saturation (m^3 m^{-3}). Sc is a correction coefficient following Wever et al. (2014). The parameters α, n and m are tuning~~fit~~ coefficients, with α being related to the maximum pore size and n and m being related to the pore size distribution. These three parameters, referred to as the van Genuchten parameters, are specific to the modelled porous medium and for snow; a common approach is to use the parameterisation developed by Yamaguchi et al. (2012) in a laboratory study:

$$\alpha = 4.4\ 10^{6} \cancel{*\ 10^{6}} \left(\frac{\rho}{2r}\right)^{-0.98} \tag{13}$$

$$n = 1 + 2.7\ 10^{-3} \cancel{*\ 10^{-3}} \left(\frac{\rho}{2r}\right)^{0.61} \tag{14}$$

$$m = 1 - \frac{1}{n} \tag{15}$$

Yamaguchi et al. (2012) measured the water-retention curve for a range of grain radii (0.025 to 2.9 mm) and densities (361 to 636 kg m^{-3}) in different snow samples by using a gravity drainage column method.

The porosity is the part of the volume not occupied by the solid matrix and, in the case of firn, is defined as:

$$P = 1 - \frac{\rho}{\rho_i} \tag{16}$$

The volumetric liquid water content at saturation is proportional to the porosity (Wever et al., 2014):

$$\theta_{sat} = P\ \frac{\rho_i}{\rho_w} \tag{17}$$

Note that water is not assumed to fill the entire pore space in saturated conditions and the correction factor $\frac{\rho_i}{\rho_w}$ included in Eq. (17) accounts for the required space to allow the liquid water to freeze. It is reasonable to use this correction factor since Yamaguchi et al. (2010) found that trapped air still occupies 10 % of the porosity in saturated snow. ~~included in Eq. (17) accounts for the required space to allow the liquid water to freeze.~~

The parameter θ_{sat} thus represents the pore space available for liquid water and from there we can define the effective saturation as:

$$Se = \frac{\theta - \theta_r}{\theta_{sat} - \theta_r} \tag{18}$$

and Se must be bounded between 0 and 1. In completely dry layers, a zero effective saturation would lead to infinite values in the head pressure calculation and thus, we use a numerical adjustment to avoid this happening (see Supplementary Material S1.3).~~Appendix A3).~~ The residual water content θ_r is defined as the amount of liquid water that cannot be removed by gravity as it is held by capillary tension~~suction~~ at the surface of the solid grains. Following Yamaguchi et al. (2010), a constant value of θ_r = 0.02 can be taken but in case of refreezing, θ can approach zero and θ_r must be adjusted accordingly. We take θ_r following a piecewise function:

$$\theta_r = \min[0.02, 0.9\ \theta] \tag{19}$$

The numerical requirement of an effective saturation value strictly greater than zero causes the persistence of very low flow rates, even for liquid water contents close to the residual water content. Over long time periods, layers cannot hold any residual water content and eventually dry out under the effect of gravity. By taking the coefficient 0.9 in Eq. (19) instead of 0.75 used in snow models (Wever et al., 2014; D'Amboise et al., 2017), we partially reduce this effect because this lowers the effective saturation value Se for any value of volumetric water content θ approaching zero.

~~Another issue with the numerical requirement of an effective saturation value strictly superior to zero is that very low flow rates persist, even for liquid water contents close to the residual water content. Over long time periods, layers cannot hold any residual water content and eventually dry out under the effect of gravity, contrarily to BK. By taking the coefficient 0.9 in Eq. (19) instead of 0.75 used in snow models (Wever et al., 2014; D'Amboise et al., 2017), we partially reduce this effect.~~

The hydraulic conductivity ($K(\theta)$) is the ability of the fluid to flow through the porous medium under a certain hydraulic gradient dependent~~that depends~~ on pressure head and gravity. Thus, $K(\theta)$ depends on the effective saturation and on the properties of both the porous medium and the fluid; fluid flow is enhanced in highly saturated layers. The hydraulic conductivity is described by the van Genuchten-Mualem model (Mualem, 1976; van Genuchten, 1980)~~(Mualem, 1976; van Genuchten, 1980)~~:

$$K(\theta) = Ksat\, Se^{1/2} \left[1 - \left(1 - Se^{\frac{1}{m}}\right)^{m}\right]^2 \tag{20}$$

where $Ksat$ is the hydraulic conductivity in saturated conditions (Se = 1). For the case of water flow through snow, it has been inferred using three-dimensional images of the microstructure by Calonne et al. (2012) as:

$$Ksat = 3.0\, r^2 \exp(-0.013\, \rho) \left(\frac{g\, \rho_w}{\mu}\right) \tag{21}$$

Where g is the gravitational acceleration (9.8 m s^{-2}) and μ is 0.001792 kg m^{-1} s^{-1}, the dynamic viscosity of liquid water at 273.15 K. Equation (21) shows that simulated water flow is faster in layers with coarser grains and lower densities. These conditions correspond to cases where the connectivity between the pore spaces is high. With respect to the hydraulic conductivity parameterisation, we additionally modify the permeability of ice layers. The hydraulic conductivity of any layer with density exceeding~~above~~ the impermeability threshold is set to zero, rendering it impermeable to incoming flow and leading to the ponding of water on top of that layer and subsequent enhancement of runoff rates (Sect. 3.4.2).~~it.~~ This RE implementation completely describes R1M and provides the basis of DPM, further detailed in the next section.

Details of the numerical implementations that are required to maintain stability and to improve computational efficiency for the RE calculations are discussed in the Supplementary Material~~Appendix~~.

3.3 Dual-permeability model

Physical models of preferential flow in snow are still scarce (Hirashima et al., 2014; Wever et al., 2016). In this section, we explain how the SNOWPACK dual-permeability model (Wever et al., 2016) is implemented in the CFM. The firn column is separated into two domains and~~;~~ water flow in both is governed by the RE (~~described in~~ Sect. 3.2)~~.~~. We define F as the pore space allocated to the preferential flow domain and accordingly 1-F as the pore space for the matrix flow domain. Wever et al. (2016) used a grain-size dependence for F, but their regression was performed on only four data points measured in idealised snow laboratory conditions (Katsushima et al., 2013). The experimental grain-sizes ranged from 0.1 to 0.8 mm and the water input from 480 to 550 mm per day, which is not representative of firn conditions in Greenland (Figs. 1 and 2). Moreover, due to the typical grain-size ranges in firn (Gow et al., 2004; Lyapustin et al., 2009)~~(Gow et al., 2004; Lyapustin et al., 2009)~~, the model would regularly be forced to use for F the minimal value for numerical stability implemented in SNOWPACK. To deal with this uncertain parameter but still retain fidelity with respect~~remain as close as possible~~ to the SNOWPACK implementation, we favour the use of a constant value based on observations in natural snow. Marsh and Woo (1984) and Williams et al. (2010) reported that rapid flow paths occupy respectively 22% and 5% to 30% of the area and we thus fix the value F = 0.2. The~~However, the~~ extension of the preferential flow area within the snowpack is very likely to be a function of grain-size and meltwater influx and~~, but even in laboratory conditions~~ these dependencies are~~must~~ still uncertain~~be investigated further~~ (Avanzi et al., 2016). The value of F thus determines the value of the saturated liquid water content θ_{sat} in both domains and instead of Eq. (17), we write:

$$\begin{cases} \theta_{sat,m} = (1-F)P\,\frac{\rho_i}{\rho_w} \\ \theta_{sat,p} = F\,P\,\frac{\rho_i}{\rho_w} \end{cases} \tag{22}$$

where from hereon~~now on~~, the subscripts m and p stand for matrix and preferential flow domain respectively. Equation (22) shows that the volumetric water content in the preferential flow domain is smaller than that in the matrix flow domain. All the input of meltwater is added to the matrix flow domain. For the regulation~~regulations~~ of the exchange~~exchanges~~ of water between~~ both~~ domains, we also closely follow the transfer processes of SNOWPACK (Wever et al., 2016) which are executed at the same 15-minute time step. We briefly summarize the transfer processes below.

Water from the matrix flow domain can enter the preferential flow domain of the layer below if the pressure head in the layer reaches the water entry suction, h_{we}, of the underlying layer. The parameter can be expressed as (Katsushima et al., 2013; Hirashima et al., 2014; Wever et al., 2016):

$$h_{we} = 0.0437(2r)^{-1} + 0.01074 \tag{23}$$

The amount of water transferred into the preferential flow domain equals the amount of water in excess of h_{we}. If after the transfer, Se in the matrix flow domain still exceeds Se in the preferential flow domain of the underlying layer, their respective Se are equalised by transferring the appropriate amount of water from the overlying matrix flow domain to the underlying preferential flow domain. In addition, in every individual firn layer where Se in the matrix flow domain exceeds Se in the preferential flow domain, matrix and preferential Se are equalised by transferring water from the matrix flow domain to the preferential flow domain. This serves to avoid the presence of horizontal pressure gradients in wet snow.

Water can flow from the preferential flow domain to the matrix domain by two processes. The first process is when the saturation in the preferential flow domain exceeds a threshold value Θ. Wever et al. (2016) determined Θ by tuning its value to best match observations. When this threshold is reached, the amount of water corresponding to the cold content of the layer flows back into the matrix domain. If there is still water in excess of the threshold in the preferential flow domain, saturation in both domains is set equal to one another. The second process simulates the heat flow from the preferential flow domain (at the melting point) to the colder surrounding matrix domain. Instead of transferring sensible heat, this process allows liquid water and its inherent latent heat to be exchanged to account for a theoretical heat flow, Q, and thus approximating Fourier's law:

$$Q = k_s \frac{(T-T_0)}{\left(\sqrt{\frac{1+F}{2\pi}}-\sqrt{\frac{F}{\pi}}\right)}\cancel{\frac{(T-273.15)}{\left(\sqrt{\frac{1+F}{2\pi}}-\sqrt{\frac{F}{\pi}}\right)}} \qquad (24)$$

This formulation assumes a linear horizontal temperature gradient in the matrix and a circular shape of the preferential flow path's perimeter. From Eq. (24), the corresponding water transfer is calculated as:

$$\Delta\theta_{p\rightarrow m} = \frac{2\,N\,\sqrt{\pi\,F}\,Q\,\Delta t_{15}}{L_f\,\rho_w} \qquad (25)$$

where Δt_{15} is the 15 minutes time step (s), L_f is the specific latent heat of fusion (335 500 J kg^{-1}) and N is a tuning parameter representing the number of preferential flow paths per square meter (m^{-2}). In their study, Wever et al. (2016) arrived at a best parameter set for Θ and N of 0.1 and 0 m^{-2} based on comparisons of ice-layer occurrence and runoff amounts with observations in alpine snowpacks. Note that the use of a null value for N is implausible in our case of firn-column simulations. Indeed, this would imply that liquid water would persist and flow deeper in the preferential flow domain in saturation conditions below the Θ value until the bottom of a subfreezing firn column, which can be up to 70 meters thick in some areas of the GrIS. Therefore, we use the smallest non-zero value of N tested by Wever et al. (2016) and the parameters Θ and N are fixed to 0.1 and 0.2 m^{-2} respectively.

The hydraulic conductivity of ice layers is not artificially~~synthetically~~ set to zero in the preferential flow domain as it is in the matrix flow domain. Preferential flow thus provides a way for water to flow through an ice layer, reproducing observations that ice layers are not totally impermeable barriers and can lead to localised piping events (Marsh and Woo, 1984; Pfeffer and Humphrey, 1998; Williams et al., 2010; Sommers et al., 2017). An exception for this is the bottom of the domain: as preferential flow is stopped at the last layer, it does not percolate through the solid~~surface of the~~ ice~~ sheet~~.

3.4 Additional processes in the single- and dual-domain schemes

3.4.1 Refreezing process

In R1M and DPM a 'cold content' is calculated for every firn layer, similarly to BK (Sect. 3.1) and refreezing in both flow schemes is executed at the 15 minutes time step (equivalent to~~same frequency as~~ the time step of the~~water~~ transfer processes of DPM, Sect. 3.3).~~.~~

When refreezing occurs, every layer freezes the maximum of its liquid water content that its cold content allows. For numerical reasons, refreezing cannot dry out a layer completely; instead, a very low value of liquid water remains in every layer (see Supplementary Material S1.3).~~Appendix A3).~~ The refrozen water densifies the firn layer and modifies its hydraulic properties. The remaining liquid water is still subject to flow and infiltrates deeper into the firn column.

In DPM, refreezing is restricted to the matrix flow domain (see Supplementary Material S1.7).~~Appendix A7).~~ In the preferential flow domain, liquid water can percolate through cold layers, as~~ this~~ has been observed in field studies on the GrIS (e.g. Pfeffer and Humphrey, 1996; Humphrey et al., 2012). For this liquid water to refreeze, it first has to be transferred back to the matrix flow domain. Preferential flow thus provides a way for liquid water to bypass cold firn layers and subsequently to infiltrate deeper layers.

3.4.2 Aquifer development and lateral runoff

In R1M and DPM, lateral runoff in the firn column is simulated using the parameterisation of Zuo and Oerlemans (1996): ~~In SNOWPACK, all the water reaching the bottom of the snow column is assumed to run off. In R1M and DPM, we allow for ponding of water at the bottom of the firn column (on the top of the solid ice surface) to enable the progressive formation of firn aquifers that exist on the GrIS (Forster et al., 2014; Kuipers Munneke et al., 2014). The model identifies the layers on top of the ice sheet that are saturated with meltwater and does not perform the flow calculations in this lowest part of the domain (see Appendix A5). All the inflow of water reaching this section is added to the aquifer, hence allowing the model to progressively fill the pore space of the bottom layers in the firn column with meltwater.~~

~~Despite the conservation of the water reaching the bottom layers in the domain, lateral runoff is still implemented in the rest of the column and is simulated by using the parameterised formulation of Zuo and Oerlemans (1996):~~

$$\frac{dRu}{dt} = \frac{L_{excess}}{\tau_{Ru}} \tag{26}$$

$$\tau_{Ru} = c_1 + c_2 \exp(-c_3\, S) \tag{27}$$

where Ru is the amount of meltwater that runs off (m), L_{excess} is the excess of liquid water amount with respect to the residual water content (m) and τ_{Ru} is a characteristic runoff time (s). The constants c_1, c_2 and c_3 are parameters derived by comparison with observations by Zuo and Oerlemans (1996) for the GrIS and S is the surface slope. The meltwater input is immediately treated as lateral runoff if the surface layer is an impermeable ice layer or if it is saturated.

Equation (26) leads to the complete drainage of a layer with a zero slope in only 26 days, precluding the formation and persistence of perennial firn aquifers. Therefore, we don’t apply Eq. (26) in the layers at the bottom of the firn column. All the inflow of water reaching this section is added to the aquifer, allowing the model to progressively fill the pore space of the bottom layers in the firn column with meltwater~~which precludes the formation and persistence of perennial firn aquifers. Therefore, runoff is not applied in the layers at the bottom of the firn column where a firn aquifer is building up. The water in such aquifers in the lowest layers has been demonstrated to be ponding over long time periods (Forster et al., 2014) and is affected by other drainage processes not represented in the model such as entering crevasses (Poinar et al., 2017) and possibly catastrophic water release events (Koenig et al., 2014). However, not applying any runoff could theoretically lead to an infinite liquid water accumulation until the water table reaches the surface of the firn layer and we use a pragmatic approach to solve this issue. At the firn aquifer site, Koenig et al. (2014) measured a total water mass of 18.7 kg in 12 cm diameter boreholes, which thus corresponds to 1.65 m w.e. Because of the dearth of data indicating how much water might be stored in PFAs and~~

~~the difficulty of accounting for horizontal drainage processes in a one-dimensional model, we use this value as a model threshold: any amount of water in excess of this value becomes runoff. In firn aquifers forming at the bottom of the firn column, the saturation in both domains is equalised~~.

Firn aquifers are known to be affected by drainage mechanisms not represented in the model, for example via crevasses (Poinar et al., 2017), and possibly hydrofracture and rapid drainage events (Koenig et al., 2014). Miller et al. (2018) found discharge rates within the firn aquifer to be 4.3 x 10^{-6} m s^{-1} by borehole dilution tests in the field. We tested this approach in our model by applying this value as a constant discharge rate for aquifers formed in our simulations. We found however that, using this approach, an aquifer was not sustained; suggesting that such discharge rates must be dependent on the total amount of water within the aquifer and are likely temporally variable. To account for drainage processes and yet allow the formation of an aquifer, we therefore limited the amount of water stored in the firn aquifer to 1.65 m w.e., i.e. the water level measured in the field by Koenig et al. (2014). In firn aquifers forming at the bottom of the firn column, the saturation in both domains is equalised and the model does not perform flow calculation in this lowest part of the domain (see Appendix A5).

3.5 Investigating model sensitivity

In Sections 2 and 3, we highlight several factors influencing BK, R1M and DPM. For each of the schemes, we analyse results generated using three possible impermeability thresholds: 780 kg m^{-3} (ip780), 810 kg m^{-3} (ip810) and 830 kg m^{-3} (ip830). This provides a way to compare the sensitivity of the simple BK and of the physically based schemes (R1M and DPM) to a common parameter. For BK, we try two different formulations of the water-holding capacity: constant at 0.02 (wh02) and according to the parameterisation of Coléou and Lesaffre (1998), Eq. (9) (whCL). For R1M and for DPM, we test two different grain-size implementations: the Linow et al. (2012) surface grain-size calculation, Eq. (5),~~)~~ coupled to the Katsushima et al. (2009) grain growth rate, Eq. (6) (grLK),~~)~~ and the grain-size implementation of Arthern et al. (2010), Eq. (8) (grA). It is important to examine model sensitivity to the grain-size variable as almost all the hydraulic parameters of the RE depend on it. The different sensitivity tests are summarised in Table 1.

4 Results

In this section, we describe and discuss the model performance~~performances~~ at each of the four sites tested (DYE-2, NASA-SE, KAN-U and FA13). We begin~~systematically start~~ by comparing BK, R1M and DPM in a base case parameterisation: BK wh02 ip810, R1M grLK ip810 and DPM grLK ip810 respectively. Then, we perform~~proceed to~~ various tests to investigate the sensitivity of the flow schemes to variations in their parameter values. We refer to ice layers as layers with a density value exceeding the impermeability threshold in the model, and to liquid water input as the total of meltwater and rain influx. The DPM approach features two tuning parameters, N and Θ. Model results and depth-density profiles were found to be weakly sensitive to the value of N and Θ and so we omit consideration of these from the remainder of our study. Results of simulations and observations are inter-compared based on the~~The~~ firn air content (FAC~~;) is~~ the depth integrated porosity in a firn column) ~~. We introduce this quantity because we make use of it to compare results of simulations with each other and with observations. We systematically quantify FAC~~ over the top~~first~~ 15 m of firn and the temperature at 10m depth. Comparing the modelled FAC and 10 m depth temperature values with observed data depicts the ability of the tested models to reproduce the bulk condition of the upper firn column. We also qualitatively assess the degree to which the models to form a ‘realistic’ ice layer distribution and depth-density profile. One would not expect simulated values of either to match observations precisely given the high spatial variability of firn structure (Marchenko et al., 2017), but it is indicative of the models’ performance in reproducing heterogeneity in firn density.

4.1 DYE-2

DYE-2 has a typical liquid water input between 0.1 and 0.3 m w.e. yr^{-1} (Fig. 2), which is moderate in the context of our study sites. The extreme melt year of 2012 (Nghiem et al., 2012) is an exception, with an estimated input of more than 0.7 m w.e. Using BK, almost all of this meltwater refreezes locally and runoff is close to zero (Table 2) until the 2012 summer when ice layers ($\rho \geq 810$ kg m^{-3}) start forming in the top 2 m (Fig. 3a). Runoff increases in the subsequent years because meltwater reaches these ice layers. In R1M and DPM, small amounts of runoff occur between 1980 and 2011 due to the lateral runoff implementation, Eq. (26). Beginning in summer 2004, some ice layers start to form in R1M (Fig. 3b) due to the refreezing of water held close to the surface by capillary forces. Over the 2012 summer, surface layers are progressively melted, bringing ice layers closer to the surface. The ponding and refreezing of water on the top ice layer allows it to thicken. This then acts as an impermeable barrier to vertical percolation from 2012 onwards, resulting in a more than sixfold increase in runoff (Table 2). In contrast, runoff remains low in DPM, in which several ice layers form in the upper firn as early as summer 1996 (Fig. 3c). These ice layers generally form deeper than 2 m due to more effective water transfer from the near-surface to lower layers; preferential flow provides a path for ponding meltwater in the matrix flow domain to bypass ice layers and continue to percolate vertically, thus maintaining low runoff amounts. Preferential flow brings part of the 2012 meltwater to depths greater than 12 m. For each flow scheme, the modelled FAC underestimates the observed value by 4-16%. This can partly be attributed to the tendency of the CROCUS scheme to slightly overestimate densification rates in the upper part of polar firn (Gascon et al., 2014). FAC is underestimated more strongly in DPM (16 %) than in BK and R1M (4 %) because in DPM the deeper firn is not isolated from surface meltwater percolation (Table 2).

Modelled density profiles using each flow scheme are compared with observations (Fig. 4a). Mean density is reproduced reasonably well using~~with~~ each of the three flow schemes, but no configuration is able to qualitatively reproduce the strong variability in density observed. For example, numerous high-density layers separated by much lower density intervals are clear in the observations. Regardless of the flow scheme, only a few ice layers are formed in the model and these tend to be confined to the upper 6 m, which has been affected by the higher melting rates of the recent years. In older firn deposited under lower-melt conditions, the number of density peaks and their amplitude is underestimated even more strongly. Several ice layers are observed in the 10 – 20 m depth range~~; where~~ only DPM simulates the presence of ice layers here.

The three flow schemes lead to significantly different firn thermal conditions. The temperature~~temperatures~~ at 10 m depth of BK and R1M agree well with observations (+0.2 and -0.4 K). In contrast, 10 m temperature is strongly overestimated in DPM (+2.7 K) because it allows percolation at depth, subsequent refreezing, and latent heat release. The summer 2012 percolation raises the 10 m depth temperature to within a few degrees of melting using DPM. Since the DPM method seems to exaggerate deep percolation, we tested a lower impermeability threshold (DPM grLK ip780) which should favour the formation of shallow ice layers, the ponding of water in the matrix flow domain, more lateral runoff and colder temperatures at depth. The ice layers do form slightly earlier in the melt seasons but not noticeably shallower than in DPM ip810. The partitioning between runoff and refreezing is barely affected and the 10 m temperature bias remains (Table 2).

The BK method gives a density profile closer to R1M than to DPM. In order to mimic the behaviour of DPM we increase the impermeability threshold in BK (BK wh02 ip830) to make it more effective in transporting water vertically; however, model results are only weakly affected by this change (Table 2). We also modify the water-holding capacity in BK according to the parameterisation of Coléou and Lesaffre (1998) (BK whCL ip810) which allows more water to be retained in the low-density layers close to the surface. Ice layers appear earlier in the simulation and at shallower depths (Fig. 3d). This increases the amount of runoff in BK whCL ip810 with respect to BK wh02 ip810 (+4 % of the water input over the entirety of the transient model run); however, in the surface layers, where high amounts of water are retained, refreezing dominates. As a result, much less water percolates to the deeper firn and there is less refreezing and latent heat release. All of this leads to a significantly higher FAC (+4 %) and colder 10 m temperature (-1.5 K) relative to BK wh02 ip810.~~).~~

For models based on the RE (R1M and DPM), we test sensitivity to grain-size by implementing a parameterisation for grain growth based on Arthern et al. (2010) (denoted~~experiments~~ grA). Using this parameterisation, grain-sizes tend to be smaller, and so more water tends to be retained and refrozen close to the surface due to stronger capillary forces. Compared to the R1M grLK ip810 experiment, the R1M grA ip810 causes formation of ice layers earlier in the simulation (beginning in 1996) and shallower in the firn column (Fig. 3e), favouring water ponding and subsequent runoff (+7 % of the water input over the entirety of the transient model run). Stronger capillarity also means that saturation is higher for percolation to occur, which in turn increases the simulated runoff since more water is in excess of the residual water content. The enhanced runoff and shallower percolation lead to a higher FAC (+4 %) and a colder 10 m temperature (-0.6 K). In DPM, the flow and refreezing patterns are also altered by the grain-size formulation: DPM grA ip810 produces ice layers much earlier (beginning in summer 1981), at shallower depths and in larger numbers (Fig. 3f). Runoff is however only slightly increased (+2%). The FAC remains similar to DPM grLK ip810, but the 10 m temperature is 0.3 K lower and the warm bias is thus reduced (an 11 % decrease) (Table 2).

Finally, we investigate differences in the depth-density profiles simulated at DYE-2 attributed to different firn-densification formulations in contrast to those observed due to the use of different flow schemes. We first choose to apply the DPM grLK ip810 flow scheme with the additional firn-densification formulations of Herron and Langway (1980) (HL) and of Kuipers Munneke et al. (2015) (KM), both calibrated for GrIS firn. The HL and KM models are forced with the same three-hourly climatic forcing as the CROCUS (base case) model. The FAC (-5 %), 10 m temperature (+0.4 K) and mean density profile (Fig. 4b) predicted by the HL densification model agree reasonably well with that predicted by~~the~~ CROCUS ~~model~~, although HL predicts greater density variability due to its stronger dependence on the annual temperature cycle. In contrast, the KM model predicts much higher densification rates and thus greater densities, with several thick ice layers in the 3-8 m depth range, some exceeding a meter thickness. This results in a much lower FAC value compared to the CROCUS model (-24 %) and in this case, differences between flow schemes are small with respect to the choice of the densification formulation. Since the warm bias of DPM can cause temperature-dependent densification formulations to overestimate densities, we also compare the three densification formulations coupled to R1M grLK ip810 (Fig. 4c). Similar to the results using the DPM flow scheme, the HL profile agrees reasonably well with the CROCUS model (FAC value is -7 %) but predicts that a meter-thick ice layer formed at 5 m depth (Fig. 4c) during the 2012 summer. Discrepancies between CROCUS and KM are only slightly reduced using R1M; for example, the FAC predicted by KM is 20% less than that predicted by CROCUS. This can be attributed to greater densities at depth (>8 m) and to much higher densities in the depth range 3-5 m. The latter corresponds to the layers affected by meltwater refreezing and considerable latent heat release in the 2012 summer.

4.2 NASA-SE

NASA-SE is a site characterised by high accumulation rates, ranging between 0.5 and 0.8 m w.e. yr^{-1}, and low rates of liquid water input, typically between 0.01 and 0.15 m w.e. yr^{-1} (Fig. 2). Under these conditions, abundant pore space and cold content are available for prompt refreezing of the summer meltwater so one would expect~~expects~~ a smaller sensitivity of the model to the flow scheme applied. In BK, no runoff is produced over the entire simulation (Table 3) since refreezing of small amounts of melt does not lead to the formation of impermeable ice layers. R1M and DPM have very low runoff amounts with a small spike in the summer of 2012 when there was 0.38 m w.e. of liquid water input. No ice layer forms in the top 15 m of the firn column using any of the liquid water schemes, in agreement with the observed core (Fig. 5a). Changing the impermeability threshold results in identical model results since no layer exceeds the lowest possible value in the depth range where water percolates. The three water-transport schemes predict a similar FAC; they all underestimate the observed value by approximately 3% (Table 3). This is because the mean firn density is well-captured by the model but somewhat overestimated at depths greater than 8 m~~in the lower part of the core~~ (Fig. 5a). R1M simulates a single density peak at 8 m depth (Fig. 5a), corresponding to the 2012 summer meltwater percolation, due to capillary forces effectively retaining the relatively high meltwater volume produced in that year close to the surface and exposing it to delayed refreezing once these layers cool below the freezing point. DPM also produces a density peak (albeit a much smaller one) at a similar depth, and more-effective downward percolation results in a uniform increase in density over the next 3 m. Finally, BK also produces a small density peak; however, this is at a greater depth of 9 m since it assumes water flow to be instantaneous in a time step and the major part of the refreezing occurs as water reaches deeper cold layers. Again, none of the percolation schemes capture~~scheme captures~~ the observed variability in density. Also, despite the low melt/accumulation ratio, the three percolation schemes overestimate the 10 m temperature by 1.4-2.2 K (Table 3).

Increasing the water-holding capacity in BK (BK whCL ip810) leads to a minor increase in the FAC (< 1%) and a 0.9 K cooling of the 10 m temperature, because the surface layers have a relatively low density (surface boundary condition of 240 kg m^{-3} at this site) and thus retain high amounts of water with the whCL~~CL~~ parameterisation (Table 3). The R1M and the DPM density profiles are weakly sensitive to a change in the grain-size formulation from grLK to grA (Table 3). This is due to the small meltwater amounts with meltwater refreezing only slightly closer to the surface because of the stronger capillarity retention in the grA models. However, we note~~it is noteworthy~~ that simply changing the grain-size formulation in R1M from grLK to grA leads to a 0.4 K colder 10 m temperature and thus decreases the bias with respect to observations by 28 % (Table 3).

We used the R1M grLK ip810 model with the HL and the KM densification formulations in order to prevent the DPM's warm bias from skewing the modelled densification rates. As expected in this relatively dry site, the modelled profiles are much more sensitive to the dry-densification than to the percolation scheme (Table 3 and Fig. 5a and b). The ~~aim of this paper is not to discuss the specificities of the dry-densification schemes, but the~~ maximal difference in FAC between~~among~~ the three densification formulations tested is 20% compared to less than 1 % between~~among~~ the three flow schemes and their possible parameterisations. In contrast with the DYE-2 simulations, the CROCUS model predicts the fastest densification and thus the lowest FAC. HL and KM predict 20% and 11% greater FAC than CROCUS, respectively, and CROCUS is in closest agreement with the observations, underestimating FAC by just 3%.~~.~~

4.3 KAN-U

KAN-U is a high-melt site with an average melt rate over the 1980-2013 period of 0.33 m w.e. yr^{-1}, and in the last three years of our simulation (2010-2013), the RCM calculates annual melt exceeding annual accumulation (Fig. 2). Since surface temperatures are relatively high (annual mean around -8 °C), refreezing of the summer meltwater depletes the cold content over large depth ranges. Beginning in summer 1990 in the BK simulation, some ice layers are present in the depth range 3-8 m (Fig. 6a), allowing part of the meltwater to runoff and impeding percolation to greater depths. At the start of 2012, there is a thick ice layer in the upper 4 m and another one forms at the surface during the summer. As a result, refreezing is constrained to the uppermost firn layers and a large part of the water input runs off (Table 4). In R1M, the high water content and the almost-continuous presence of ice layers in the upper 5 m from summer 1986 onwards (Fig. 6b) cause relatively high runoff rates throughout the simulation (28 % of the water input over the entirety of the transient model run). As in the BK simulation, runoff is particularly high in 2012 due to ice layers impeding vertical percolation below 1 m (Table 4). In the DPM simulation, the preferential flow mechanism leads to the formation of multiple ice layers in the depth range 4-10 m from 1987 onwards (Fig. 6c). Runoff rates remain low but there is a notable increase in 2012. This is due to the formation of ice layers close to the surface, which allows ponding of water in the matrix flow domain. The preferential flow domain is unable to accommodate all the ponding water, and part of it is treated as lateral runoff (Eq. (26)). While matrix flow typically remains constrained to the upper 5 m (Fig. 7a), the recent (2010 to 2012) high-melt summers cause preferential flow to reach much greater depths (e.g. up to 35 m in the 2012 summer (Fig. 7b)). Since preferential flow can transfer water below ice layers, the refreezing process can fill the pore space available at depth, leading to substantial thickening of the ice layers. As a result, the FAC is much smaller in the DPM simulation than in the BK (-39 %) and the R1M (-35 %) simulations, in which runoff limits the amount of meltwater refreezing.

The observations reveal a thick, almost continuous ice slab over the depth range of 1-7 m (Fig. 8a). Below it, the density is more variable but remains generally high causing a low FAC (Table 4). Both the BK and the R1M simulation significantly overestimate the FAC (+59% and +50 %). In contrast, the average FAC of~~%) whereas~~ the DPM simulation is~~agrees~~ very close to~~well with~~ the observed value (-2 %), however~~%). However~~, the DPM density profile shows an almost continuous ice slab from 3 to 17 m depth (Fig. 8a) and does not reproduce the lower density intervals observed. This demonstrates an important limitation of the liquid water schemes: since water cannot be retained in layers exceeding the impermeability threshold, these layers can only further densify by the dry densification mechanism and not by water refreezing. The~~Therefore, the~~ overestimation of the ice slab thickness in the DPM profile is thus compensated by the underestimation of its density, which leads to the good agreement with the observed FAC value. BK reproduces the presence of the ice slab at 1 m depth, but it underestimates its thickness and simulated~~shows~~ a thick (2 m)~~large~~ low-density region~~section~~ (Fig. 8a). Below the observed ice slab, the agreement with observed~~the~~ average density is reasonable but ~~the model underestimates density~~ variability in density is underestimated. Despite also underestimating the thickness of the ice slab, the R1M profile agrees better with the observed density profile: it produces only two thin, low-density layers in the slab, and more high density peaks and ice layers below 7 m which is~~are~~ in better agreement with the observed density variability.

With respect to the 10 m temperature, the BK method is biased cold but gives results in reasonable agreement with the observations (-1.7 K). This~~), whereas the cold~~ bias is more pronounced in R1M (-2.6 K). In contrast, DPM largely overestimates the 10 m temperature (+4.5 K), as a result of~~which stems from~~ its overestimation of percolation and subsequent refreezing at depth~~great depths~~.

Changing the impermeability threshold for DPM (DPM wh02 ip780 and ip830) does not alter the ~~general~~ pattern of the modelled depth-density profile, but the corresponding changes to the density ~~values~~ of the ice slab has an impact on~~become consistent with the impermeability threshold applied which affects~~ the FAC ~~accordingly~~ (+15 % for ip780 and -9 % for ip830).

Other factors further affect the FAC: runoff rates slightly decrease with higher impermeability thresholds (Table 4) and the mass of the ice layers increases the overburden stress on the firn column below, increasing the densification rate. In addition, higher (lower) impermeability thresholds lead to warmer (colder) 10 m temperatures (+~~(-1.6 K for ip780 and +~~1.1 K for ip830 and -1.6 K for ip780), due to enhanced latent heat release. Compared to BK wh02 ip810, decreasing the impermeability threshold (BK wh02 ip780) leads to formation of ice layers in earlier years and closer to the surface and thus more runoff (+3 % of the water input over the entirety of the transient model run), which in turn increases the FAC (+5 %) and decreases the 10 m temperature (-0.5 K). Increasing the threshold (BK wh02 ip830) has the opposite effect (-8 % for the FAC and +0.8 K for the 10 m temperature compared to BK wh02 ip810).~~).~~ If we instead allow for a greater water-holding capacity (BK whCL ip810), the partitioning between runoff and refreezing remains very similar (Table 4). However, the FAC and the 10 m temperature are changed (+3 % and -1.7 K compared to BK wh02 ip810).~~).~~ The lower temperature is due to latent heat release from refreezing being more concentrated in the surface layers (Fig. 6d). The formation of ice layers earlier in the year and at shallower depths allows part~~parts~~ of the underlying firn to remain free of refreezing, which increases the FAC. Furthermore, colder temperatures cause a higher firn viscosity thus decreasing the densification rates. Since the R1M formulation both overestimates the FAC and underestimates the 10 m temperature, we test an increase in its impermeability threshold (R1M grLK ip830), allowing for deeper percolation. Both the decrease in FAC (-1 %) and increase in 10 m temperature (+0.1 K) compared to R1M grLK ip810 are minor.

With the grA formulation in DPM (DPM grA ip810), water is more efficiently transferred vertically through the preferential flow domain, which causes an increase in the number of ice layers formed during the simulation (Fig. 6f), a slight decrease in FAC (-2 %) and a slight increase in the 10 m temperature (+0.1 K) relative to DPM grLK ip810.~~).~~ The nearly-continuous ice slab, which extends to 17 m depth below the final winter accumulation, explains the weak sensitivity of the final FAC and 10 m temperature values of DPM to grain-size. In contrast, applying the grA formulation in R1M (R1M grA ip810) leads to a considerable increase in FAC (+11 %) and a decrease in 10 m temperature (-0.7 K) compared to R1M grLK ip810.~~).~~ This is due to higher water content during percolation events and, especially in the most recent years of our simulation, refreezing and ice-layer formation at shallower depths (Fig. 6e). This increases the runoff and isolates the deeper firn from meltwater percolation. As in the cases of DYE-2 and NASA-SE, the change in FAC due to different grain-size formulations in R1M is greater than the change due to switching from BK to R1M (Table 4).

The modelled depth-density profiles also differ according to the densification formulation used (Fig. 8b). We compare the different densification formulations using R1M grLK ip810, thus avoiding the effect of the strong temperature bias of DPM on the densification process. Densification in KM is sensitive to high firn temperatures, and it predicts the highest densities: it produces the highest density values in the ice slab range, the most ice layers below the ice slab and the lowest FAC value (-27 % compared to the CROCUS formulation). HL behaves in a similar way to CROCUS in the upper 5 m, apart from a much lower density interval in the 2-2.5 m depth range. In deeper firn, densities simulated using HL tend to lie between those simulated using KM and CROCUS, and its FAC difference with the CROCUS (-9 %) is less than that of KM. The DPM scheme simulates a depth-density profile of an ice slab over a 14 m range, which is in stark contrast with BK and R1M. Apart from this, the choice of the densification formulation has a greater influence on the model than the choice of liquid water scheme and of any of their respective parameterisations presented here, in spite of the high water input at this site.

4.4 FA13

The FA13 site is representative of conditions in the southeast part of the GrIS; it has both high accumulation and high melt rates (mean 1980-2012 rates of 1.09 and 0.64 m w.e. yr^{-1} respectively, Fig. 2). This favours the insulation of summer percolating meltwater from winter atmospheric temperatures, typically leading to the formation of PFAs (Kuipers Munneke et al., 2014). Here, the initial conditions and the spin-up process cause the deep firn to be close to the melting point at the start of the transient run.

The warm firn, combined with the high water influx, allows liquid water to reach greater depths than at the other sites in all three flow schemes. Additionally, the firn – ice transition depth becomes important in the FA13 simulations. The observed core shows that the 810 kg m^{-3} density is reached and maintained from 24 m depth. The CROCUS densification scheme predicts that this density horizon occurs at 60 m depth. Since CROCUS has been developed for seasonal snow, the densification at high overburden stress is probably not well captured by the model (Stevens, 2018). Because of this, we base our simulations for FA13 on the HL densification model, which predicts this transition depth to be around 21 m.

The total refreezing rates are similar for the three flow schemes (Table 5). Since the deep firn is close to the melting point, the total refreezing amounts are essentially determined by the cold content provided in winter and the precise behaviour of the percolation has a minor impact. However, variability of refreezing with depth differs between schemes, which leads to differences in the 15 m FAC values (Table 5) and in the modelled depth-density profiles (Fig. 9a, b and c and Fig. 10a). FAC is consistently underestimated (-23 to -30 %) because firn density is overestimated above 10 m. R1M and DPM overestimate density most strongly with FAC values 9 and 10 % smaller than BK respectively, and both schemes simulate the presence of a thick ice layer in the upper 10 m of the firn, which is~~was~~ not observed in the core. The BK model produces only a single thin ice layer in the 10 upper meters (0.2 m thick at 9 m depth), which is in good agreement with the observations (showing a single thin ice layer at 7.5 m depth). Below 10 m, the modelled densities are generally in better agreement and all the schemes produce several ice layers (Fig. 10a and Fig. 9a, b and c).

In the absence of any shallow ice layer throughout most of the simulation (Fig. 9a, b and c), meltwater is free to percolate through the winter accumulation layers and to deplete their cold content. The flow schemes have different abilities to store liquid water, which leads to small variations in runoff and refreezing rates. In BK, water is retained according to the water-holding capacity (Fig. 11a) and refreezes during subsequent winters. In contrast, DPM allows percolation down to the firn –

ice sheet transition where it ponds to form an aquifer (Fig. 11d and e). This leads to a significant reduction of runoff amounts during the aquifer build-up (-6 % of the water input over the entirety of the transient model run compared to BK) and the water remaining in the firn column is essentially constrained by the maximal amount of water we allow in the aquifer (1.65 m). In theory, the same mechanism could be simulated by R1M but the percolating water is depleted before it reaches the bottom of the firn column (Fig. 11b). This is due to refreezing, to the lateral runoff parameterisation and to the presence of ice layers in the upper 10 m. No water persists through the winter seasons, which illustrates the model artefact that the effective saturation must be strictly positive for the stability of the RE (Sect. 3.2). Thus, the refreezing rates are slightly lower than in BK since no residual water is stored and later exposed to winter refreezing (Table 5).

The build-up of the aquifer starts very early (in the summer of 1981) when DPM is turned on in the transient run due to the low refreezing capacity of the deep firn. The depth of this aquifer is constrained by the impermeability threshold applied, which determines where the model places the firn ice transition. This depth is at~~of~~ 33 m in 1981 and 21 m in 2013, the decrease being caused by enhanced densification. The aquifer is fed only by preferential flow (Fig. 11e) since matrix flow cannot reach the water table due to runoff, refreezing and the presence of ice layers in the firn column.

From 1994 and onwards the total simulated water content in summer is only regulated by the maximum allowed in the model (1.65 m). Since the water table is at a shallow depth towards the end of the simulation (7.5 m), the propagation from the surface of the cold winter temperatures can refreeze part of the saturated layers. This leads to the formation and progressive thickening of the shallow, thick ice layer. Also, the shallowness of the aquifer causes 23% of the porosity in the top 15 m to be filled with liquid water and the 10 m temperature to be at the melting point.

The higher impermeability threshold in DPM grLK ip830 increases the depth of the calculated firn – ice transition, producing a deeper aquifer that extends between 12 and 29 m depth at the end of the simulation, similar~~compared~~ to the 12-37 m depth range observed by Koenig et al. (2014). Compared to DPM grLK ip810, the~~The~~ increased depth leads to less refreezing in the shallowest layers of the aquifer and thus a higher FAC value (+3 %) and ~~to~~ a 10 m temperature below the melting point.
The grain-size formulation following Arthern et al. (2010) (DPM grA ip810) reduces the ability of preferential flow to transport water down to the firn – ice transition but instead favours formation of discrete ice layers in the firn column (Fig. 9f~~8f~~). In this case the aquifer does not start to form until summer 1988, but the final aquifer structure (also between 7.5 and 21 m), the FAC value (-3 % for grA), and the partitioning between refreezing and runoff are similar to those simulated using grLK (Table 5). In R1M, the sensitivity to grain-size is noticeable in the firn-structure evolution with differences in ice-layer formation between R1M grLK ip810 and R1M grA ip810 (Fig. 9b~~8b~~ and e). The final FAC value (+4 % for grA) and the meltwater partitioning remain similar (Table 5) between R1M grLK and R1M grA,~~),~~ as for the case of DPM grLK and DPM grA. This can be explained by the total refreezing's stronger dependence on the firn thermal structure than on the percolation pattern at this site.

Increasing the water-holding capacity in BK (BK whCL ip810) leads to a significantly lower FAC value (-12 %): more water refreezes in the near-surface layers, which reduces the runoff and enhances densification in the entire underlying firn column. Also, more water remains stored at depth throughout the different winter seasons (Fig. 11c), and some is still present at the end of the simulation (0.09 m) between 16 and 23 m depth. However, this small amount retained by the water-holding capacity is much less than is stored in the saturated layers of the aquifer simulated in DPM.

We compare the three different densification models (CROCUS, HL, KM) using the R1M grLK ip810 flow scheme and these show important differences in the final modelled depth-density profiles (Fig. 10b). CROCUS agrees reasonably well with HL in the top 6 m but, as mentioned above, it has a strong low density bias at greater depths. Since CROCUS simulates lower densification rates, its underestimation of the FAC value in the 15 upper meters (-21 %) is smaller than in HL (-30 %), but it is clearly not representative of the density conditions below 15 m. KM predicts a firn column below the last winter's accumulation entirely at the ice density. The model thus identifies a firn – ice sheet transition at shallow depth (~2 m), which the water can reach before being depleted by the lateral runoff parameterisation and saturated layers can thus build up. This further amplifies the densification since the saturated layers at the transition depth are exposed to refreezing. Hence, in 2012, runoff combined with refreezing exceeds the liquid water input (Table 5). This occurs because~~) since~~ some layers wherein water had been stored in previous years reach the 810 kg m^{-3} density, causing the stored water to be considered as runoff by the model. Whereas the FAC values are generally close for the different flow schemes and their parameterisations (maximal difference of 12 %), CROCUS and KM reach values 14 % higher and 34 % lower than HL respectively.

5 Discussion

The three liquid water schemes show consistent behaviour between sites. R1M generally predicts slower downward percolation~~greater retention~~ of water than the other schemes, which leads to more near-surface refreezing~~ and thus more pore space and lower temperatures in deeper firn. In addition~~, the formation of near-surface ice layers, more ~~close to the surface favours~~ lateral runoff and thus ~~contributes to~~ lower densities and lower~~colder~~ temperatures in deeper~~the deep~~ firn. As a result, when compared to observations R1M tends to reach higher FAC values and to underestimate 10 m temperatures. The BK formulation with the Coléou and Lesaffre (1998) parameterisation for the water-holding capacity leads to the same effects, but they are amplified. The underestimation of the 10 m temperature is stronger~~biases are colder~~, suggesting that BK whCL does not allow for deep enough percolation. BK with the lower water-holding capacity (BK wh02) leads to a partitioning of the water input between refreezing and runoff similar to the more complex R1M at the four sites. As a result, the FAC values predicted by BK wh02 and R1M generally agree (maximum difference less than 10 %), as do the temperatures at 10 m depth (maximum difference less than 1 K). The FAC values and 10 m temperatures of R1M at the end of the model runs always lie in the range of the ones obtained with different parameterisations of BK. This suggests that BK can produce results similar to R1M, provided it is parameterised appropriately.

DPM exhibits~~shows~~ a different behaviour: it effectively brings water to greater depths, depleting~~ and depletes~~ the deep-firn pore space and cold content. Even in the presence of shallow ice layers hindering matrix flow, the preferential flow implementation still ensures efficient vertical water transport, and runoff amounts remain low. This suggests that transfer mechanisms to the preferential flow domain implemented in DPM are more effective in draining ponding water than the lateral runoff parameterisation. Due to large FAC underestimation and 10 m temperature overestimation, the data-model mismatch of DPM with respect to these variables is significantly greater than that of R1M and BK.~~ However,~~ DPM is better at producing density variability in depth, which is underestimated in all schemes at all sites. Also, in contrast to the two other schemes, DPM can form ice layers even in summers of average melt, and it is able to simulate the persistence of deep saturated firn layers at the FA13 site. In this respect our findings support those of Wever et al. (2016) who highlight the tendency of DPM to produce ice layers at various depths in alpine snowpack simulations, and thus to reproduce depth-density variability. It is important to bear in mind that we only use the dual permeability water~~flow~~ scheme of SNOWPACK in DPM and not the other physics of this model; the results produced by the full SNOWPACK model would be different because it has its own formulations for snow mechanical and thermal properties. In particular, DPM relies heavily on the grain-size, and it would thus benefit from better representations of the firn's structural properties. Moreover, the primary purpose of the DPM implementation in SNOWPACK is to reproduce the occurrence of ice layers in a seasonal alpine snow pack (Wever et al., 2016), whereas in this study we evaluate its ability to simulate representative firn depth-density profiles over the course of numerous decades.

BK with low water-holding capacity is usually used to mimic preferential flow (Reijmer et al., 2012). However, our findings suggest that, in fact, this more closely represents matrix flow as modelled using the Richards Equation. We suggest that in order to use BK in this way, percolation of some meltwater in the presence of ice layers should be considered.

The lack of ~~density~~ variability in density in the modelled profiles cannot only be attributed to inaccuracies in the percolation-refreezing process. This is demonstrated in the example of NASA-SE: the layers of the density peak observed around 1 m depth (Fig. 4a and b) were deposited during the final winter of the simulation (2015-2016). As such, these have only been influenced by the percolation and refreezing of negligible amounts of liquid water. The consistent underestimation of density variability across all schemes indicates that one or several other factors that are not or poorly represented by firn models likely play a crucial role in firn evolution. These factors may include horizontal water flow, prolonged ponding~~variable density~~ of water in soaked firn close to the surface, variability in fresh snow density, the~~,~~ effects of firn microstructure and~~on densification,~~ impurity content on densification, wind packing and short-term weather fluctuations. Moreover, the validity of the firn model relies on the accuracy of the climatic forcing.

~~At KAN-U, despite imperfect agreement with the observed density profile (Fig. 7a), DPM predicts the 15 m FAC accurately (Table 4). This could suggest that it predicts the correct amount of refreezing at this site integrated over the top 15 m. On the other hand, this model-data agreement could result from numerous errors in the model compensating for each other. DPM strongly overestimates temperature at 10 m depth, suggesting that this refreezing is occurring too deep in the firn column. It likely overestimates the percolation whereas in reality, water may pond for longer in soaked firn close to the surface (Pfeffer and Humphrey, 1996). The subsequent refreezing allows for more of the released latent heat to be dissipated towards the atmosphere. It is also possible that DPM overestimates the total refreezing and that enhanced densification causes part of the FAC depletion.~~At all sites, interchanging the HL, KM and CROCUS formulations for firn densification generally leads to more variability in the results than using different water flow schemes. This highlights the need to understand the causes of disparity between densification models under various climatic conditions and thus to proceed to further model intercomparison experiments (Lundin et al., 2017). The existing firn-densification formulations are likely not suited for representing densification in conditions of high water contents and high refreezing rates. Our study indicates that firn-densification models could be improved by accounting for the latent heat source as well as the effects of liquid water and of refreezing cycles on firn viscosity and densification rates. For example, the KM and HL densification equations were established for dry firn (Herron and Langway, 1980; Kuipers Munneke et al., 2015a). In the CROCUS scheme, firn viscosity is adjusted according to the water content, but our results show that the modification in the parameterisation is insufficient to reproduce the observed densities at KAN-U. ~~At all sites, interchanging the HL, KM and CROCUS formulations for firn densification generally leads to more variability in the results than using different water flow schemes.~~ A simple example of the densification schemes in HL and KM not representing reality becomes apparent when applying the percolation-refreezing schemes: in reality, densification is dependent on the overburden stress, but these models use accumulation rate as a proxy for stress. Consequently, in these models the redistribution of mass due to runoff and percolation does not affect the densification rates, despite the effect it has on the firn column mass. The absence of a preferential flow scheme is often presented as a possible explanation for firn-density overestimation close to the surface (e.g. Gascon et al., 2014; Kuipers Munneke et al., 2014; Steger et al., 2017a).~~(e.g. Gascon et al., 2014; Kuipers Munneke et al., 2014; Steger et al., 2017).~~ However, our results suggest that simply adding a one-dimensional preferential flow scheme, although physically detailed, to firn-densification models does not solve this issue. The water that is transported quickly from the shallow layers must flow back into the matrix domain at some point. If this occurs in the shallow layers, the density-overestimation issue remains; if this occurs in deep layers it can lead to unrealistic temperature signatures. There~~The representation of preferential flow physics requires improvements and there~~ are several other possible factors for densification errors at ~~such~~ high melt sites, including exaggerated sensitivity of the model to temperature because the densification model is not suited for conditions with substantial latent heat release.

We compare the results reached at KAN-U with previous firn modelling studies at this site. Langen et al. (2017) also used the CROCUS densification scheme and a water flow scheme conceptually comparable to R1M but with a simplified solving process of the RE. Their results show a density profile entirely at ice density from 4 m depth and an overestimation of the temperature at 10 m depth (+3 to +5 K). In our study, the R1M results show lower deep densities and a 10 m temperature underestimation. These discrepancies can be attributed to differences in 1) model implementation, 2) climatic forcing and 3) details of the water flow scheme. Model resolution is likely of importance here: Langen et al. (2017) used a coarser vertical resolution, disfavouring the formation of thin impermeable layers, allowing liquid water to flow more readily to greater depths and refreeze, thus causing greater density and higher temperature values. Steger et al. (2017b) used the SNOWPACK densification model (recall: we use different densification physics to SNOWPACK in this study) with a bucket scheme, similar to BK, and the same climatic forcing as in this study. Their model output shows a firn column fully compacted to ice at KAN-U. They attribute this to the overestimation of densification rates by the densification model used and also argued that some other effects could be at play such as the surface density applied. The 10 m temperature is underestimated in their result, likely due to the absence of percolation of water through ice and thus no latent heat release at depth.

Both DPM and R1M exhibit significant sensitivity to the choice of the grain-size formulation (grLK or grA). Modifying this formulation in R1M affects the model results more than changing to the use of BK at all sites apart from FA13 where the magnitudes of change are comparable. For example, the change of grain size at FA13 in R1M leads to a difference of 4 % in FAC and 1.2 K in 10 m temperature, and in DPM, the patterns of ice layer formation are significantly different at all sites where such ice layers form. This highlights another significant difficulty for percolation schemes: the dependence of water flow on the firn's structural properties. Field evidence demonstrates the crucial role of structural transitions, even at the scale of centimeters, on the behaviour of water flow in firn (Marsh and Woo, 1984; Pfeffer and Humphrey, 1996, 1998; Williams et al., 2010). With respect to this, the advanced flow schemes applied in this study have some limitations. Firstly, the structural properties of grains in the firn layer are poorly constrained by observations. Secondly, the parameterisations linking the structural and hydraulic properties on which R1M and DPM rely were derived from a limited number of laboratory experiments. These are typically performed at a very small scale (e.g. shallow snow columns with diameter of 5 cm in the experiments of Yamaguchi et al. (2012)), and are mostly based on homogeneous snow in terms of grain-size and temperature (Yamaguchi et al. 2012~~Yamaguchi et al. 2012~~; Katsushima et al., 2013). The much larger scale of the GrIS firn layer, the spatial and temporal heterogeneity of its structural properties, and its climatic and glaciological settings render the validity of these idealised parameterisations questionable. Finally, the density dependence of the parameters makes them sensitive to errors in the densification process. Thus, a better knowledge of firn structural properties would only be profitable to water flow schemes if we have a clear understanding of the link between snow structure and its hydraulic properties and vice versa.

Another major limitation of the implementation of physically detailed liquid water flow schemes in one-dimensional firn models is the fact that water flow is in reality three dimensional. Water can flow horizontally on top of buried ice lenses or on thin, near-surface ice crusts caused by daily refreezing (Marsh and Woo, 1984; Pfeffer and Humphrey, 1996). Even at depths greater than 10 m, large masses of liquid water can persist through the winter and move laterally over considerable distances (Humphrey et al., 2012). In one-dimensional models, the key to solving this issue is to accurately partition between vertical percolation and lateral flow; this likely requires a better approach than the lateral runoff parameterisation we implement here. As an example, at FA13 all three water-transport schemes overestimate the density in the 10 upper meters except in the last winter's accumulated layers (0 – 2 m depth), where there is a good agreement with observations (Fig. 10a). This suggests a consistent overestimation of the summer meltwater refreezing and underestimation of lateral runoff. Also, the need to use a limit for the PFA water content demonstrates that some processes not represented in the model must regulate its water volume; these are likely lateral movement driven by hydraulic pressure gradients and connections with englacial and subglacial hydrological systems. A one-dimensional preferential flow scheme aims to correctly partition the water input between matrix flow and fast preferential flow; there are several other difficulties with this approach. These include accurately determining how deep the water can be transported by preferential flow, how much water refreezes and how much is stored as liquid water, and the amount of lateral flow at different depths in the firn column. Similarly, the same considerations apply to liquid water flowing in from upstream grid cells. The representation of preferential flow physics thus requires improvements to address some deficiencies. We highlight (1) that too much water is transported through preferential flow or at exaggerated depths as demonstrated by the consistent overestimation of 10 m temperature, (2) the need to consider lateral flow as the tendency to underestimate FAC shows and (3) the large sensitivity of the ice layer formation process to grain size, which should be overcome or should be addressed by further observational studies of grain metamorphism in firn.

Our results also suggest that more observations of firn-temperature variability in time and depth would likely be useful for the evaluation of existing flow schemes and the development of new ones. Modelled temperature profiles show both the depth and volume of refreezing due to the release of latent heat. Moreover, deep meltwater refreezing causes marked and long-lasting temperature increases due to insulation from the overlying firn, and temperature measurements in depth can be powerful indicators of the occurrence of deep percolation and refreezing events. On the other hand, comparisons between modelled and observed density profiles are strongly affected by the choice and accuracy of the densification formulation, the variability of surface density, several other factors influencing model outputs mentioned above and possible uncertainties in field measurements. Such uncertainties are related to the strong spatial variability of firn structure (Marchenko et al., 2017), which can be observed by comparing density profiles of cores drilled at nearby locations. However, the modelled temperature profile also depends on the accuracy of the climatic forcing, of the heat-transport scheme and of the thermal-conductivity parameterisation. The latter is a function of density, thus erroneous depth-density profiles inevitably lead to an inaccurate heat-transport process. As an example of the influence of various sources of errors, the warm 10 m temperature bias of all the schemes at NASA-SE (Table 3) is unlikely to be only due to the percolation-refreezing process.

6 Conclusion

We implemented three liquid water schemes of different levels of physical complexity in a firn model using a fine vertical resolution: a bucket scheme, Richards Equation in a matrix flow scheme, and Richards Equation in a preferential flow scheme.

To our knowledge, this is the first study to apply the Richards Equation as well as a preferential flow scheme in firn-densification simulations on the GrIS.

Our three liquid water flow schemes predict significantly different vertical patterns of refreezing and consequently modelled densities, firn air content values and 10 m temperatures. The preferential flow scheme effectively evacuates meltwater from the surface layers and leads to underestimation of firn air content and overestimation of 10 m temperatures. Compared to the preferential flow scheme, the single-domain Richards Equation scheme generally showed biases of the opposite signs and of much lower magnitudes, suggesting it slightly underestimates percolation depths. The simpler bucket scheme predicted refreezing rates, firn air contents and 10 m temperatures similar to those obtained by the single-domain Richards Equation; by adjusting its water-holding capacity and impermeable density parameters, it could produce the same results. Using the Coléou and Lesaffre (1998) parameterisation for the water-holding capacity in the bucket scheme led to underestimation of percolation depths. The bucket scheme with lower water-holding capacity and the single-domain Richards Equation scheme predicted firn air contents and 10 m temperatures in closest agreement with observations. However, the preferential flow scheme was found to perform better than the simpler flow schemes in reproducing the density variability with depth and the water-saturated conditions at the bottom of the firn column at a site of a perennial firn aquifer.

We identified the multidimensionality of liquid water flow as the prominent challenge for water percolation schemes. Because firn models are currently one dimensional, an accurate partitioning between horizontal and vertical flow is likely to be at least as difficult and as important as the separation between slow matrix and rapid preferential flow. Other difficulties related to water-flow representation include the uncertainties in firn hydraulic properties and in firn micro- and macro-structure on the GrIS. This is further demonstrated by our results showing the sensitivity of the Richards Equation-based schemes on the grain-size formulation. However, the absence of any large-scale field observations of water flow in firn makes it difficult to constrain its implementation and to validate model behaviour. Here, we aimed to assess the applicability of ~~By using~~ flow schemes developed for seasonal snow models to the Greenland~~, the goal of this study was to identify limitations in implementing such schemes in~~ firn ~~and research needed to improve liquid water schemes~~. Whilst we did apply some modifications to account for the differences between snow and firn, we suggest that more modifications are likely required since the spatial scales and the structural characteristics of seasonal snowpacks and firn are different.

There is no large scale detailed observation available of liquid water content and percolation pattern during melting events in firn. This renders~~are a number of effects that influence firn density, which hamper~~ the validation of a particular flow scheme difficult and validation relies~~based~~ on temperature and ~~observed depth~~ density profiles. However, there are a number of effects that influence firn density and temperature, all potentially contributing to mismatch between modelled and observed values.

As an example, the density variability in depth was largely underestimated regardless of the flow scheme. This suggests that there are uncaptured complexities in the percolation and refreezing mechanisms that need to be better taken into account such as water ponding and the effect of grain shape on water flow. Furthermore, this shows~~incorporated into models and also~~ that firn-model development must focus on including complex processes currently poorly or not represented, such as surface-density variability, wet firn densification and firn structural effects on densification. We note also that our assessment considers only a single profile from each site, captured at one time point, and further work is required to assess the impact of liquid water percolation on transient firn evolution. A comprehensive exploration of the various firn models and their parameter spaces could help identify priorities for further model developments based on minimising data-model mismatch and overall uncertainty. In line with this, we showed that output from three common firn-densification models shows greater variability than the output from single densification model using the different flow schemes. In order to capture the multiple impacts of liquid water on firn densification, future models require an improved liquid water flow scheme, accurate boundary conditions, and formulations developed explicitly to simulate densification of wet firn.

Author contributions. VV and AL conceived this study. VV performed the development of the water flow schemes, performed the model experiments and led writing of the manuscript. AL supervised the work. MS contributed to development of the water flow schemes and model experiments. MMF provided the firn core data of the FirnCover Project. BN and MRB provided the RACMO2.3 forcing data. All authors provided comments and suggested edits to the manuscript.

Acknowledgements. We thank Laura Koenig for making available the FA13 firn core data in the SUMup dataset (https://doi.org/10.5194/essd-10-1959-2018).~~.~~ We thank Horst Machguth for making available the KAN-U firn core data. We thank the Geological Survey of Denmark and Greenland for making temperature measurements at KAN-U available in the PROMICE dataset (https://www.promice.dk/WeatherStations.html).~~.~~ Keith Beven is acknowledged for insight into the subject of hydrology. Nander Wever is acknowledged for support in the understanding of the SNOWPACK model. Part of the funding for this research was provided by the Centre for Polar Observation and Modelling. We thank two anonymous reviewers and Baptiste Vandecrux for providing insightful and constructive comments.

Competing interests. The authors declare that they have no conflict of interest.

~~Appendix A: Model Implementation~~

~~The model uses a finite-volume scheme with each layer being an independent volume. We use the general mixed-form Picard iteration scheme to solve the RE, as it has been demonstrated that the mixed form of RE can be efficiently used in finite-difference schemes because of its accuracy and its robustness with respect to mass conservation (Celia et al., 1990). The Picard scheme discretises the model using central finite differences for the space derivative and a backward Euler method for the time derivative. The iterative process calculates the value of the pressure head at each iteration and then adjusts the liquid water content according to the water retention curve, Eq. (12). Hydraulic parameters are updated and iterations are repeated until convergence of the solution is achieved. Boundary conditions are the rate of meltwater input at the surface and a no-flow condition at the bottom. Solving the RE in the firn column presents numerical challenges. We adopt an implementation strategy~~

~~based on the works of Wever et al. (2014) and D'Amboise et al. (2017) who implemented the RE in the snow models SNOWPACK and CROCUS respectively. Here, we give more details about this methodology.~~

~~A1 Convergence criteria~~

~~For the solution reached by the Picard iteration scheme to be considered convergent, it must fulfil different criteria. The convergence criteria between two successive iterations are defined for the head pressure (ε_h) and liquid water content (ε_θ) values as well as for the mass balance error (ε_{MB}) of individual layers. These three criteria are fixed to 10^{-3} m, 10^{-5} and 10^{-8} m respectively, following Huang et al. (1996) and Wever et al. (2014). For each layer, we select ε_θ or ε_h according to the effective saturation. Huang et al. (1996) showed that using ε_θ allows faster convergence. However, it cannot be used in very saturated layers and thus we apply ε_h for layers where effective saturation exceeds 0.99, in accordance with Wever et al. (2014). The mass-balance criterion is always applied to every layer, regardless of the saturation.~~

~~A2 Hydraulic conductivity calculation~~

~~As we use a central finite difference approach to compute RE, the fluxes are assumed to occur on the interface between adjacent layers. Incoming and outgoing fluxes are computed and this requires the hydraulic conductivity value to be calculated at the top and bottom of every layer *i* and not at the centre. We use the upstream-weighting technique (Forsyth et al., 1995):~~

$$\cancel{K_{i+\frac{1}{2}} = \begin{cases} K_i, \ if \ \frac{\Delta h}{\Delta z} - 1 \leq 0 \\ K_{i+1}, \ if \ \frac{\Delta h}{\Delta z} - 1 > 0 \end{cases}} \qquad \text{(A1)}$$

~~The advantage of this formulation over a simple arithmetic mean is that it does not lead to oscillatory solutions, regardless of the mesh size (Forsyth et al., 1995; Szymkiewicz, 2009).~~

~~A3 Dry layers~~

~~For numerical stability, a snow layer cannot be completely dry (i.e. $\theta = 0$). Therefore, two cases must be considered: dry layers and refreezing layers. At the start of the flow routine, all layers are initialised with a very low θ value, θ_{dry}. The value must be sufficiently low to avoid influencing the refreezing process but sufficiently high to lead to a convergent solution (D'Amboise et al., 2017). In this study, the θ_{dry} value is fixed at 10^{-6} as this is a tenth of the ε_θ criterion. This corresponds to a 1 m thick snow layer holding 1 µm of liquid water. When the flow routine is called in the firn model, the water content of every dry layer is thus synthetically raised to θ_{dry}, which corresponds to a pre-wetting. The porosity of ice layers that are at high densities (>900 kg m^{-3}) is thus adjusted in order to raise their water content to θ_{dry} in both domains.~~

~~Similarly, there is a risk for θ reaching too-low values when refreezing occurs. Therefore, refreezing is allowed only if the θ value is above 0.01% (Wever et al., 2014). This value is above θ_{dry} to avoid refreezing and corresponding latent heat release of the very low amounts of water resulting from the fluxes between layers that are initialised at θ_{dry}. Only at the last time step of the flow routine is the refreezing process allowed to decrease the volumetric water content until θ_{dry}. After that, the pre-wetting~~

~~amounts of liquid water are subtracted at the end of the flow routine to maintain the mass conservation property of the firn model. At the end of the flow routine, if all the layers have a water content below ε_θ, we consider the firn column to be completely dry again so that the flow routine does not have to be called until the next melt event and computational time is largely saved.~~

~~A4 Dynamical time step adjustment~~

~~The numerical solving of RE uses a dynamically adjusted time step. Certain situations, such as the arrival of the wetting front at a stratigraphic transition, require a very small time step whereas larger time steps can be used in other cases without affecting numerical stability. Thus, the time step is adjusted according to the number of iterations, n_{it}, required to achieve convergence of the solution at the previous time step: decreased for a large number of iterations and increased for few iterations. Also, as in Wever et al. (2014) and D'Amboise et al. (2017), a back step case is used: the calculation is stopped and the time step automatically decreased if the solution fails to converge in 15 iterations or if warning signs of instability appear (positive pressure head values, effective saturation exceeding 1 or differences in successive pressure head values exceeding 10^{-3} m). The time step is bounded between 10^{-20} s and 900 s. The procedure can be summarised as follows:~~

$$\Delta t_{RE}^{t} = \begin{cases} 1.25\ \Delta t_{RE}^{t-1}, & if\ n_{it} \leq 5 \\ \Delta t_{RE}^{t-1}, & if\ 5 < n_{it} < 10 \\ 0.5\ \Delta t_{RE}^{t-1}, & if\ 10 \leq n_{it} \leq 15 \\ back\ step, & if\ n_{it} > 15 \end{cases} \tag{A2}$$

~~A5 Saturated layers and aquifer treatment~~

~~If water reaches an impermeable ice layer, the layer above progressively becomes saturated. This means that its hydraulic conductivity progressively increases. As a consequence, the incoming flow becomes very large whereas the outgoing flow is forced to be zero. To deal with this issue, the layer has to be set impermeable once close to saturation and this process must go on for layers above when these reach saturation in turn. When an aquifer is present at the bottom of the domain, the amount of water is held in memory at the start of the flow routine and the end of the domain is set as the top of the aquifer. All the percolating water reaching the end of the domain is added to the aquifer amount and at the end of the routine, this total amount is redistributed in the bottom layers.~~

~~A6 Partial RE solving~~

~~In order to save computational time, the RE is not necessarily solved for the entire domain. If a significant part of the lowest layers is dry, we do not proceed to the calculations for this lower dry part. Starting from the surface, we look for the lowest layer where the water content is at least ε_θ + 0.01 % (above the minimum water content after refreezing). Then we take as lower limit for the RE calculation the layer situated 50 cm below this lowest wet layer. This is recalculated at every time step of the RE solving, making the 50 cm addition largely sufficient to capture the wetting of the dry lower part. If the lowest wet~~

~~layer is less than 50 cm above the end of the domain, then the RE is calculated on the entire domain. This is applied in both the matrix and the preferential flow domains.~~

~~A7 Refreezing in the preferential flow domain~~

~~Contrarily to the SNOWPACK model, there is a particular circumstance for which we apply refreezing directly in the preferential flow domain: if a cold front (subfreezing temperatures) propagates from the surface into a wet firn column, all the water present in the matrix flow domain will progressively be refrozen, starting from the surface layer. It would be unrealistic to keep liquid water present in the preferential flow domain of layers that are above this cold front. Thus, if starting from the surface, the entire firn column until a particular layer that holds some liquid water in the preferential flow domain is at subfreezing temperatures, this liquid water is refrozen. In such cases, the firn column is dry in both domains until the depth delimited by the cold front. Simulations without this refreezing implementation reached very similar results but required more computational time.~~

~~A8 Merging process~~

~~The CFM usually considers every accumulation event as a new layer. However, as we use three hourly accumulation forcing, the firn layer could consist of a high number of extremely fine layers. Because the calculation time for the RE is very dependent on the number of distinct layers in the firn column, we chose to merge any layer thinner than 2 cm with the underlying layer. If this was applied to the surface layer, every accumulation event of less than 2 cm snow would be immediately merged with the previous surface layer. In the case where a high number of successive snowfall events would be below the 2 cm threshold, these would all be merged within the same layer, possibly becoming very thick. To avoid this, the newly added snow layer is merged with the previous surface layer only if the latter is below the 2 cm threshold. However, newly-added layers that are less than 0.01 mm thick are always merged with the layer below. It is important to keep a high vertical resolution when simulating the percolation process with the RE, as this flow equation is highly sensitive to structural heterogeneities in the firn. If the merging process is too lenient, this leads to the smoothing of heterogeneities such as sharp grain-size or density transitions. Moreover, using a coarse resolution would lead to only an approximation of the water percolation because water content is always homogeneous in a single layer. Thus, as soon as water percolates at the top of a given layer, it is distributed in the entire layer.~~

References

Anderson, E. A.: A point energy and mass balance model of a snow cover, NOAA Tech. Rep. NWS, 19, 1976.

Arthern, R. J., Vaughan, D. G., Rankin, A. M., Mulvaney, R. and Thomas, E. R.: In situ measurements of Antarctic snow compaction compared with predictions of models, J. Geophys. Res. Earth Surf., 115, 1–12, doi:10.1029/2009JF001306, 2010.

Avanzi, F., Hirashima, H., Yamaguchi, S., Katsushima, T. and De Michele, C.: Observations of capillary barriers and preferential flow in layered snow during cold laboratory experiments, Cryosph., 10, 2013–2026, doi:10.5194/tc-10-2013-2016, 2016.

Calonne, N., Geindreau, C., Flin, F., Morin, S., Lesaffre, B., Rolland Du Roscoat, S. and Charrier, P.: 3-D image-based numerical computations of snow permeability: Links to specific surface area, density, and microstructural anisotropy, Cryosphere, 6, 939–951, doi:10.5194/tc-6-939-2012, 2012.

Celia, M. A., Bouloutas, E. T. and Zarba, R. L.: A General Mass-Conservative Numerical Solution for the Unsaturated Flow Equation, Water Resour. Res., 26, 1483–1496, doi:10.1029/90wr00196, 1990.

Coléou, C. and Lesaffre, B.: Irreducible water saturation in snow: experimental results in a cold laboratory, Ann. Glaciol., 26, 64–68, doi:10.3189/1998AoG26-1-64-68, 1998.

Cox, C., Humphrey, N. and Harper, J.: Quantifying meltwater refreezing along a transect of sites on the Greenland Icesheet, Cryosph., 8, 5485–5509, doi:10.5194/tcd-8-5485-2014, 2015.

D'Amboise, C. J. L., Müller, K., Oxarango, L., Morin, S. and Schuler, T. V.: Implementation of a physically based water percolation routine in the CROCUS (V7) snowpack model, Geosci. Model Dev. Discuss., 1–32, doi:10.5194/gmd-2017-56, 2017.

Fettweis, X.: Reconstruction of the 1979–2006 Greenland ice sheet surface mass balance using the regional climate model MAR, Cryosph., 1, 21–40, doi:10.5194/tc-1-21-2007, 2007.

Forster, R. R., Box, J. E., van den Broeke, M. R., Miège, C., Burgess, E. W., van Angelen, J. H., Lenaerts, J. T. M., Koenig, L. S., Paden, J., Lewis, C., Gogineni, S. P., Leuschen, C. and McConnell, J. R.: Extensive liquid meltwater storage in firn within the Greenland ice sheet, Nat. Geosci., 7, 95–98, doi:10.1038/ngeo2043, 2014.

Forsyth, P. A., Wu, Y. S. and Pruess, K.: Robust numerical methods for saturated-unsaturated flow with dry initial conditions in heterogeneous media, Adv. Water Resour., 18, 25–38, doi:10.1016/0309-1708(95)00020-J, 1995.

Gascon, G., Sharp, M., Burgess, D., Bezeau, P., Bush, A. B. G., Morin, S. and Lafaysse, M.: How well is firn densification represented by a physically based multilayer model? Model evaluation for Devon Ice Cap, Nunavut, Canada, J. Glaciol., 60, 694–704, doi:10.3189/2014JoG13J209, 2014.

Gregory, S. A., Albert, M. R. and Baker, I.: Impact of physical properties and accumulation rate on pore close-off in layered firn, Cryosphere, 8, 91–105, doi:10.5194/tc-8-91-2014, 2014.

Gow, A., Meese, D. and Bialas, R.: Accumulation variability, density profiles and crystal growth trends in ITASE firn and ice cores from West Antarctica, Annals of Glaciology, 39, 101–109, 2004.

Harper, J., Humphrey, N., Pfeffer, W. T., Brown, J. and Fettweis, X.: Greenland ice-sheet contribution to sea-level rise buffered by meltwater storage in firn, Nature, 491, 240–243, doi:10.1038/nature11566, 2012.

Helsen, M. M., van den Broeke, M. R., van de Wal, R. S. W., van de Berg, W. J., van Meijgaard, E., Davis, C. H., Li, Y. and Goodwin, I.: Elevation changes in antarctica mainly determined by accumulation variability, Science (80-.)., 320, 1626–1629, doi:10.1126/science.1153894, 2008.

Herron, M. and Langway, C.: Firn densification: an empirical model, J. Glaciol., 25, 1980.

Hirashima, H., Yamaguchi, S., Sato, A. and Lehning, M.: Numerical modeling of liquid water movement through layered snow based on new measurements of the water retention curve, Cold Reg. Sci. Technol., 64, 94–103, doi:10.1016/j.coldregions.2010.09.003, 2010.

Hirashima, H., Yamaguchi, S. and Katsushima, T.: A multi-dimensional water transport model to reproduce preferential flow in the snowpack, Cold Reg. Sci. Technol., 108, 80–90, doi:10.1016/j.coldregions.2014.09.004, 2014.

Huang, K., Mohanty, B. P. and van Genuchten, M. T.: Method To Solve the Variably Saturated Flow Equation, J. Hydrol., 178, 69–91, 1996.

Humphrey, N. F., Harper, J. T. and Pfeffer, W. T.: Thermal tracking of meltwater retention in Greenland's accumulation area, J. Geophys. Res. Earth Surf., 117, 1–11, doi:10.1029/2011JF002083, 2012.

Jordan, R.: Effects of capillary discontinuities on water flow and water retention in layered snowcovers, Def. Sci. J., 45, 79–91, 1995.

Katsushima, T., Kumakura, T. and Takeuchi, Y.: A multiple snow layer model including a parameterization of vertical water channel process in snowpack, Cold Reg. Sci. Technol., 59, 143–151, doi:10.1016/j.coldregions.2009.09.002, 2009.

Katsushima, T., Yamaguchi, S., Kumakura, T. and Sato, A.: Experimental analysis of preferential flow in dry snowpack, Cold Reg. Sci. Technol., 85, 206–216, doi:10.1016/j.coldregions.2012.09.012, 2013.

Koenig, L. S., Miège, C., Forster, R. R. and Brucker, L.: Initial in situ measurements of perennial meltwater storage in the Greenland firn aquifer, Geophys. Res. Lett., 41, 81–85, doi:10.1002/2013GL058083, 2014.

Kuipers Munneke, P., Ligtenberg, S. R. M., van den Broeke, M. R., van Angelen, J. H. and Forster, R. R.: Explaining the presence of perennial liquid water bodies in the firn of the Greenland Ice Sheet, Geophys. Res. Lett., 41, 476–483, doi:10.1002/2013GL058389, 2014.

Kuipers Munneke, P., Ligtenberg, S. R. M., Suder, E. A. and van den Broeke, M. R.: A model study of the response of dry and wet firn to climate change, Ann. Glaciol., 56, 1–8, doi:10.3189/2015AoG70A994, 2015a.

Kuipers Munneke, P., Ligtenberg, S. R. M., Noël, B. P. Y., Howat, I. M., Box, J. E., Mosley-Thompson, E., McConnell, J. R., Steffen, K., Harper, J. T., Das, S. B. and van den Broeke, M. R.: Elevation change of the Greenland ice sheet due to surface mass balance and firn processes, 1960-2013, Cryosph., 9, 3541–3580, doi:10.5194/tcd-9-3541-2015, 2015b.

Langen, P. L., Fausto, R. S., Vandecrux, B., Mottram, R. H. and Box, J. E.: Liquid Water Flow and Retention on the Greenland Ice Sheet in the Regional Climate Model HIRHAM5: Local and Large-Scale Impacts, Front. Earth Sci., 4, doi:10.3389/feart.2016.00110, 2017.

Li, J. and Zwally, H. J.: Modeling of firn compaction for estimating ice-sheet mass change from observed ice-sheet elevation change, Ann. Glaciol., 52, 1–7, doi:10.3189/172756411799096321, 2011.

Linow, S., Hörhold, M. W. and Freitag, J.: Grain-size evolution of polar firn: A new empirical grain growth parameterization based on X-ray microcomputer tomography measurements, J. Glaciol., 58, 1245–1252, doi:10.3189/2012JoG11J256, 2012.

Lyapustin, A., Tedesco, M., Wang, Y., Aoki, T., Hori, M., and Kokhanovsky, A.: Retrieval of snow grain size over Greenland from MODIS, Remote Sens. Environ., 113, 2463–2475, doi:10.1016/j.rse.2009.05.008, 2009.

Machguth, H., Macferrin, M., van As, D., Box, J. E., Charalampidis, C., Colgan, W., Fausto, R. S., Meijer, H. A. J., Mosley-Thompson, E. and van de Wal, R. S. W.: Greenland meltwater storage in firn limited by near-surface ice formation, Nat. Clim. Chang., 6, 390–393, doi:10.1038/nclimate2899, 2016.

Marsh, P. and Woo, M. -K: Wetting front advance and freezing of meltwater within a snow cover: 1. Observations in the Canadian Arctic, Water Resour. Res., 20, 1853–1864, doi:10.1029/WR020i012p01853, 1984.

McMillan, M., Leeson, A., Shepherd, A., Briggs, K., Armitage, T., Hogg, A., Kuipers Munneke, P., van den Broeke, M., Noël, B., van de Berg, W. J., Ligtenberg, S., Horwath, M., Groh, A., Muir, A. and Gilbert, L.: A high-resolution record of Greenland mass balance, Geophys. Res. Lett., 7002–7010, doi:10.1002/2016GL069666.Received, 2016.

Morris, E. M. and Wingham, D. J.: Densification of polar snow: Measurements, modeling, and implications for altimetry, J. Geophys. Res. Earth Surf., 119, 349–365, doi:10.1002/2013JF002898, 2014.

Mualem, Y.: A new model for predicting the hydraulic conductivity of unsaturated porous media, Water Resour. Res., 12, 564–566, 1976.

Nghiem, S. V., Hall, D. K., Mote, T. L., Tedesco, M., Albert, M. R., Keegan, K., Shuman, C. A., DiGirolamo, N. E., and Neuman, G.: The Extreme Melt across the Greenland Ice Sheet in 2012, Geophys. Res. Lett., 39, L20502, doi:10.1029/2012GL053611, 2012.

Noël, B., van de Berg, W. J., van Wessem, J. M., van Meijgaard, E. and van As, D.: Modelling the climate and surface mass balance of polar ice sheets using RACMO2 – Part 1 : Greenland (1958 – 2016), Cryosph., 811–831, 2018.

Parry, V., Nienow, P., Mair, D., Scott, J., Hubbard, B., Steffen, K. and Wingham, D.: Investigations of meltwater refreezing and density variations in the snowpack and firn within the percolation zone of the Greenland ice sheet, Ann. Glaciol., 46, 61–68, doi:10.3189/172756407782871332, 2007.

Pfeffer, W. T. and Humphrey, N. F.: Determination of timing and location of water movement and ice-layer formation by temperature measurements in sub-freezing snow, J. Glaciol., 1996.

Pfeffer, W. T. and Humphrey, N. F.: Formation of ice layers by infiltration and refreezing of meltwater, Ann. Glaciol., 83–91, 1998.

Poinar, K., Joughin, I., Lilien, D., Brucker, L., Kehrl, L. and Nowicki, S.: Drainage of Southeast Greenland Firn Aquifer Water through Crevasses to the Bed, Front. Earth Sci., 5(February), 1–15, doi:10.3389/feart.2017.00005, 2017.

Reeh, N.: A nonsteady-state firn-densification model for the percolation zone of a glacier, J. Geophys. Res. Earth Surf., 113(3), 1–13, doi:10.1029/2007JF000746, 2008.

Reijmer, C. H., van den Broeke, M. R., Fettweis, X., Ettema, J. and Stap, L. B.: Refreezing on the Greenland ice sheet: A comparison of parameterizations, Cryosphere, 6, 743–762, doi:10.5194/tc-6-743-2012, 2012.

Shepherd, A., Ivins, E., Rignot, E., Smith, B., van den Broeke, M., Velicogna, I., Whitehouse, P., Briggs, K., Joughin, I., Krinner, G., Nowicki, S., Payne, T., Scambos, T., Schlegel, N., Geruo, A., Agosta, C., Ahlstrøm, A., Babonis, G., Barletta, V., Blazquez, A., Bonin, J., Csatho, B., Cullather, R., Felikson, D., Fettweis, X., Forsberg, R., Gallee, H., Gardner, A., Gilbert, L., Groh, A., Gunter, B., Hanna, E., Harig, C., Helm, V., Horvath, A., Horwath, M., Khan, S., Kjeldsen, K. K., Konrad, H., Langen, P., Lecavalier, B., Loomis, B., Luthcke, S., McMillan, M., Melini, D., Mernild, S., Mohajerani, Y., Moore, P., Mouginot, J., Moyano, G., Muir, A., Nagler, T., Nield, G., Nilsson, J., Noel, B., Otosaka, I., Pattle, M. E., Peltier, W. R., Pie, N., Rietbroek, R., Rott, H., Sandberg-Sørensen, L., Sasgen, I., Save, H., Scheuchl, B., Schrama, E., Schröder, L., Seo, K. W., Simonsen, S., Slater, T., Spada, G., Sutterley, T., Talpe, M., Tarasov, L., van de Berg, W. J., van der Wal, W., van Wessem, M., Vishwakarma, B. D., Wiese, D. and Wouters, B.: Mass balance of the Antarctic Ice Sheet from 1992 to 2017, Nature, 558, 219–222, doi:10.1038/s41586-018-0179-y, 2018.

Simonsen, S. B., Stenseng, L., Adalgeirsdóttir, G., Fausto, R. S., Hvidberg, C. S. and Lucas-Picher, P.: Assessing a multilayered dynamic firn-compaction model for Greenland with ASIRAS radar measurements, J. Glaciol., 59, 545–558, doi:10.3189/2013JoG12J158, 2013.

Sommers, A. N., Rajaram, H., Weber, E. P., MacFerrin, M. J., Colgan, W. T. and Stevens, C. M.: Inferring Firn Permeability from Pneumatic Testing: A Case Study on the Greenland Ice Sheet, Front. Earth Sci., 5(March), 1–12, doi:10.3389/feart.2017.00020, 2017.

Steger, C. R., Reijmer, C. H., van den Broeke, M. R., Wever, N., Forster, R. R., Koenig, L. S., Kuipers Munneke, P., Lehning, M., Lhermitte, S., Ligtenberg, S. R. M., Miège, C. and Noël, B. P. Y.: Firn Meltwater Retention on the Greenland Ice Sheet: A Model Comparison, Front. Earth Sci., 5(January), doi:10.3389/feart.2017.00003, 2017.

Stevens, C. M.: Investigations of physical processes in polar firn through modeling and field measurements, PhD dissertation, University of Washington, Seattle, 2018.

Szymkiewicz, A.: Approximation of internodal conductivities in numerical simulation of one-dimensional infiltration, drainage, and capillary rise in unsaturated soils, Water Resour. Res., 45, 1–16, doi:10.1029/2008WR007654, 2009.

van Angelen, J. H., van den Broeke, M. R., Wouters, B. and Lenaerts, J. T. M.: Contemporary (1960–2012) Evolution of the Climate and Surface Mass Balance of the Greenland Ice Sheet, Surv. Geophys., 35, 1155–1174, doi:10.1007/s10712-013-9261-z, 2014.

van As, D., Box, J. E. and Fausto, R. S.: Challenges of Quantifying Meltwater Retention in Snow and Firn: An Expert Elicitation, Front. Earth Sci., 4(November), 1–5, doi:10.3389/feart.2016.00101, 2016.

van den Broeke, M. R., Enderlin, E. M., Howat, I. M., Kuipers Munneke, P., Noël, B. P. Y., van de Berg, W. J., van Meijgaard, E. and Wouters, B.: On the recent contribution of the Greenland ice sheet to sea level change, Cryosphere, 10, 1933–1946, doi:10.5194/tc-10-1933-2016, 2016.

van Genuchten, M.: A closed form equation for predicting the hydraulic conductivity of unsaturated soils., Soil Sci. Soc. Am. J., 44, 892–898, 1980.

van Kampenhout, L., Lenaerts, J. T. M., Lipscomb, W. H., Sacks, W. J., Lawrence, D. M., Slater, A. G. and van den Broeke, M. R.: Improving the Representation of Polar Snow and Firn in the Community Earth System Model, J. Adv. Model. Earth Syst., 9, 2583–2600, doi:10.1002/2017MS000988, 2017.

van Pelt, W. J. J., Oerlemans, J., Reijmer, C. H., Pohjola, V. A., Pettersson, R. and van Angelen, J. H.: Simulating melt, runoff and refreezing on Nordenskiöldbreen, Svalbard, using a coupled snow and energy balance model, Cryosphere, 6, 641–659, doi:10.5194/tc-6-641-2012, 2012.

Vionnet, V., Brun, E., Morin, S., Boone, A., Faroux, S., Le Moigne, P., Martin, E. and Willemet, J. M.: The detailed snowpack scheme CROCUS and its implementation in SURFEX v7.2, Geosci. Model Dev., 5, 773–791, doi:10.5194/gmd-5-773-2012, 2012.

Waldner, P. A., Schneebeli, M., Schultze-Zimmermann, U. and Flühler, H.: Effect of snow structure on water flow and solute transport, Hydrol. Process., 18, 1271–1290, doi:10.1002/hyp.1401, 2004.

Wever, N., Fierz, C., Mitterer, C., Hirashima, H. and Lehning, M.: Solving Richards Equation for snow improves snowpack meltwater runoff estimations in detailed multi-layer snowpack model, Cryosphere, 8, 257–274, doi:10.5194/tc-8-257-2014, 2014.

Wever, N., Würzer, S., Fierz, C. and Lehning, M.: Simulating ice layer formation under the presence of preferential flow in layered snowpacks, Cryosphere, 10, 2731–2744, doi:10.5194/tc-10-2731-2016, 2016.

Williams, M. W., Erickson, T. A. and Petrzelka, J. L.: Visualizing meltwater flow through snow at the centimetre-to-metre scale using a snow guillotine, Hydrol. Process., 24, 2098–2110, doi:10.1002/hyp.7630, 2010.

Yamaguchi, S., Katsushima, T., Sato, A. and Kumakura, T.: Water retention curve of snow with different grain sizes, Cold Reg. Sci. Technol., 64, 87–93, doi:10.1016/j.coldregions.2010.05.008, 2010.

Yamaguchi, S., Watanabe, K., Katsushima, T., Sato, A. and Kumakura, T.: Dependence of the water retention curve of snow on snow characteristics, Ann. Glaciol., 53, 6–12, doi:10.3189/2012AoG61A001, 2012.

Zuo, Z. and Oerlemans, J.: Modelling albedo and specific balance of the Greenland ice sheet: Calculations for the Søndre Stromfjord transect, J. Glaciol., 42, 305–316, doi:10.3198/1996JoG42-141-305-317, 1996.

Bucket Model (BK~~BM~~)					Single-domain RE (R1M)					Dual-Permeability RE (DPM)				
Impermeability threshold (ip)			Water-holding capacity (wh)		Impermeability threshold (ip)			Grain-size formulation (gr)		Impermeability threshold (ip)			Grain-size formulation (gr)	
780	810	830	0.02	CL	780	810	830	LK	A	780	810	830	LK	A

Table 1. Summary of the sensitivity tests

	Refreezing / Inflow (1980-2011)	Refreezing / Inflow (2012-2016)	Runoff / Inflow (1980-2011)	Runoff / Inflow (2012-2016)	Top 15 m FAC [m] (anomaly vs observations)	T 10m [K] (anomaly vs observations [K])
BK (wh02 ip810)	0.96	0.67	0.01	0.31	5.01 (-4 %)	260.88 (+0.21)
R1M (grLK ip810)	0.91	0.63	0.05	0.35	4.99 (-4 %)	260.27 (-0.40)
DPM (grLK ip810)	0.95	0.95	0.02	0.03	4.38 (-16 %)	263.39 (+2.72)
Observations	/	/	/	/	5.21	260.67
DPM (grLK ip780)	0.95	0.96	0.02	0.02	4.39 (-16 %)	263.45 (+2.78)
BK (wh02~~wh2~~ ip780)	0.96	0.60	0.02	0.38	5.15 (-1 %)	260.68 (+0.01)
BK (whCL ip810)	0.92	0.62	0.05	0.36	5.21 (+0 %)	259.40 (-1.27)
BK (wh02 ip830)	0.97	0.68	0.00	0.31	4.96 (-5 %)	260.98 (+0.31)
R1M (grA ip810)	0.83	0.59	0.14	0.38	5.19 (-0 %)	259.64 (-1.03)
DPM (grA ip810)	0.93	0.93	0.04	0.05	4.40 (-16 %)	263.08 (+2.41)
HL DPM (grLK ip810)	0.95	0.96	0.02	0.02	4.16 (-20 %)	263.78 (+3.11)
KM DPM (grLK ip810)	0.95	0.95	0.02	0.02	3.35 (-36 %)	262.74 (+2.07)
HL R1M (grLK ip810)	0.90	0.72	0.07	0.26	4.65 (-11 %)	260.41 (-0.26)
KM R1M (grLK ip810)	0.91	0.75	0.06	0.23	4.00 (-23 %)	260.26 (-0.41)

Table 2. Model outputs at DYE-2 site. / indicates no data.

	Refreezing / Inflow (1980-2011)	Refreezing / Inflow (2012-2015)	Runoff / Inflow (1980-2011)	Runoff / Inflow (2012-2015)	Top 15 m FAC [m] (anomaly vs observations)	T 10m [K] (anomaly vs observations [K])
BK (wh02 ip810)	0.97	0.97	0.00	0.00	6.78 (-3 %)	257.91 (+1.94)
R1M (grLK ip810)	0.94	0.89	0.02	0.08	6.78 (-3 %)	257.39 (+1.42)
DPM (grLK ip810)	0.95	0.94	0.01	0.03	6.77 (-3 %)	258.18 (+2.21)
Observations	/	/	/	/	6.98	255.97
BK (whCL ip810)	0.95	0.94	0.00	0.02	6.81 (-2 %)	256.97 (+1.00)
R1M (grA ip810)	0.92	0.83	0.04	0.13	6.83 (-2 %)	256.99 (+1.02)
DPM (grA ip810)	0.95	0.92	0.01	0.04	6.78 (-3 %)	258.11 (+2.14)
HL R1M (grLK ip810)	0.93	0.86	0.04	0.11	8.13 (+17 %)	258.19 (+1.22)
KM R1M (grLK ip810)	0.93	0.86	0.03	0.10	7.53 (+8 %)	257.74 (+1.77)

Table 3. Model outputs at NASA-SE site. / indicates no data.

	Refreezing / Inflow (1980-2011)	Refreezing / Inflow (2012)	Runoff / Inflow (1980-2011)	Runoff / Inflow (2012)	Top 15 m FAC [m] (anomaly vs observations)	T 10m [K] (anomaly vs observations [K])
BK (wh02 ip810)	0.81	0.18	0.17	0.81	3.92 (+59%)	263.93 (-1.73)
R1M (grLK ip810)	0.74	0.20	0.23	0.79	3.69 (+50 %)	263.09 (-2.57)
DPM (grLK ip810)	0.91	0.77	0.07	0.23	2.40 (-2 %)	270.18 (+4.52)
Observations	/	/	/	/	2.46	265.66
DPM (grLK ip780)	0.91	0.75	0.07	0.25	2.77 (+13 %)	268.63 (+2.97)
DPM (grLK ip 830)	0.90	0.82	0.07	0.18	2.18 (-11%)	271.31 (+5.65)
BK (wh02 ip780)	0.78	0.19	0.21	0.81	4.11 (+67 %)	263.46 (-2.20)
BK (whCL ip810)	0.78	0.22	0.19	0.78	4.05 (+65 %)	262.23 (-3.43)
BK (wh02 ip830)	0.83	0.21	0.15	0.79	3.61 (+47 %)	264.69 (-0.97)
R1M (grLK ip830)	0.76	0.20	0.22	0.79	3.64 (+48 %)	263.21 (-2.45)
R1M (grA ip810)	0.66	0.26	0.31	0.73	4.08 (+66 %)	262.41 (-3.25)
DPM (grA ip810)	0.87	0.69	0.10	0.30	2.36 (-4 %)	270.28 (+4.62)
HL R1M (grLK ip810)	0.74	0.18	0.23	0.82	3.36 (+37 %)	263.34 (-2.32)
KM R1M (grLK ip810)	0.74	0.20	0.23	0.80	2.70 (+10%)	262.82 (-2.84)

Table 4. Model outputs at KAN-U site. / indicates no data.

	Refreezing / Inflow (1980-2011)	Refreezing / Inflow (2012)	Runoff / Inflow (1980-2011)	Runoff / Inflow (2012)	Top 15 m FAC [m] (anomaly vs observations)	T 10m [K] (anomaly vs observations [K])	Remaining water [m]
BK (HL wh02 ip810)	0.55	0.28	0.45	0.73	3.82 (-23 %)	271.75 (+0.10)	0
R1M (HL grLK ip810)	0.50	0.28	0.49	0.71	3.47 (-30 %)	270.94 (-0.71)	0
DPM (HL grLK ip810)	0.51	0.32	0.38	0.70	3.45 (-30 %) of which 0.81 m of water	273.15 (+1.5)	1.53
Observations	/	/	/	/	4.96	271.65	1.65
BK (HL whCL ip810)	0.60	0.23	0.38	0.81	3.38 (-32 %)	270.99 (-0.66)	0.09
R1M (HL grA ip810)	0.46	0.30	0.52	0.69	3.60 (-27 %)	269.77 (-1.88)	0
DPM (HL grA ip810)	0.51	0.36	0.39	0.70	3.36 (-32 %) of which 0.83 m of water	273.15 (+1.5)	1.48
DPM (HL grLK ip830)	0.51	0.29	0.39	0.70	3.57 (-28 %) of which 0.38 m of water	272.13 (+0.48)	1.64
CROCUS R1M (grLK ip810)	0.49	0.31	0.49	0.68	3.94 (-21%)	271.46 (-0.19)	0
KM R1M (grLK ip810)	0.51	0.37	0.45	0.99	2.29 (-54 %)	270.90 (-0.75)	0

Table 5. Model outputs at FA13 site. / indicates no data.

Variable/Parameter	Symbol	Value [unit]
Density	ρ	[kg m^{-3}]
Ice density	ρ_i	917 [kg m^{-3}]
Water density	ρ_w	1000 [kg m^{-3}]
Temperature	T	[K]
Mean annual surface temperature	T_{av}	[K]
Mean annual accumulation rate	$\dot{b}$	[m s^{-1}]
Gas constant	R	8.314 [J mol^{-1} K^{-1}]
Gravitational acceleration	g	9.81 [m s^{-2}]
Overburden pressure	σ	[kg m^{-1} s^{-2}]
Snow viscosity	η	[kg m^{-1} s^{-1}]
Firn viscosity parameters	η_0	7.62237 [kg s^{-1} m^{-1}]
	a_η	0.1 [K^{-1}]
	b_η	0.023 [m^3 kg^{-1}]
	c_η	358 [kg m^{-3}]
	f_1	4 [/]
	f_2	[/]
Firn thermal conductivity	k_s	[W m^{-1} K^{-1}]
Pressure head	h	[m]
Hydraulic conductivity	$K(\theta)$	[m s^{-1}]
Hydraulic conductivity at saturation	$Ksat$	[m s^{-1}]
Grain radius	r	[m]
Grain radius at surface	r_0	[m]
Grain growth activation energy	E_g	42.4 10^3 [J mol^{-1}]
Grain growth rate constant	k_g	1.3 10^{-7} [m^2 s^{-1}]
Initial grain-size parameters	b_0	0.781 [/]
	b_1	0.0085 [/]
	b_2	-0.279 [/]
Dynamic viscosity of liquid water at 273.15 K	μ	0.001792 [kg m^{-1} s^{-1}]
Volumetric water content	θ	[/]
Water holding capacity	θ_h	[/]
Mass proportion corresponding to water holding capacity	W_w	[/]
Residual water content	θ_r	[/]
Porosity	P	[/]
Fraction of the pore space allocated to preferential flow	F	0.02 [/]
Saturated water content	θ_{sat}	[/]
Effective saturation	Se	[/]
van Genuchten parameters	α, n, m	[/]
Water entry suction	h_{we}	[m]
Heat flow	Q	[J m^{-2} s^{-1}]
Specific latent heat of fusion	L_f	[J kg^{-1}]

~~Concentration of preferential flowpaths~~	~~N~~	~~[m^{-2}]~~
~~Preferential flow saturation threshold~~	~~Θ~~	~~0.1 [/]~~
~~Lateral runoff~~	~~Ru~~	~~[m]~~
~~Water in excess of the residual water content~~	~~L_{excess}~~	~~[m]~~
~~Characteristic runoff time~~	~~τ_{Ru}~~	~~[s]~~
~~Surface slope~~	~~S~~	~~[/]~~
	~~c_1~~	~~$1.296\ 10^5$ [s]~~
~~Runoff parameters~~	~~c_2~~	~~$2.16\ 10^6$ [s]~~
	~~c_3~~	~~140 [/]~~
~~Mass liquid water content~~	~~$\theta_{weight,\%}$~~	~~[%]~~

~~**Table A1. Variables and parameters notation**~~

~~Liquid water scheme [Abbreviation]~~	~~Bucket model [BK]; Single-domain Richards Equation [R1M]; Dual-permeability Richards Equation [DPM]~~
~~Compaction scheme [Abbreviation]~~	~~CROCUS [CR]; Herron and Langway (1980) [HL]; Kuipers Munneke et al. (2015) [KM]~~
~~Impermeability threshold [Abbreviation]~~	~~780 kg m^{-3} [ip780]; 810 kg m^{-3} [ip810]; 830 kg m^{-3} [ip830]~~
~~Water holding capacity [Abbreviation]~~	~~Constant at 2 % [wh02]; Coléou and Lesaffre (1998) [whCL]~~
~~Grain-size formulation [Abbreviation]~~	~~Linow et al. (2012) at surface and Katsushima et al. (2009) growth [grLK]; Constant at surface and Arthern et al. (2010) growth [grA]~~

~~**Table A2. Options for simulation experiments and their respective abbreviations**~~

	~~Liquid water scheme~~	~~Compaction scheme~~	~~Impermeability threshold~~	~~Water holding capacity~~	~~Grain-size formulation~~
~~BK (wh02 ip810)~~	~~BK~~	~~CROCUS~~	~~810~~	~~0.02~~	~~/~~
~~R1M (grLK ip810)~~	~~R1M~~	~~CROCUS~~	~~810~~	~~/~~	~~LK~~
~~DPM (grLK ip810)~~	~~DPM~~	~~CROCUS~~	~~810~~	~~/~~	~~LK~~
~~DPM (grLK ip780)~~	~~DPM~~	~~CROCUS~~	~~780~~	~~/~~	~~LK~~
~~DPM (grLK ip830)~~	~~DPM~~	~~CROCUS~~	~~830~~	~~/~~	~~LK~~
~~BK (wh02 ip780)~~	~~BK~~	~~CROCUS~~	~~780~~	~~0.02~~	~~/~~
~~BK (whCL ip810)~~	~~BK~~	~~CROCUS~~	~~810~~	~~CL~~	~~/~~
~~BK (wh02 ip830)~~	~~BK~~	~~CROCUS~~	~~830~~	~~0.02~~	~~/~~
~~R1M (grLK ip830)~~	~~R1M~~	~~CROCUS~~	~~830~~	~~/~~	~~LK~~
~~R1M (grA ip810)~~	~~R1M~~	~~CROCUS~~	~~810~~	~~/~~	~~A~~
~~DPM (grA ip810)~~	~~DPM~~	~~CROCUS~~	~~810~~	~~/~~	~~A~~
~~HL DPM (grLK ip810)~~	~~DPM~~	~~HL~~	~~810~~	~~/~~	~~LK~~
~~KM DPM (grLK ip810)~~	~~DPM~~	~~KM~~	~~810~~	~~/~~	~~LK~~
~~HL R1M (grLK ip810)~~	~~R1M~~	~~HL~~	~~810~~	~~/~~	~~LK~~
~~KM R1M (grLK ip810)~~	~~R1M~~	~~KM~~	~~810~~	~~/~~	~~LK~~

~~**Table A3. Details of the acronyms of the simulation experiments presented**~~

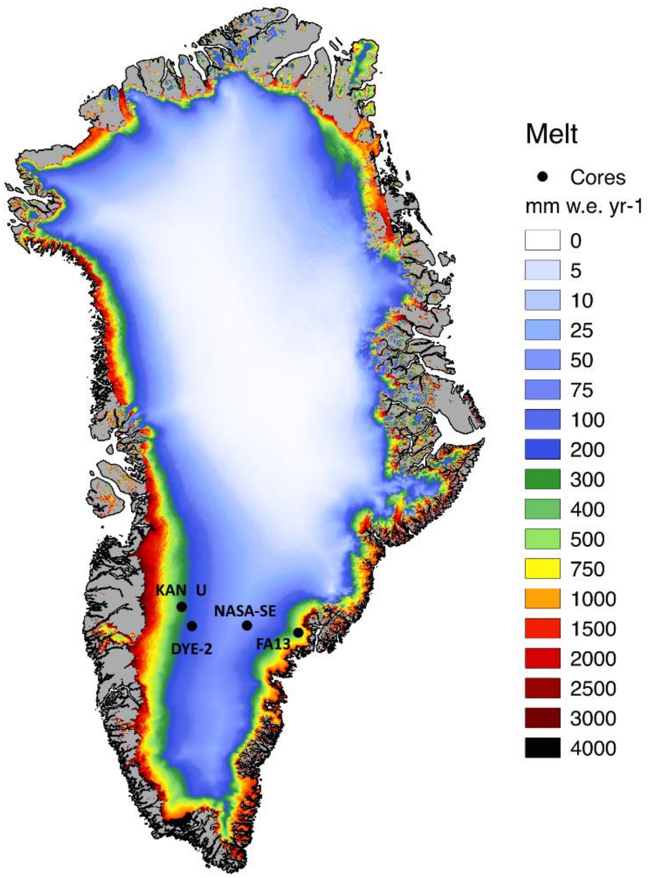

Figure 1. Study sites locations and mean annual melt rates (1958-2017) from RACMO2.3p2

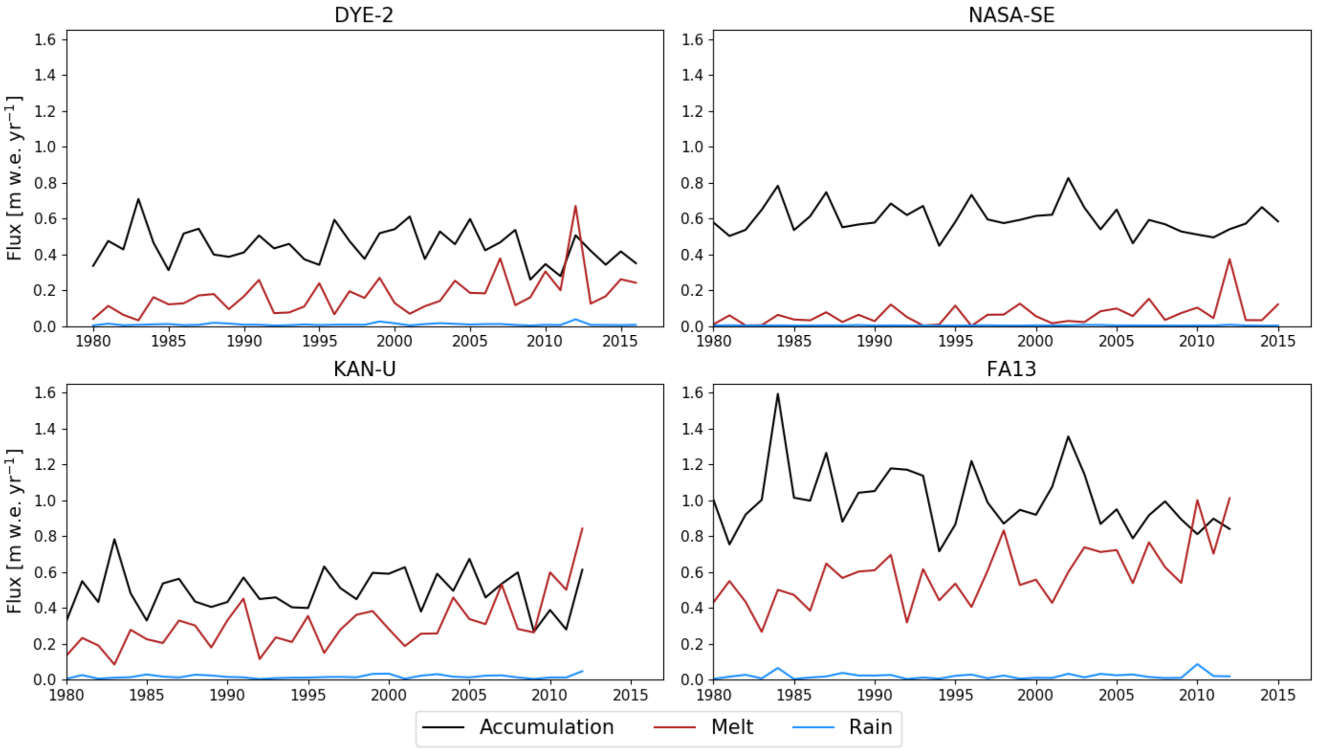

Figure 2. Annual surface mass fluxes from RACMO2.3p2 at the study sites (1980-drilling date)

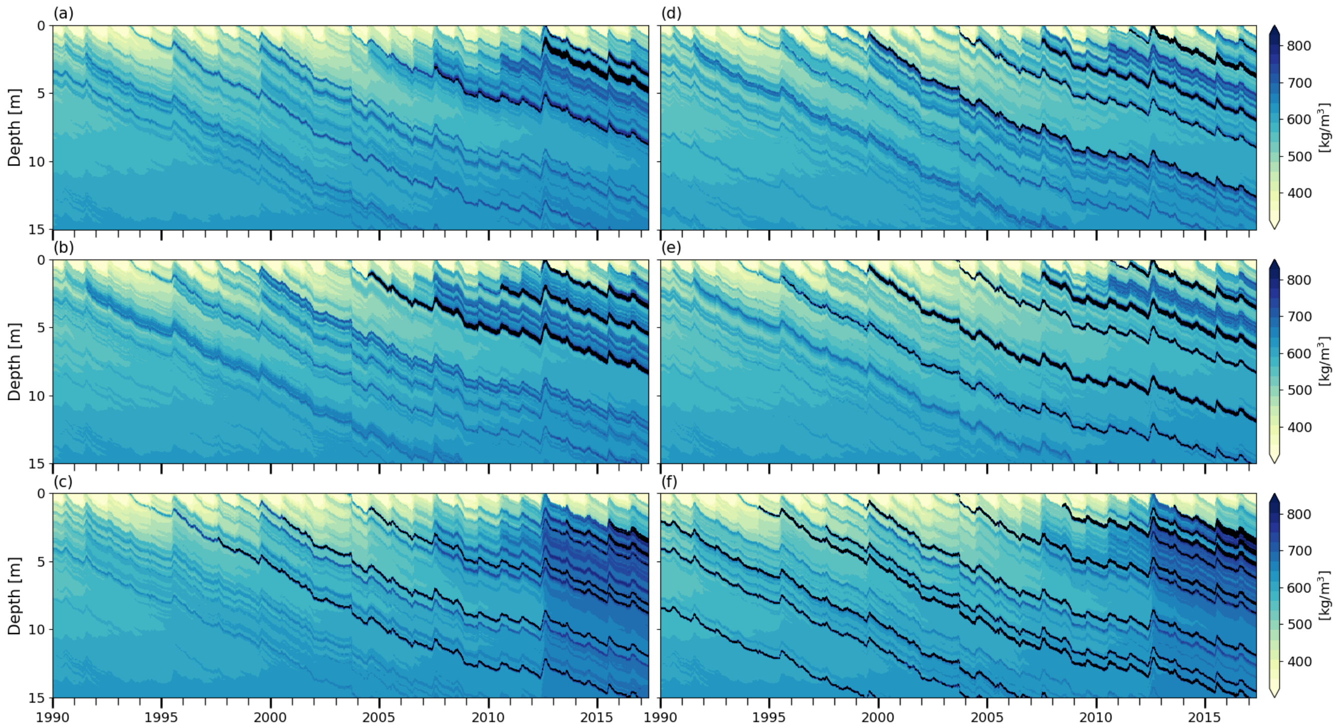

Figure 3. **Modelled~~Modeled~~ firn density at DYE-2 (a) BK wh02 ip810, (b) R1M grLK ip810, (c) DPM grLK ip810, (d) BK whCL ip810, (e) R1M grA ip810, (f) DPM grA ip810, black indicates solid ice. ~~layers~~**

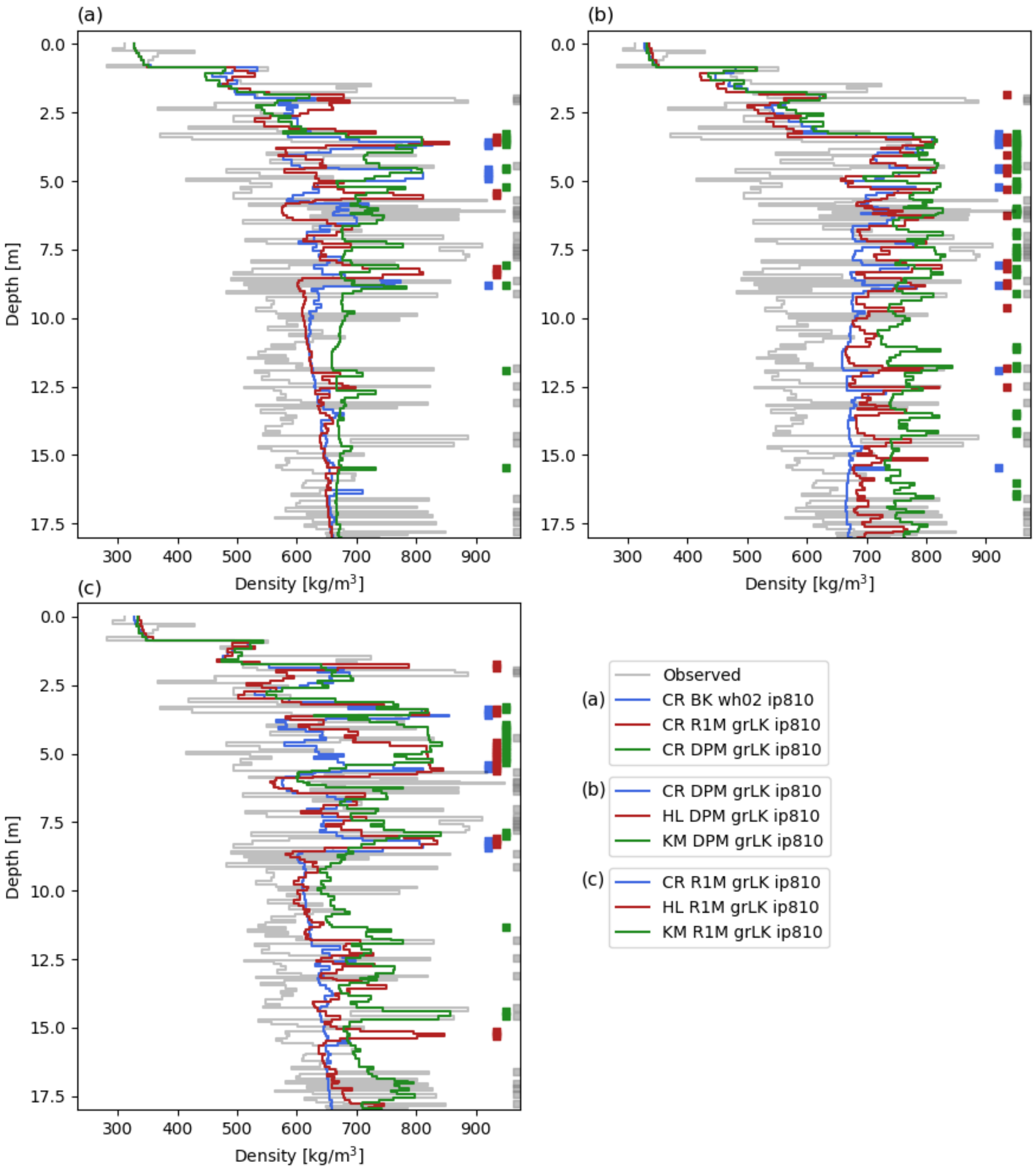
(a)
(b)
(c)
Depth [m]
Density [kg/m^3]
Observed
(a) CR BK wh02 ip810
CR R1M grLK ip810
CR DPM grLK ip810
(b) CR DPM grLK ip810
HL DPM grLK ip810
KM DPM grLK ip810
(c) CR R1M grLK ip810
HL R1M grLK ip810
KM R1M grLK ip810

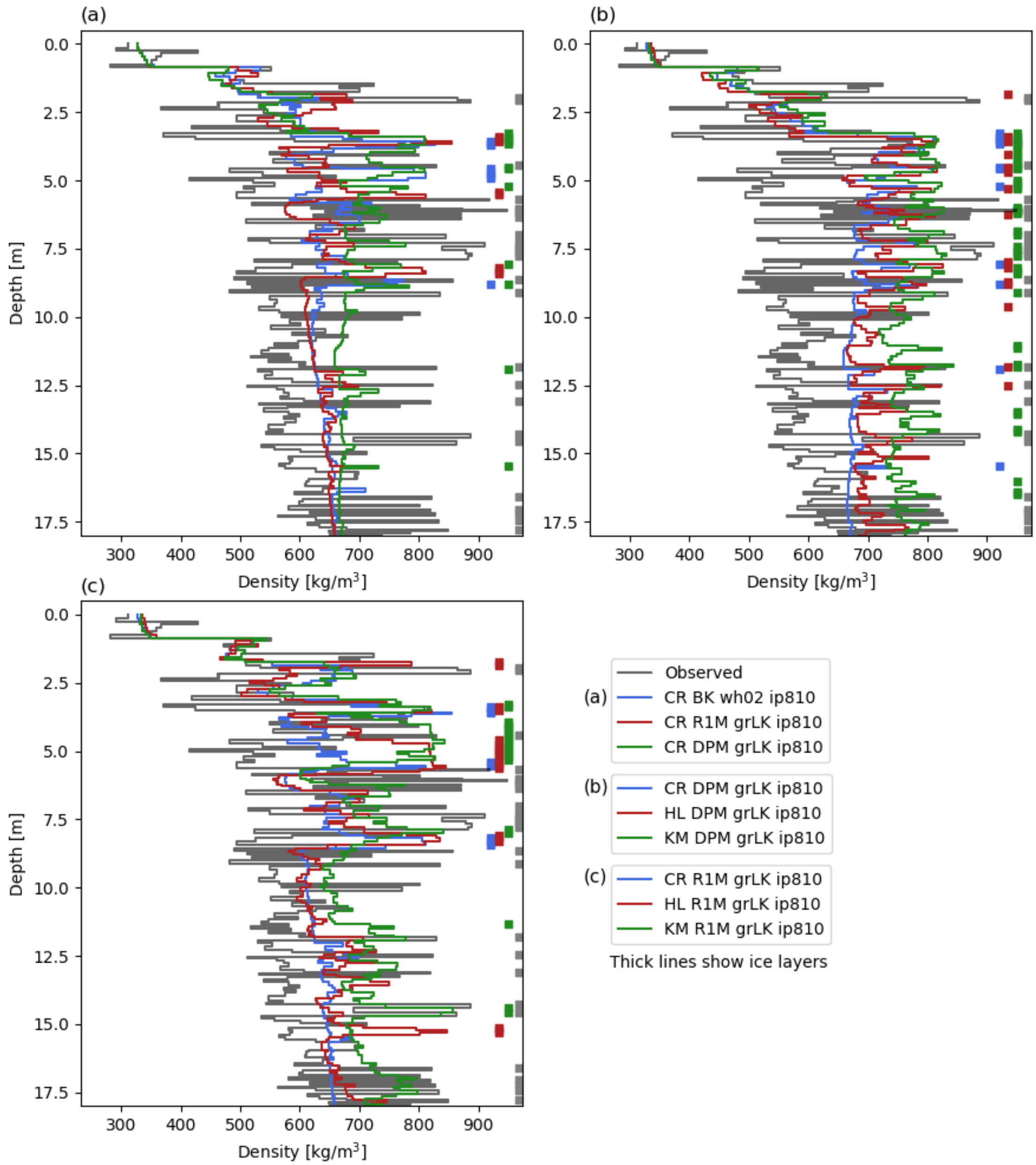

Figure 4. Measured and modelled depth-density profiles at DYE-2 on 11/05/2017. Thick vertical lines show ice layers. The modelled densities are averaged at the vertical resolution of the drilled core. CR: CROCUS, HL: Herron and Langway, KM: Kuipers Munneke.

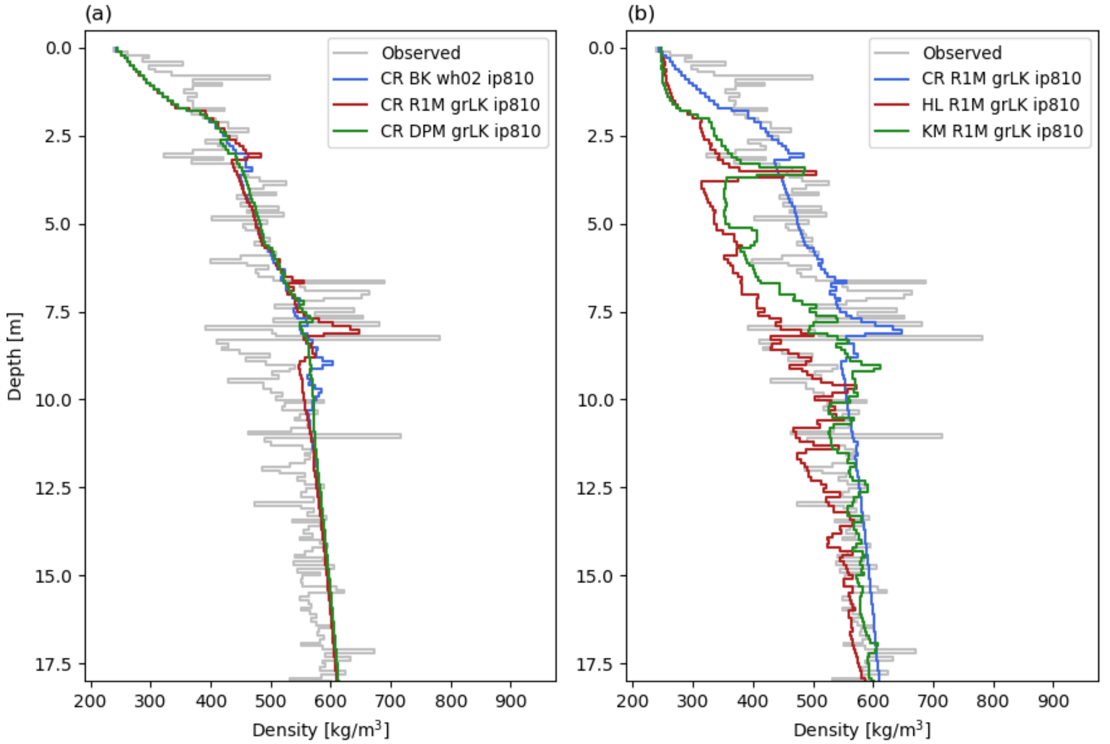
(a)
Observed
CR BK wh02 ip810
CR R1M grLK ip810
CR DPM grLK ip810
Depth [m]
Density [kg/m^3]
(b)
Observed
CR R1M grLK ip810
HL R1M grLK ip810
KM R1M grLK ip810
Depth [m]
Density [kg/m^3]

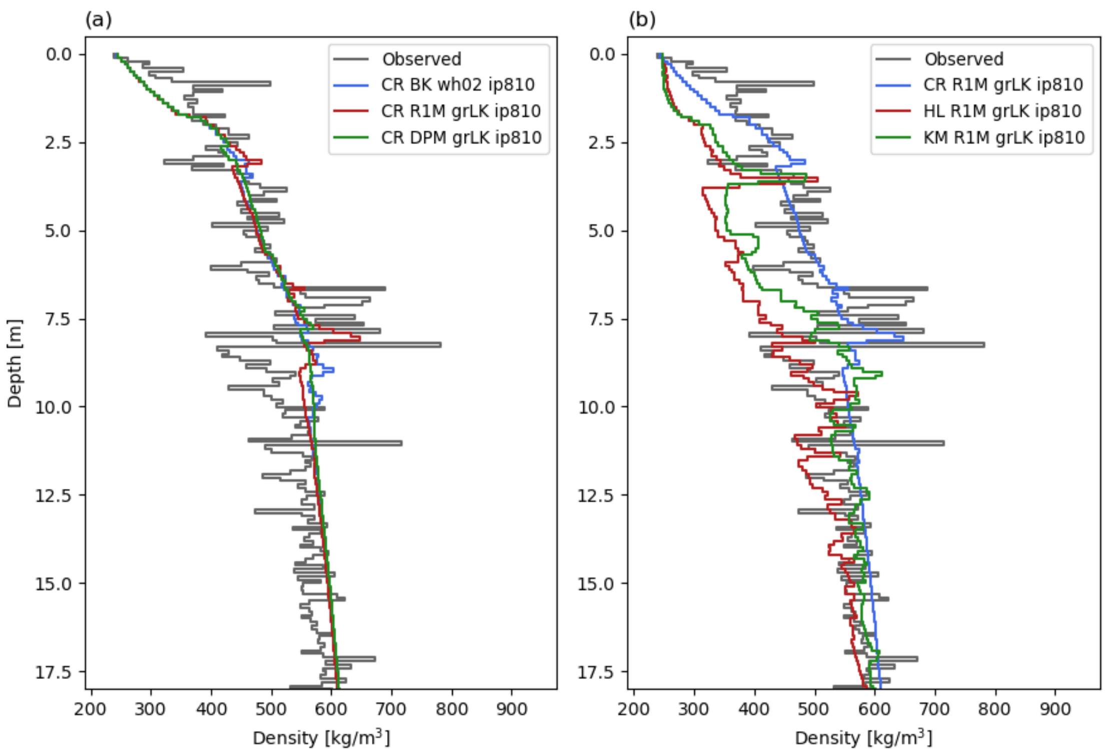
(a)
Observed
CR BK wh02 ip810
CR R1M grLK ip810
CR DPM grLK ip810
Depth [m]
Density [kg/m^3]
(b)
Observed
CR R1M grLK ip810
HL R1M grLK ip810
KM R1M grLK ip810
Depth [m]
Density [kg/m^3]

Figure 5. Measured and modelled depth-density profiles at NASA-SE on 04/05/2016. The modelled densities are averaged at the vertical resolution of the drilled core. CR: CROCUS, HL: Herron and Langway, KM: Kuipers Munneke.

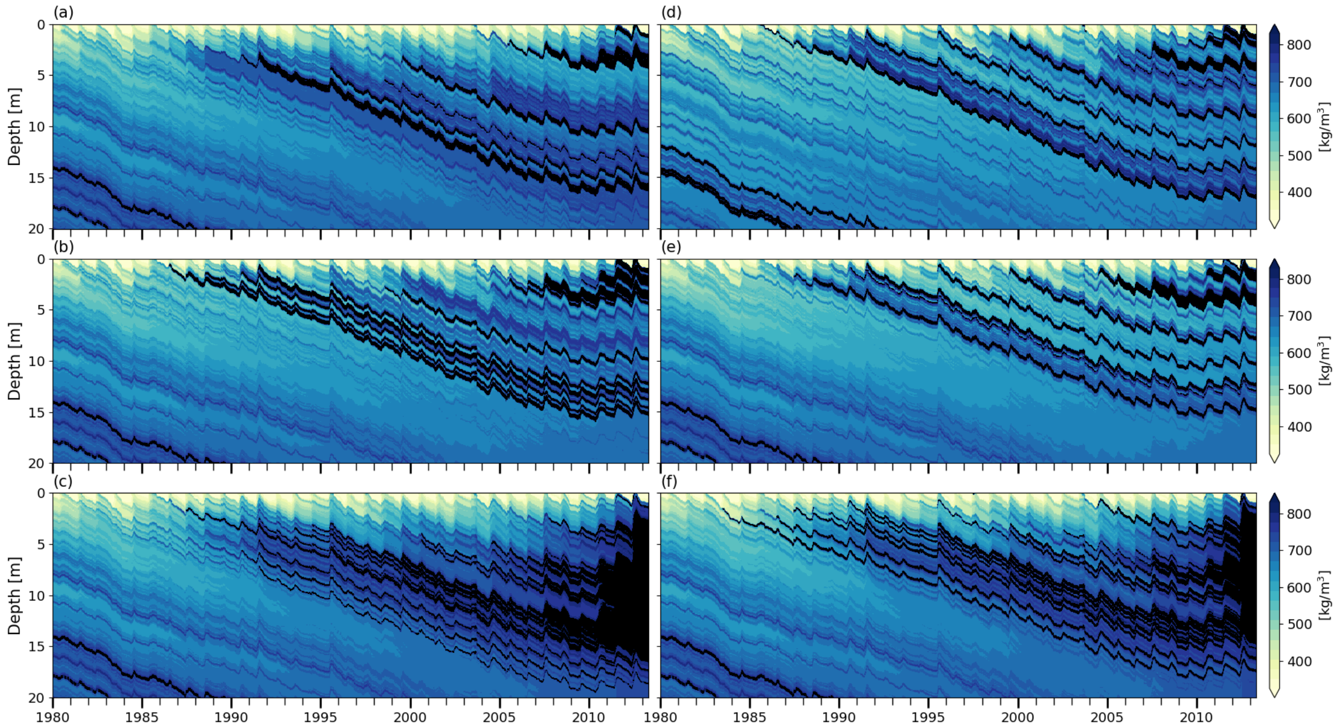

Figure 6. Modelled firn density at KAN-U. (a) BK wh02 ip810, (b) R1M grLK ip810, (c) DPM grLK ip810, (d) BK whCL ip810, (e) R1M grA ip810, (f) DPM grA ip810, black indicates ice layers

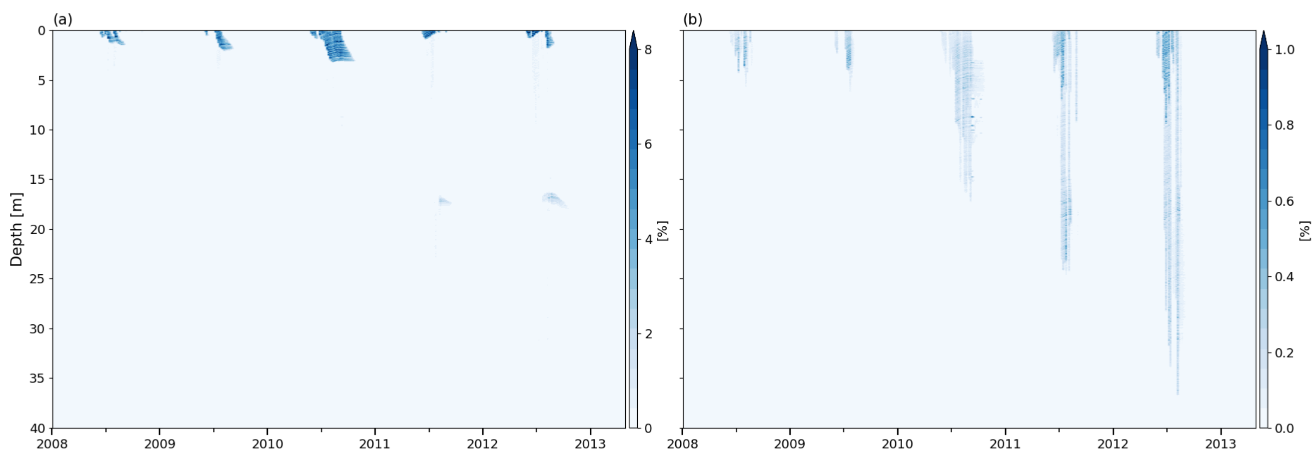

Figure 7. Volumetric water content at KAN-U site for DPM grLK ip810 in (a) Matrix flow domain, (b) Preferential flow domain, note difference in~~notice the different~~ scales

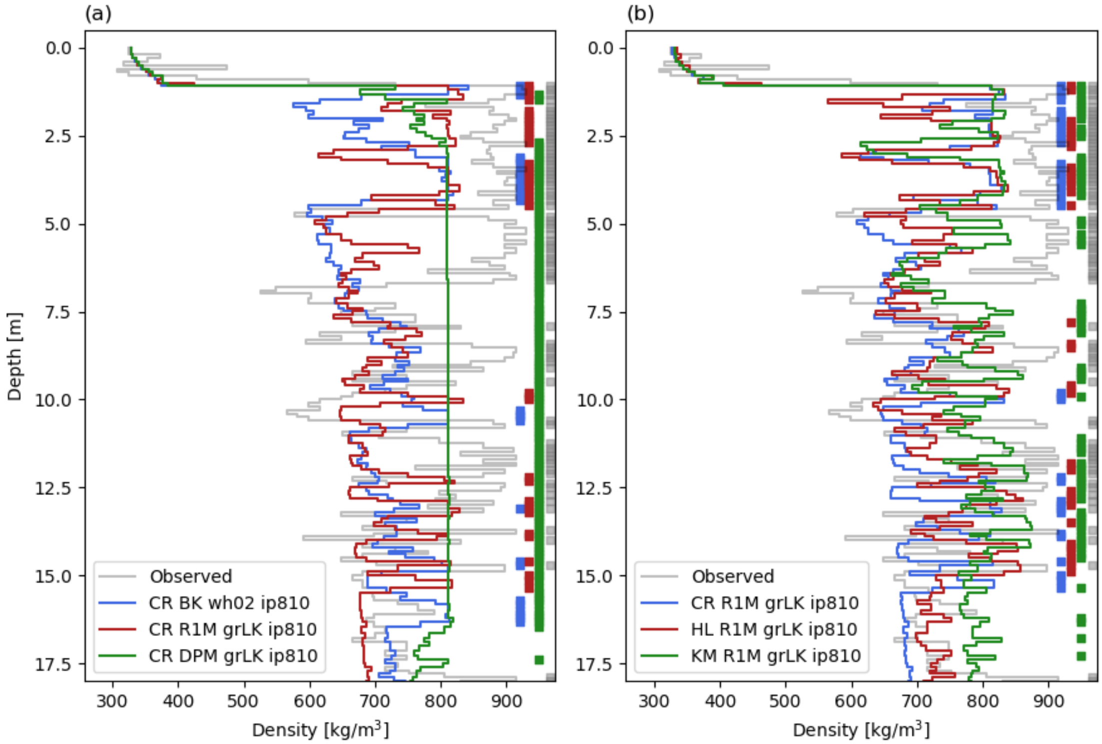

(a)
(b)
Depth [m]
0.0
2.5
5.0
7.5
10.0
12.5
15.0
17.5
300
400
500
600
700
800
900
Density [kg/m^3]
Observed
CR BK wh02 ip810
CR R1M grLK ip810
CR DPM grLK ip810
CR R1M grLK ip810
HL R1M grLK ip810
KM R1M grLK ip810

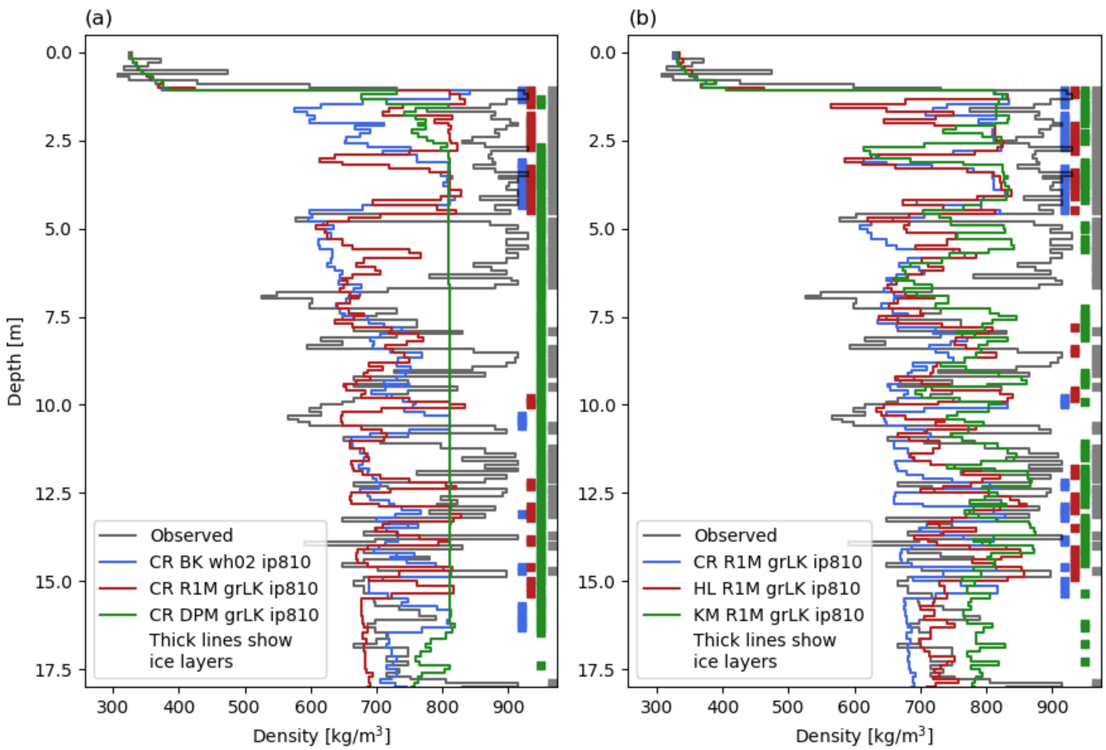

Figure 8. Measured and modelled depth-density profiles at KAN-U on 28/04/2013. Thick vertical lines show ice layers. The modelled densities are averaged at the vertical resolution of the drilled core. CR: CROCUS, HL: Herron and Langway, KM: Kuipers Munneke.

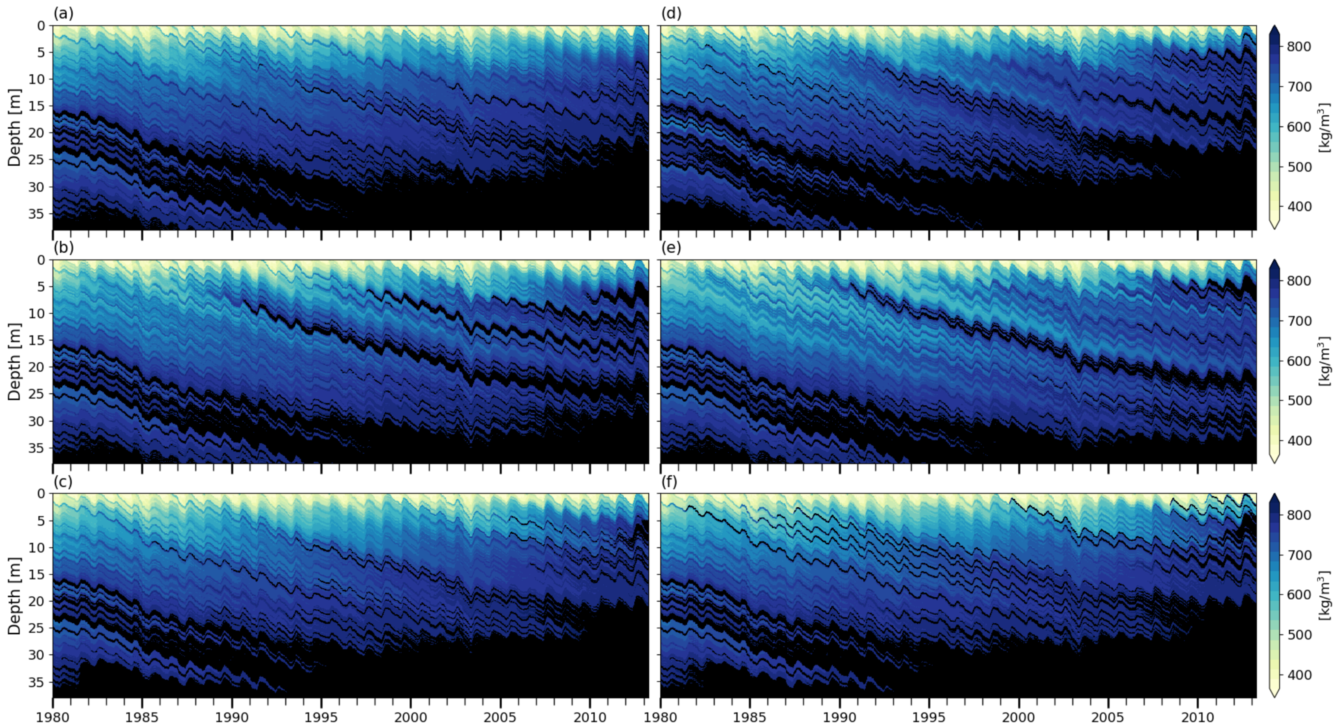

Figure 9. Firn density at FA13 (a) BK wh02 ip810, (b) R1M grLK ip810, (c) DPM grLK ip810, (d) BK whCL ip810, (e) R1M grA ip810, (f) DPM grA ip810, black indicates solid ice.~~ layers~~

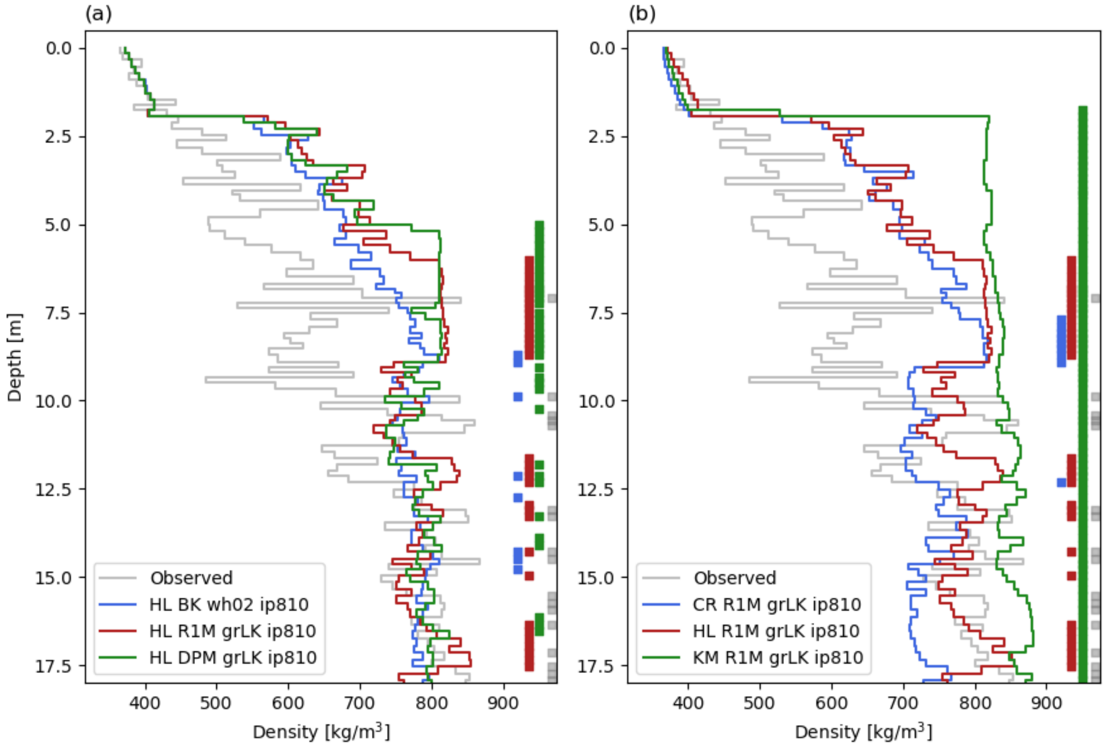
(a)
(b)
Depth [m]
Density [kg/m³]
Observed
HL BK wh02 ip810
HL R1M grLK ip810
HL DPM grLK ip810
Observed
CR R1M grLK ip810
HL R1M grLK ip810
KM R1M grLK ip810

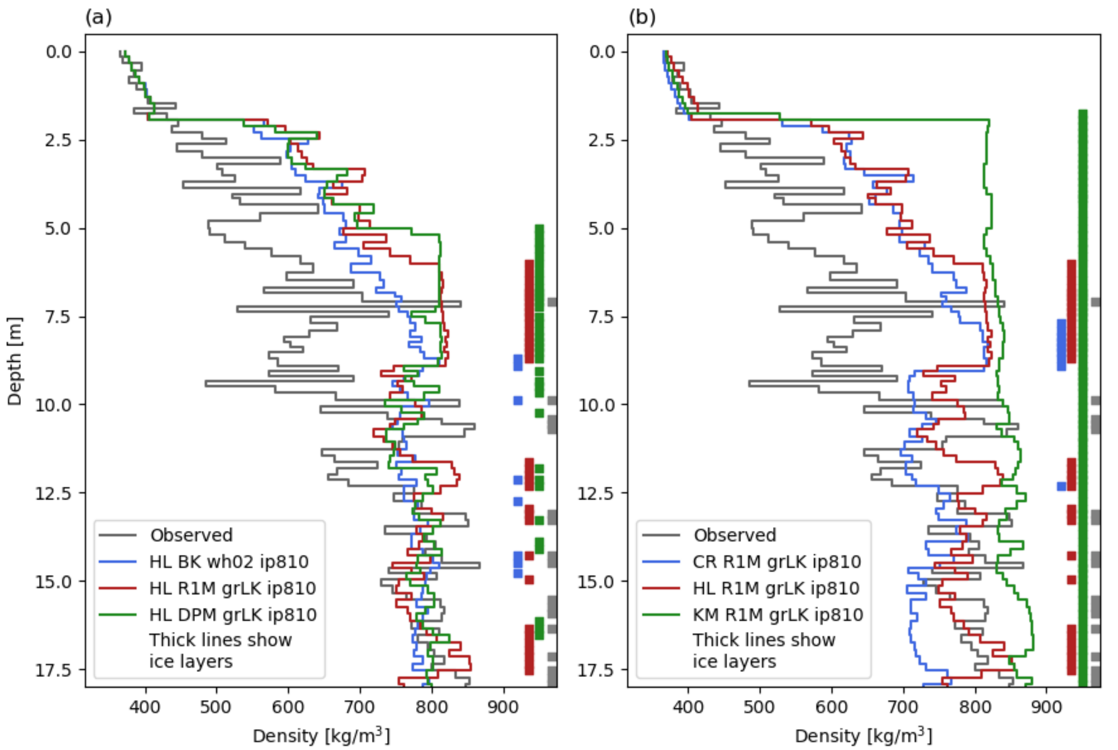
(a)
(b)
Depth [m]
Density [kg/m³]
Observed
HL BK wh02 ip810
HL R1M grLK ip810
HL DPM grLK ip810
Thick lines show
ice layers
Observed
CR R1M grLK ip810
HL R1M grLK ip810
KM R1M grLK ip810
Thick lines show
ice layers

Figure 10. Measured and modelled depth-density profiles at FA13 on 10/04/2013. Thick vertical lines show ice layers. The modelled densities are averaged at the vertical resolution of the drilled core. CR: CROCUS, HL: Herron and Langway, KM: Kuipers Munneke.

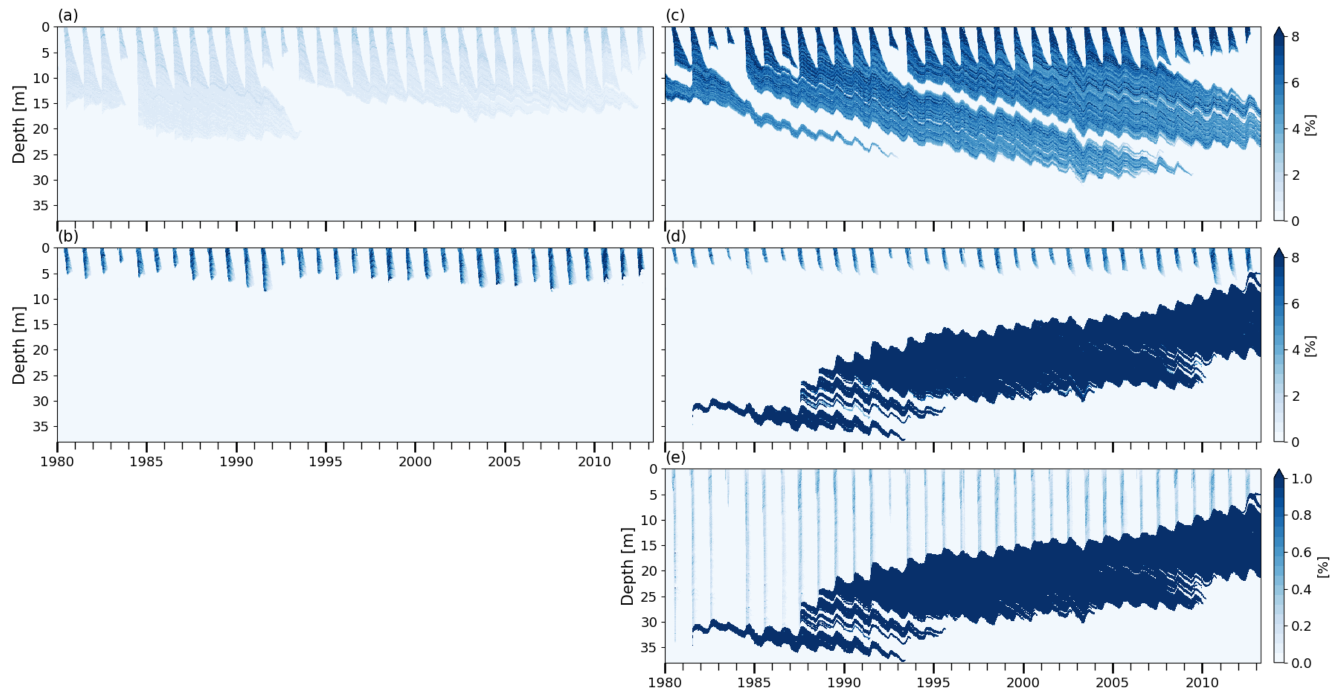

Figure 11. Volumetric water content at FA13 (a) BK wh02 ip810, (b) R1M grLK ip810, (c) BK whCL ip810, (d) Matrix flow domain of DPM grLK ip810, (e) Preferential flow domain of DPM grA ip810, note difference in scale for panel (e) ~~notice the different scales~~

S1 Model Implementation

The model uses a finite-volume scheme with each layer being an independent volume. We use the general mixed-form Picard iteration scheme to solve the RE, as it has been demonstrated that the mixed form of RE can be efficiently used in finite-difference schemes because of its accuracy and its robustness with respect to mass conservation (Celia et al., 1990). The Picard scheme discretises the model using central finite differences for the space derivative and a backward Euler method for the time derivative. The iterative process calculates the value of the pressure head at each iteration and then adjusts the liquid water content according to the water retention curve, Eq. (12). Hydraulic parameters are updated and iterations are repeated until convergence of the solution is achieved. Boundary conditions are the rate of meltwater input at the surface and a no-flow condition at the bottom. Solving the RE in the firn column presents numerical challenges. We adopt an implementation strategy based on the works of Wever et al. (2014) and D'Amboise et al. (2017) who implemented the RE in the snow models SNOWPACK and CROCUS respectively. Here, we give more details about this methodology.

S1.1 Convergence criteria

For the solution reached by the Picard iteration scheme to be considered convergent, it must fulfil different criteria. The convergence criteria between two successive iterations are defined for the head pressure (ε_h) and liquid water content (ε_θ) values as well as for the mass balance error (ε_{MB}) of individual layers. These three criteria are fixed to 10^{-3} m, 10^{-5} and 10^{-8} m respectively, following Huang et al. (1996) and Wever et al. (2014). For each layer, we select ε_θ or ε_h according to the effective saturation. Huang et al. (1996) showed that using ε_θ allows faster convergence. However, it cannot be used in very saturated layers and thus we apply ε_h for layers where effective saturation exceeds 0.99, in accordance with Wever et al. (2014). The mass-balance criterion is always applied to every layer, regardless of the saturation.

S1.2 Hydraulic conductivity calculation

As we use a central finite difference approach to compute RE, the fluxes are assumed to occur on the interface between adjacent layers. Incoming and outgoing fluxes are computed and this requires the hydraulic conductivity value to be calculated at the top and bottom of every layer *i* and not at the centre. We use the upstream-weighting technique (Forsyth et al., 1995):

$$K_{i+\frac{1}{2}} = \begin{cases} K_i,\ if\ \frac{\Delta h}{\Delta z} - 1 \leq 0 \\ K_{i+1},\ if\ \frac{\Delta h}{\Delta z} - 1 > 0 \end{cases} \quad \text{(S1)}$$

The advantage of this formulation over a simple arithmetic mean is that it does not lead to oscillatory solutions, regardless of the mesh size (Forsyth et al., 1995; Szymkiewicz, 2009).

S1.3 Dry layers

For numerical stability, a snow layer cannot be completely dry (i.e. $\theta = 0$). Therefore, two cases must be considered: dry layers and refreezing layers. At the start of the flow routine, all layers are initialised with a very low θ value, θ_{dry}. The value must be sufficiently low to avoid influencing the refreezing process but sufficiently high to lead to a convergent solution (D'Amboise et al., 2017). In this study, the θ_{dry} value is fixed at 10^{-6} as this is a tenth of the ε_θ criterion. This corresponds to a 1 m thick snow layer holding 1 µm of liquid water. When the flow routine is called in the firn model, the water content of every dry layer is thus synthetically raised to θ_{dry}, which corresponds to a pre-wetting. The porosity of ice layers that are at high densities (>900 kg m^{-3}) is thus adjusted in order to raise their water content to θ_{dry} in both domains.

Similarly, there is a risk for θ reaching too-low values when refreezing occurs. Therefore, refreezing is allowed only if the θ value is above 0.01% (Wever et al., 2014). This value is above θ_{dry} to avoid refreezing and corresponding latent heat release of the very low amounts of water resulting from the fluxes between layers that are initialised at θ_{dry}. Only at the last time step of the flow routine is the refreezing process allowed to decrease the volumetric water content until θ_{dry}. After that, the pre-wetting amounts of liquid water are subtracted at the end of the flow routine to maintain the mass conservation property of the firn model. At the end of the flow routine, if all the layers have a water content below 10^{-5}, we consider the firn column to be completely dry again so that the flow routine does not have to be called until the next melt event and computational time is largely saved.

S1.4 Dynamical time step adjustment

The numerical solving of RE uses a dynamically adjusted time step. Certain situations, such as the arrival of the wetting front at a stratigraphic transition, require a very small time step whereas larger time steps can be used in other cases without affecting numerical stability. Thus, the time step is adjusted according to the number of iterations, n_{it}, required to achieve convergence of the solution at the previous time step: decreased for a large number of iterations and increased for few iterations. Also, as in Wever et al. (2014) and D'Amboise et al. (2017), a back step case is used: the calculation is stopped and the time step automatically decreased if the solution fails to converge in 15 iterations or if warning signs of instability appear (positive pressure head values, effective saturation exceeding 1 or differences in successive pressure head values exceeding 10^3 m). The time step is bounded between 10^{-20} s and 900 s. The procedure can be summarised as follows:

$$\Delta t_{RE}^{t} = \begin{cases} 1.25\ \Delta t_{RE}^{t-1}, & if\ n_{it} \le 5 \\ \Delta t_{RE}^{t-1}, & if\ 5 < n_{it} < 10 \\ 0.5\ \Delta t_{RE}^{t-1}, & if\ 10 \le n_{it} \le 15 \\ back\ step, & if\ n_{it} > 15 \end{cases} \tag{S2}$$

S1.5 Saturated layers and aquifer treatment

If water reaches an impermeable ice layer, the layer above progressively becomes saturated. This means that its hydraulic conductivity progressively increases. As a consequence, the incoming flow becomes very large whereas the outgoing flow is forced to be zero. To deal with this issue, the layer has to be set impermeable once close to saturation and this process must go on for layers above when these reach saturation in turn. When an aquifer is present at the bottom of the domain, the amount of water is held in memory at the start of the flow routine and the end of the domain is set as the top of the aquifer. All the percolating water reaching the end of the domain is added to the aquifer amount and at the end of the routine, this total amount is redistributed in the bottom layers.

S1.6 Partial RE solving

In order to save computational time, the RE is not necessarily solved for the entire domain. If a significant part of the lowest layers is dry, we do not proceed to the calculations for this lower dry part. Starting from the surface, we look for the lowest layer where the water content is at least ε_θ + 0.01 % (above the minimum water content after refreezing). Then we take as lower limit for the RE calculation the layer situated 50 cm below this lowest wet layer. This is recalculated at every time step of the RE solving, making the 50 cm addition largely sufficient to capture the wetting of the dry lower part. If the lowest wet layer is less than 50 cm above the end of the domain, then the RE is calculated on the entire domain. This is applied in both the matrix and the preferential flow domains.

S1.7 Refreezing in the preferential flow domain

Contrarily to the SNOWPACK model, there is a particular circumstance for which we apply refreezing directly in the preferential flow domain: if a cold front (subfreezing temperatures) propagates from the surface into a wet firn column, all the water present in the matrix flow domain will progressively be refrozen, starting from the surface layer. It would be unrealistic to keep liquid water present in the preferential flow domain of layers that are above this cold front. Thus, if starting from the surface, the entire firn column until a particular layer that holds some liquid water in the preferential flow domain is at subfreezing temperatures, this liquid water is refrozen. In such cases, the firn column is dry in both domains until the depth delimited by the cold front. Simulations without this refreezing implementation reached very similar results but required more computational time.

S1.8 Merging process

The CFM usually considers every accumulation event as a new layer. However, as we use three hourly accumulation forcing, the firn layer could consist of a high number of extremely fine layers. Because the calculation time for the RE is very dependent on the number of distinct layers in the firn column, we chose to merge any layer thinner than 2 cm with the underlying layer. If this was applied to the surface layer, every accumulation event of less than 2 cm snow would be immediately merged with the previous surface layer. In the case where a high number of successive snowfall events would be below the 2 cm threshold, these would all be merged within the same layer, possibly becoming very thick. To avoid this, the newly added snow layer is merged with the previous surface layer only if the latter is below the 2 cm threshold. However, newly-added layers that are less than 0.01 mm thick are always merged with the layer below. It is important to keep a high vertical resolution when simulating the percolation process with the RE, as this flow equation is highly sensitive to structural heterogeneities in the firn. If the merging process is too lenient, this leads to the smoothing of heterogeneities such as sharp grain-size or density transitions. Moreover, using a coarse resolution would lead to only an approximation of the water percolation because water content is always homogeneous in a single layer. Thus, as soon as water percolates at the top of a given layer, it is distributed in the entire layer.

Tables

Variable/Parameter	Symbol	Value [unit]
Density	ρ	[kg m^{-3}]
Ice density	ρ_i	917 [kg m^{-3}]
Water density	ρ_w	1000 [kg m^{-3}]
Temperature	T	[K]
Mean annual surface temperature	T_{av}	[K]
Mean annual accumulation rate	$\dot{b}$	[m s^{-1}]
Gas constant	R	8.314 [J mol^{-1} K^{-1}]
Gravitational acceleration	g	9.81 [m s^{-2}]
Overburden pressure	σ	[kg m^{-1} s^{-2}]
Snow viscosity	η	[kg m^{-1} s^{-1}]
Firn viscosity parameters	η_0	7.62237 [kg s^{-1} m^{-1}]
	a_n	0.1 [K^{-1}]
	b_n	0.023 [m^3 kg^{-1}]
	c_n	358 [kg m^{-3}]
	f_1	4 [/]
	f_2	[/]
Firn thermal conductivity	k_s	[W m^{-1} K^{-1}]
Pressure head	h	[m]
Hydraulic conductivity	$K(\theta)$	[m s^{-1}]
Hydraulic conductivity at saturation	$Ksat$	[m s^{-1}]
Grain radius	r	[m]
Grain radius at surface	r_0	[m]
Grain growth activation energy	E_g	42.4 10^3 [J mol^{-1}]
Grain growth rate constant	k_g	1.3 10^{-7} [m^2 s^{-1}]
Initial grain-size parameters	b_0	0.781 [/]

	b_1	0.0085 [/]
	b_2	-0.279 [/]
Dynamic viscosity of liquid water at 273.15 K	μ	0.001792 [kg m^{-1} s^{-1}]
Volumetric water content	θ	[/]
Water-holding capacity	θ_h	[/]
Mass proportion corresponding to water-holding capacity	W_w	[/]
Residual water content	θ_r	[/]
Porosity	P	[/]
Fraction of the pore space allocated to preferential flow	F	0.02 [/]
Saturated water content	θ_{sat}	[/]
Effective saturation	Se	[/]
van Genuchten parameters	α, n, m	[/]
Water entry suction	h_{we}	[m]
Heat flow	Q	[J m^{-2} s^{-1}]
Specific latent heat of fusion	L_f	[J kg^{-1}]
Concentration of preferential flowpaths	N	[m^{-2}]
Preferential flow saturation threshold	Θ	0.1 [/]
Lateral runoff	Ru	[m]
Water in excess of the residual water content	L_{excess}	[m]
Characteristic runoff time	τ_{Ru}	[s]
Surface slope	S	[/]
	c_1	1.296 10^5 [s]
Runoff parameters	c_2	2.16 10^6 [s]
	c_3	140 [/]
Mass liquid water content	$\theta_{weight,\%}$	[%]
Correction factor in water-retention curve	Sc	$[1 + (0.0058\alpha)^n]^{-m}$ [/]

Table S1. Variables and parameters notation

Liquid water scheme [Abbreviation]	Bucket model [BK]; Single-domain Richards Equation [R1M]; Dual-permeability Richards Equation [DPM]
Compaction scheme [Abbreviation]	CROCUS [CR]; Herron and Langway (1980) [HL]; Kuipers Munneke et al. (2015) [KM]
Impermeability threshold [Abbreviation]	780 kg m^{-3} [ip780]; 810 kg m^{-3} [ip810]; 830 kg m^{-3} [ip830]
Water-holding capacity [Abbreviation]	Constant at 2 % [wh02]; Coléou and Lesaffre (1998) [whCL]
Grain-size formulation [Abbreviation]	Linow et al. (2012) at surface and Katsushima et al. (2009) growth [grLK]; Constant at surface and Arthern et al. (2010) growth [grA]

Table S2. Options for simulation experiments and their respective abbreviations

	Liquid water scheme	Compaction scheme	Impermeability threshold	Water-holding capacity	Grain-size formulation
BK (wh02 ip810)	BK	CROCUS	810	0.02	/
R1M (grLK ip810)	R1M	CROCUS	810	/	LK

DPM (grLK ip810)	DPM	CROCUS	810	/	LK
DPM (grLK ip780)	DPM	CROCUS	780	/	LK
DPM (grLK ip830)	DPM	CROCUS	830	/	LK
BK (wh02 ip780)	BK	CROCUS	780	0.02	/
BK (whCL ip810)	BK	CROCUS	810	CL	/
BK (wh02 ip830)	BK	CROCUS	830	0.02	/
R1M (grLK ip830)	R1M	CROCUS	830	/	LK
R1M (grA ip810)	R1M	CROCUS	810	/	A
DPM (grA ip810)	DPM	CROCUS	810	/	A
HL DPM (grLK ip810)	DPM	HL	810	/	LK
KM DPM (grLK ip810)	DPM	KM	810	/	LK
HL R1M (grLK ip810)	R1M	HL	810	/	LK
KM R1M (grLK ip810)	R1M	KM	810	/	LK

Table S3. Details of the acronyms of the simulation experiments presented

	Top 15 m FAC, anomaly vs observations				10 m temperature, anomaly vs observations [K]			
	DYE-2	NASA-SE	KAN-U	FA13	DYE-2	NASA-SE	KAN-U	FA13
BK (wh02 ip810)	-4 %	-3 %	+59 %	-23 %	+0.21	+1.94	-1.73	+0.10
R1M (grLK ip810)	-4 %	-3 %	+50 %	-30 %	-0.40	+1.42	-2.57	-0.71
DPM (grLK ip810)	-16 %	-3 %	-2 %	-30 %	+2.72	+2.21	+4.52	+1.5
BK (whCL ip810)	+0 %	-2 %	+65 %	-32 %	-1.27	+1.00	-3.43	-0.66
BK (wh2 ip780)	-1 %	-3 %	+67 %	-22 %	+0.01	+1.94	-2.20	-0.52
BK (wh02 ip830)	-5%	-3 %	+47 %	-23 %	+0.31	+1.94	-0.97	+0.32
R1M (grA ip810)	-0 %	-2 %	+66 %	-27%	-1.03	+1.02	-3.25	-1.88
R1M (grLK ip780)	-2 %	-3 %	+61 %	-30 %	-0.34	+1.42	-2.56	-0.72
R1M (grLK ip830)	-2 %	-3 %	+48 %	-31 %	-0.38	+1.42	-2.45	-0.43
DPM (grA ip810)	-16 %	-3 %	-4 %	-32 %	+2.41	+2.14	+4.62	+1.5
DPM (grLK ip780)	-16 %	-3 %	+13 %	-44 %	+2.78	+2.21	+2.97	+1.5
DPM (grLK ip830)	-14 %	-3 %	-11 %	-28 %	+2.73	+2.21	+5.65	+0.48

Table S3. Summary of the results of the three water schemes and their various parameterisations compared to observations

	Top 15 m FAC, anomaly vs observations				10 m temperature, anomaly vs observations [K]			
	DYE-2	NASA-SE	KAN-U	FA13	DYE-2	NASA-SE	KAN-U	FA13
CR R1M (grLK ip810)	-4 %	-3 %	+50 %	-21 %	-0.40	+1.42	-2.57	-0.19
HL R1M (grLK ip810)	-11 %	+17 %	+37 %	-30 %	-0.26	+1.22	-2.32	-0.71
KM R1M (grLK ip810)	-23 %	+8 %	+10 %	-54 %	-0.41	+1.77	-2.84	-0.75

Table S4. Summary of the results of the three densification models compared to observations

Figures

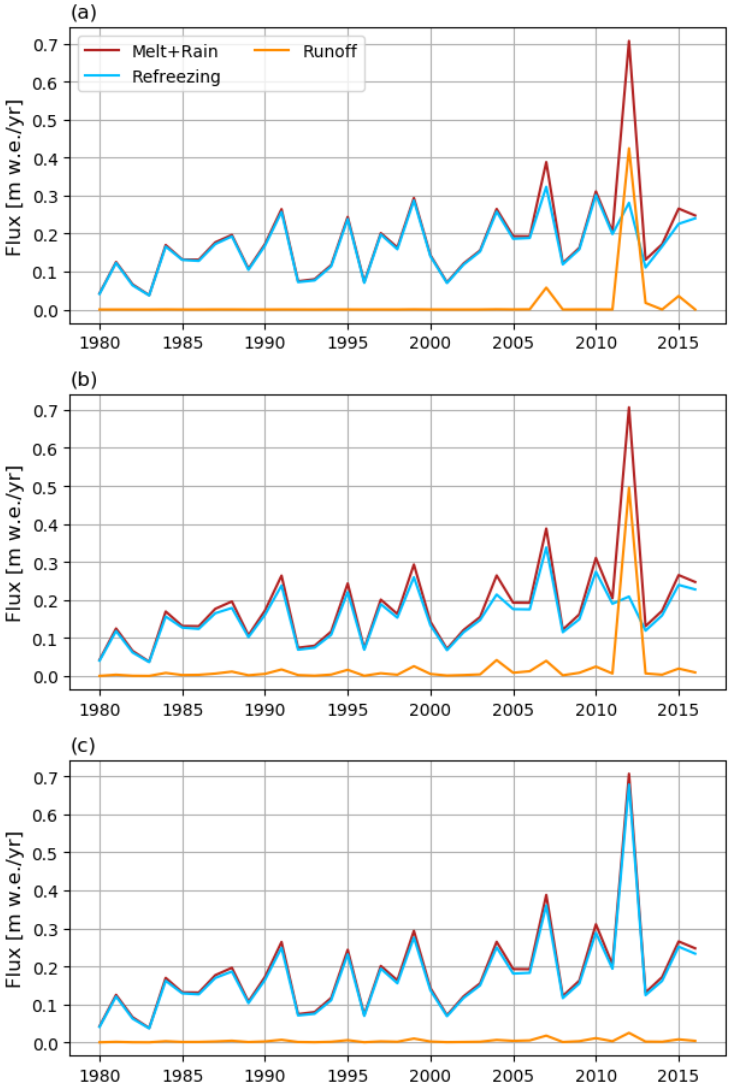

Figure S1. Annual rates of liquid water input, runoff and refreezing at DYE-2 as simulated by (a) BK wh02 ip810, (b) R1M grLK ip810 and (c) DPM grLK ip810

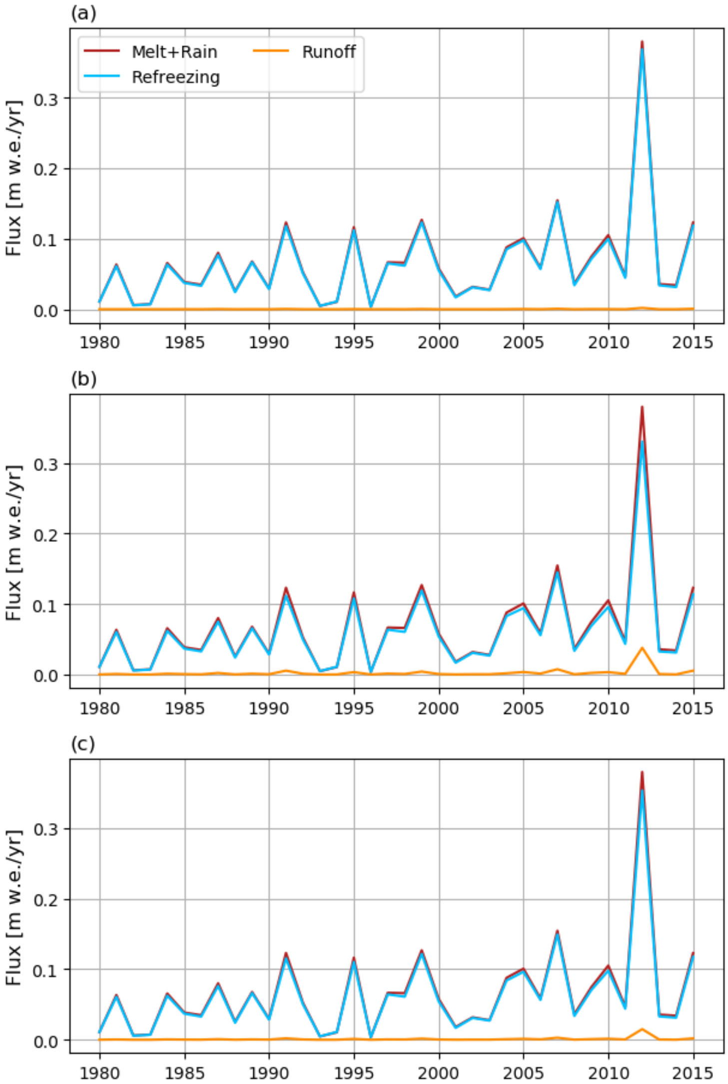

Figure S2. Annual rates of liquid water input, runoff and refreezing at NASA-SE as simulated by (a) BK wh02 ip810, (b) R1M grLK ip810 and (c) DPM grLK ip810

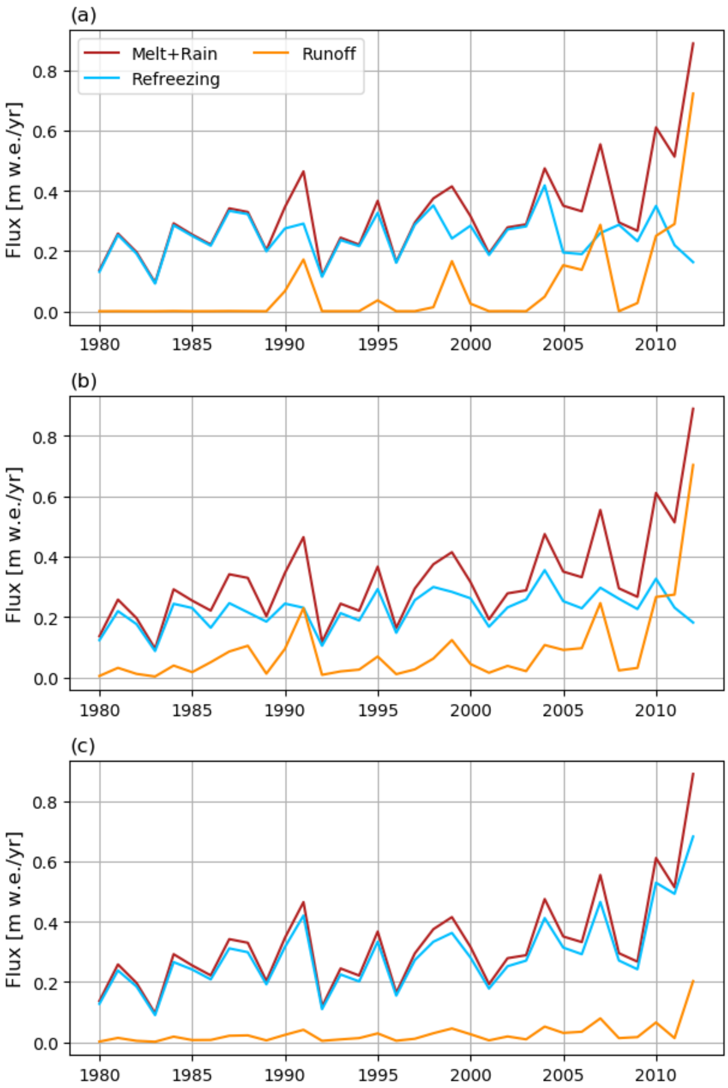

Figure S3. Annual rates of liquid water input, runoff and refreezing at KAN-U as simulated by (a) BK wh02 ip810, (b) R1M grLK ip810 and (c) DPM grLK ip810

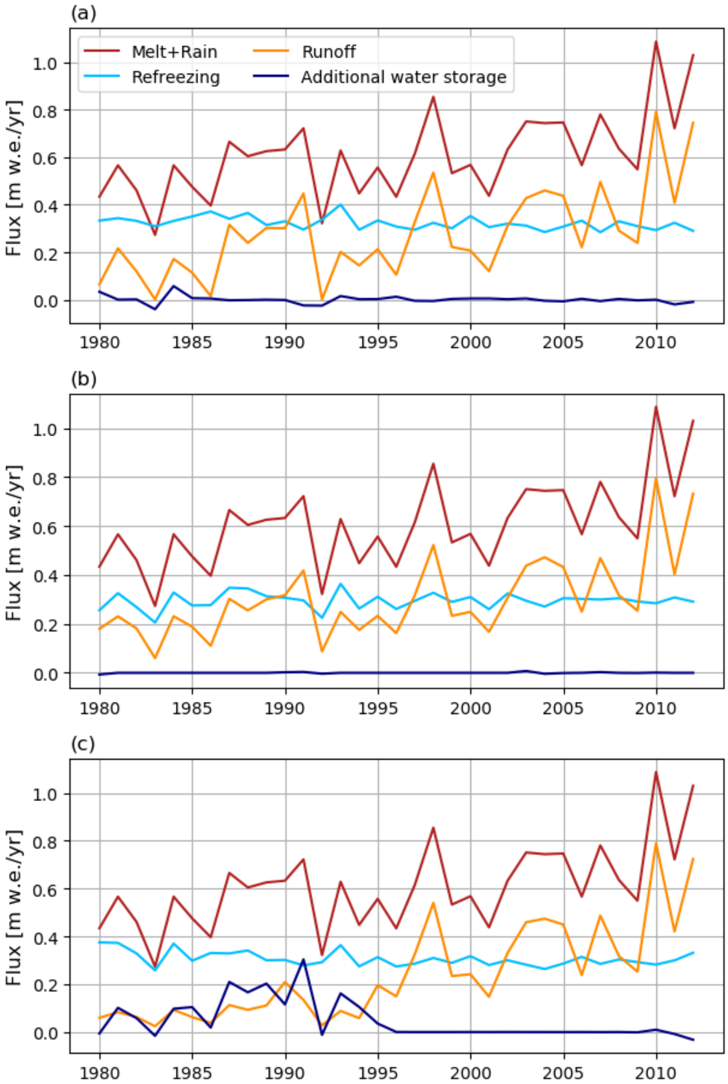

Figure S4. Annual rates of liquid water input, runoff, refreezing and storage of liquid water in the firn column at FA13 as simulated by (a) BK wh02 ip810, (b) R1M grLK ip810 and (c) DPM grLK ip810

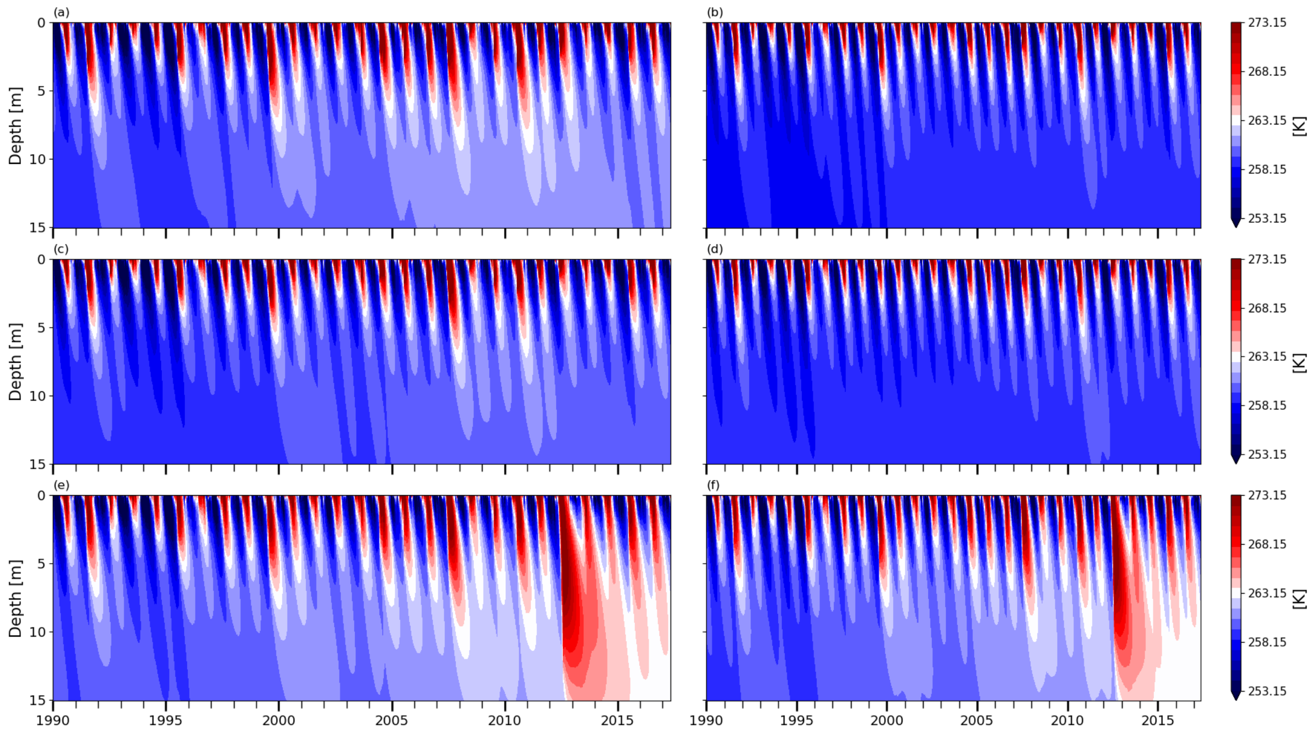

Figure S5. Modelled firn temperature at DYE-2, (a) BK wh02 ip810, (b) R1M grLK ip810, (c) DPM grLK ip810, (d) BK whCL ip810, (e) R1M grA ip810, (f) DPM grA ip810

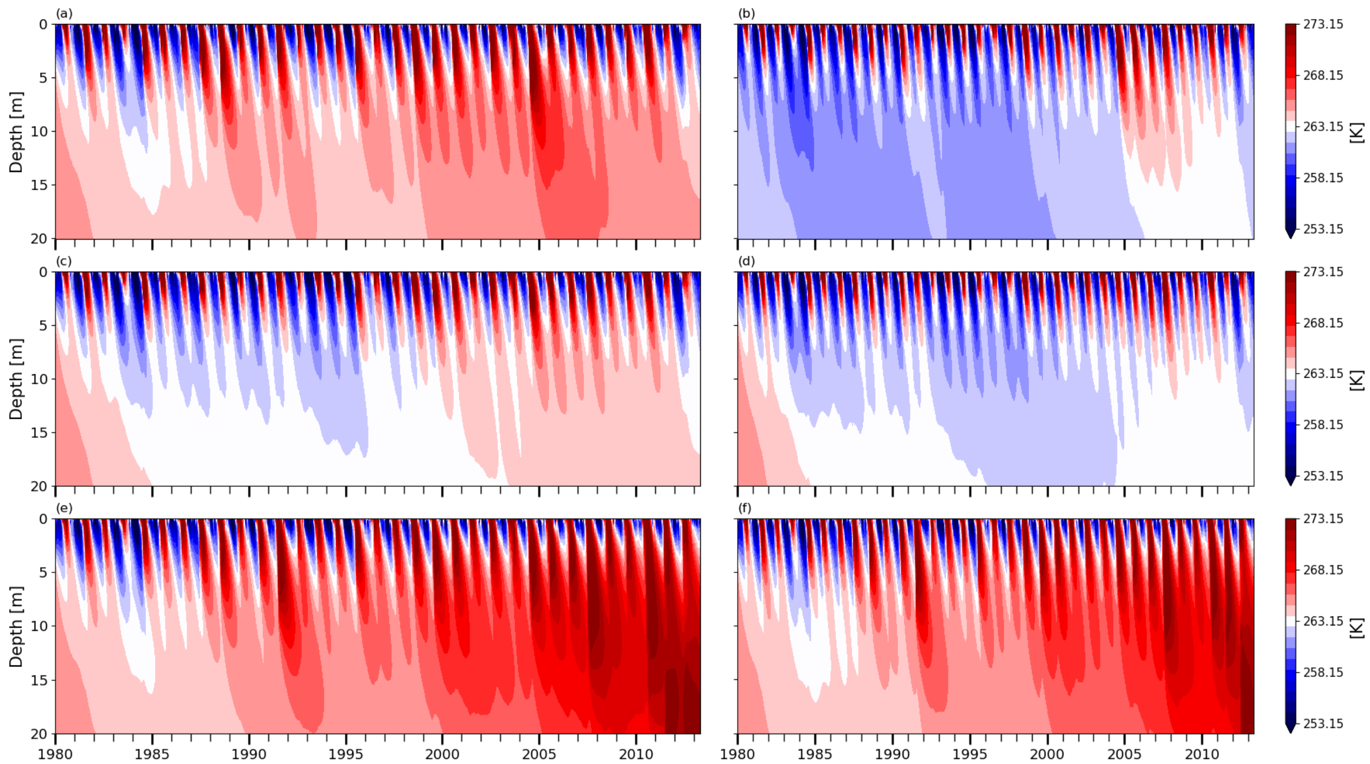

Figure S6. Modelled firn temperature at KAN-U, (a) BK wh02 ip810, (b) R1M grLK ip810, (c) DPM grLK ip810, (d) BK whCL ip810, (e) R1M grA ip810, (f) DPM grA ip810

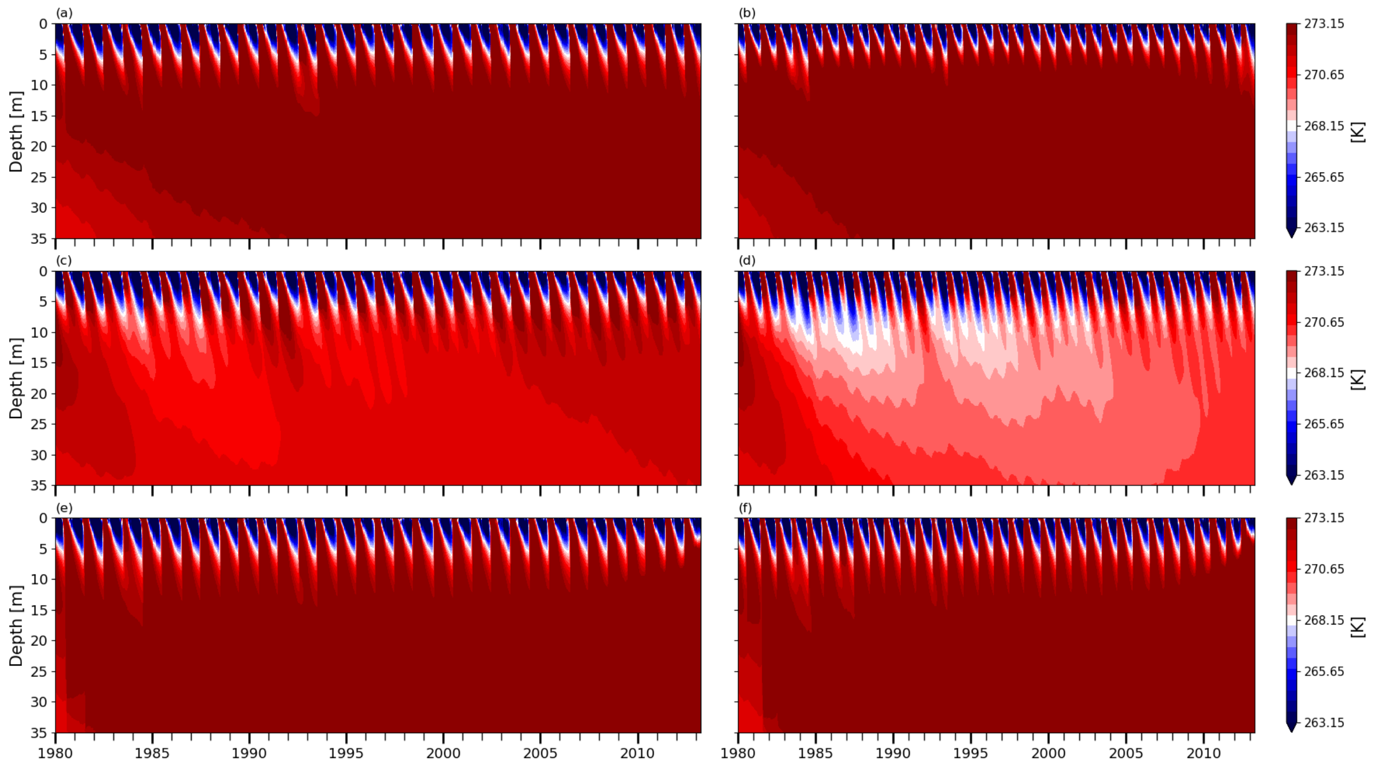

Figure S7. Modelled firn temperature at FA13, (a) BK wh02 ip810, (b) R1M grLK ip810, (c) DPM grLK ip810, (d) BK whCL ip810, (e) R1M grA ip810, (f) DPM grA ip810

References

Arthern, R. J., Vaughan, D. G., Rankin, A. M., Mulvaney, R. and Thomas, E. R.: In situ measurements of Antarctic snow compaction compared with predictions of models, J. Geophys. Res. Earth Surf., 115, 1–12, doi:10.1029/2009JF001306, 2010.

Celia, M. A., Bouloutas, E. T. and Zarba, R. L.: A General Mass-Conservative Numerical Solution for the Unsaturated Flow Equation, Water Resour. Res., 26, 1483–1496, doi:10.1029/90wr00196, 1990.

D'Amboise, C. J. L., Müller, K., Oxarango, L., Morin, S. and Schuler, T. V.: Implementation of a physically based water percolation routine in the CROCUS (V7) snowpack model, Geosci. Model Dev. Discuss., 1–32, doi:10.5194/gmd-2017-56, 2017.

Forsyth, P. A., Wu, Y. S. and Pruess, K.: Robust numerical methods for saturated-unsaturated flow with dry initial conditions in heterogeneous media, Adv. Water Resour., 18, 25–38, doi:10.1016/0309-1708(95)00020-J, 1995.

Herron, M. and Langway, C.: Firn densification: an empirical model, J. Glaciol., 25, 1980.

Huang, K., Mohanty, B. P. and van Genuchten, M. T.: Method To Solve the Variably Saturated Flow Equation, J. Hydrol., 178, 69–91, 1996.

Katsushima, T., Kumakura, T. and Takeuchi, Y.: A multiple snow layer model including a parameterization of vertical water channel process in snowpack, Cold Reg. Sci. Technol., 59, 143–151, doi:10.1016/j.coldregions.2009.09.002, 2009.

Kuipers Munneke, P., Ligtenberg, S. R. M., Noël, B. P. Y., Howat, I. M., Box, J. E., Mosley-Thompson, E., McConnell, J. R., Steffen, K., Harper, J. T., Das, S. B. and van den Broeke, M. R.: Elevation change of the Greenland ice sheet due to surface mass balance and firn processes, 1960-2013, The Cryosphere, 9, 3541–3580, doi:10.5194/tcd-9-3541-2015, 2015.

Linow, S., Hörhold, M. W. and Freitag, J.: Grain-size evolution of polar firn: A new empirical grain growth parameterization based on X-ray microcomputer tomography measurements, J. Glaciol., 58, 1245–1252, doi:10.3189/2012JoG11J256, 2012.

Machguth, H., Macferrin, M., van As, D., Box, J. E., Charalampidis, C., Colgan, W., Fausto, R. S., Meijer, H. A. J., Mosley-Thompson, E. and van de Wal, R. S. W.: Greenland meltwater storage in firn limited by near-surface ice formation, Nat. Clim. Chang., 6, 390–393, doi:10.1038/nclimate2899, 2016.

Marchenko, S., Pohjola, V., Pettersson, R., van Pelt, W. J. J., Vega, C., Machguth, H., BØggild, C. E. and Isaksson, E.: A plot-scale study of firn stratigraphy at Lomonosovfonna, Svalbard, using ice cores, borehole video and GPR surveys in 2012–14, J. Glaciol., 63(237), 67–78, doi:10.1017/jog.2016.118, 2017.

Szymkiewicz, A.: Approximation of internodal conductivities in numerical simulation of one-dimensional infiltration, drainage, and capillary rise in unsaturated soils, Water Resour. Res., 45, 1–16, doi:10.1029/2008WR007654, 2009.

Wever, N., Fierz, C., Mitterer, C., Hirashima, H. and Lehning, M.: Solving Richards Equation for snow improves snowpack meltwater runoff estimations in detailed multi-layer snowpack model, The Cryosphere, 8, 257–274, doi:10.5194/tc-8-257-2014, 2014.